UNIVERSIDAD NACIONAL AUTÓNOMA DE MÉXICO
POSGRADO EN CIENCIAS BIOLÓGICAS
FACULTAD DE CIENCIAS

EFECTO PROTECTOR DEL SULFORAFANO EN EL DAÑO RENAL CAUSADO POR LA OBSTRUCCIÓN UNILATERAL DEL URÉTER

TESIS

QUE PARA OPTAR POR EL GRADO DE:
DOCTORA EN CIENCIAS

PRESENTA:

M en C. ANA KARINA ARANDA RIVERA

TUTOR PRINCIPAL DE TESIS: DR. JOSÉ PEDRAZA CHAVERRI
FACULTAD DE CIENCIAS, UNAM
COMITÉ TUTOR: DRA. DIANA BARRERA OVIEDO
FACULTAD DE MEDICINA, UNAM
DRA. ANA MARÍA SALAZAR MARTÍNEZ
FACULTAD DE MEDICINA, UNAM

CD UNIVERSITARIA, CD. MX   Enero de 2024

UNIVERSIDAD NACIONAL AUTÓNOMA DE MÉXICO
POSGRADO EN CIENCIAS BIOLÓGICAS
FACULTAD DE CIENCIAS

EFECTO PROTECTOR DEL SULFORAFANO EN EL DAÑO RENAL CAUSADO POR LA OBSTRUCCIÓN UNILATERAL DEL URÉTER

TESIS

QUE PARA OPTAR POR EL GRADO DE:
DOCTORA EN CIENCIAS

PRESENTA:

M en C. ANA KARINA ARANDA RIVERA

TUTOR PRINCIPAL DE TESIS: DR. JOSÉ PEDRAZA CHAVERRI
FACULTAD DE CIENCIAS, UNAM
COMITÉ TUTOR: DRA. DIANA BARRERA OVIEDO
FACULTAD DE MEDICINA, UNAM
DRA. ANA MARÍA SALAZAR MARTÍNEZ
FACULTAD DE MEDICINA, UNAM

CIUDAD UNIVERSITARIA, CD. MX   Enero de 2024

M. en C. Ivonne Ramírez Wence
Directora General de Administración Escolar, UNAM
P r e s e n t e

Me permito informar a usted que en la reunión ordinaria del Comité de Posgrado en Ciencias Biológicas, celebrada el día **12 de junio de 2023** se aprobó el siguiente jurado para el examen de grado de **DOCTORA EN CIENCIAS** de la estudiante **ARANDA RIVERA ANA KARINA** con número de cuenta **517027840** con la tesis titulada: **"Efecto protector del sulforafano en el daño renal causado por la obstrucción unilateral del uréter",** realizada bajo la dirección del **DR. JOSÉ PEDRAZA CHAVERRI:**

Presidente:	**DRA. MARÍA EUGENIA GONSEBATT BONAPARTE**
Vocal:	**DRA. LAURA GABRIELA SÁNCHEZ LOZADA**
Vocal:	**DRA. GLADIS DEL CARMEN FRAGOSO GONZÁLEZ**
Vocal:	**DRA. ABEL SANTAMARÍA DEL ANGEL**
Secretario:	**DRA. DIANA BARRERA OVIEDO**

Sin otro particular, me es grato enviarle un cordial saludo.

A T E N T A M E N T E
"POR MI RAZA HABLARÁ EL ESPÍRITU"
Ciudad Universitaria, Cd. Mx., a 07 de noviembre de 2023

COORDINADOR DEL PROGRAMA

DR. ADOLFO GERARDO NAVARRO SIGÜENZA

c. c. p. Expediente del alumno

AGNS/AAC/GEMF/EARR/ipp

AGRADECIMIENTOS INSTITUCIONALES

AGRADECIMIENTOS A TÍTULO PERSONAL

A mis papás, sin ellos no hubiera tenido la confianza de llegar hasta donde estoy. Gracias por hacer que haya creído en mi y por nunca dejarme rendir, por su compañía en cada etapa, por abrazarme cuando me caigo, por las llamadas de horas. LOS AMO.

A mi hermana Nayeli, que sé que estaría orgullosa de mi. Ha sido difícil esta etapa sin ti, siempre estás en mis pensamientos. TE AMO Y EXTRAÑO.

A mi amor Alfredo y a mi hija Amaya que han estado presentes en cada reto que he llevado. LOS ADORO! A mi esposo Alfredo por su apoyo en esta etapa. Muy especialmente a mi hija Amaya que es el máximo impulso que necesito para seguir adelante. TE AMO!

A mis suegros por su apoyo en el tiempo que estuve en este camino.

A mis amigos Isabel y Bismarck. Ese viaje a Europa me hizo valorarlos más, son parte importante de toda mi transición en el doctorado. Los quiero!

A la Dra. Edilia Tapia, sin ella parte de este proyecto no hubiera sido posible, sus manos mágicas hacen maravillas en las cirugías. Gracias por apoyarme en todo el proceso y por siempre ser tan positiva.

Al Dr. Pedraza, por recibirme y hacerme parte del grupo. Por confiar en mi y apoyarme en mis decisiones.

A la Dra. Gaby, por dejarme estar en su laboratorio.

A Emiliano, por todo lo que tuvo que ver en este proyecto, mil gracias.

A los compañeros de cardiología: Quetzal, Edgar, Daniel, Misael y Diana gracias por hacer los días más amenos y hacerme reir.

ÍNDICE

LISTA DE ABEVIATURAS

α-SMA	Alfa-actina de músculo liso
$\Delta\Psi$	Potencial de membrana mitocondrial
ACO2	Aconitasa 2
AG	Ácidos grasos
AMPK	Proteína adenosin monofosfato cinasa
ANT	Translocador de nucleótidos de adenina
ATP	Adenosin trifosfato
Bcl2	Linfoma de células B 2
CD36	Grupo de diferenciación 36
Col IV	Colágeno IV
CPT1	Carnitina palmitoiltransferasa 1
DGAT1	Diacilglicerol O-aciltransferasa 1
DRP1	Proteína relacionada con la dinamina 1
ERC	Enfermedad renal crónica
ERO	Especies reactivas del oxígeno
FIS1	Proteína de fisión 1
FASN	Sintasa de los ácidos grasos
GAPDH	Gliceraldehído 3-fosfato deshidrogenasa
H_2O_2	Peróxido de hidrógeno
IL-1β	Interleucina-1 beta
KDIGO	Kidney Disease Improving Global Outcomes, por sus siglas en inglés
KIM-1	Molécula de daño renal 1
LC3-I	Proteínas asociadas a microtúbulos 1A/1B cadena ligera 3 I
LC3-II	Proteínas asociadas a microtúbulos 1A/1B cadena ligera 3 II
MET	Microscopía electrónica de transmisión
MFN	Mitofusina
NRF1	Factor nuclear respiratorio 1
NRF2	Factor nuclear respiratorio 2
Nrf2	Factor nuclear eritroide 2
OPA1	Proteína de atrofia óptica 1
OUU	Obstrucción unilateral del uréter
Parkin	E3 ubiquitina-proteína ligasa parkin
PGC-1α	Coactivador 1α del receptor activado por el proliferador de peroxisomas γ
PINK1	Cinasa 1 inducida por fosfatidilinositol-3,4,5-trisfosfato 3-fosfatasa
PVDF	Fluoruro de polivinilideno
SFN	Sulforafano
SIRT3	Sirtuína 3
SREBP1	Proteína de unión al elemento regulador de esteroles 1

STE	Sistema de transporte de electrones
TD	Túbulo distal
TFAM	Factor de transcripción mitocondrial A
TFG	Tasa de filtración glomerular
TG	Triglicéridos
TGF-β1	Factor de crecimiento transformante β1
TNB	Ácido 5-tio-2-nitrobenzoico
TP	Túbulo proximal
VDAC	Canal de aniones dependiente de voltaje

1. RESUMEN

La obstrucción unilateral del uréter (OUU) es un modelo animal realizado en roedores que permite el estudio de la nefropatía obstructiva de forma acelerada. Durante la OUU, el daño tubular y alteraciones como el estrés oxidante, la inflamación, el metabolismo de los lípidos y la disfunción mitocondrial favorecen el desarrollo de fibrosis, lo que conduce a la progresión de la enfermedad renal crónica. El sulforafano (SFN), un isotiocianato derivado de vegetales crucíferos verdes, podría mejorar las funciones mitocondriales y el metabolismo de los lípidos; sin embargo, su papel en la OUU ha sido poco explorado. Por lo tanto, nuestro objetivo fue determinar el efecto protector de SFN relacionado con las mitocondrias y el metabolismo de los lípidos en la OUU. Se encontró que en la OUU el SFN disminuyó el daño renal, atribuido a una mayor biogénesis mitocondrial. De acuerdo con lo anterior, se observó que el SFN aumenta los niveles del coactivador 1α del receptor activado por el proliferador de peroxisomas γ (PGC-1α) y el factor respiratorio nuclear 1 (NRF1). El incremento en la biogénesis incrementó los niveles proteicos del canal de aniones dependiente de voltaje (VDAC), un marcador de masa mitocondrial. Asímismo, el SFN restauró la estructura mitocondrial, así como las actividades del complejo III (CIII), la aconitasa 2 (ACO2) y la citrato sintasa que se encontraban disminuídas en la OUU. Además, el SFN mejoró el metabolismo de los lípidos, observado por la regulación a la baja del grupo de diferenciación 36 (CD36), la proteína de unión al elemento regulador de esteroles 1 (SREBP1), la sintasa de ácidos grasos (FASN) y la diacilglicerol O-aciltransferasa 1 (DGAT1), que reduce la acumulación de triglicéridos (TG). Finalmente, la restauración de la estructura mitocondrial redujo la fisión excesiva al disminuir los niveles de la proteína relacionada con la dinamina 1 (DRP1). El flujo de autofagia se restauró aún más mediante la reducción de beclin y el secuestrosoma (p62) y el aumento del linfoma de células B 2 (Bcl2) y la proporción de proteínas asociadas a microtúbulos 1A/1B cadena ligera 3 II e I (LC3II/LC3I). Estos resultados revelan que la protección por el SFN contra la lesión renal inducida por la OUU estuvo asociada al aumento de la biogénesis mitocondrial y a la mejoría del metabolismo de los lípidos.

2. ABSTRACT

Unilateral ureteral obstruction (UUO) is an animal rodent model that allows the study of obstructive nephropathy in an accelerated manner. During UUO, tubular damage is induced, and alterations such as oxidative stress, inflammation, lipid metabolism, and mitochondrial impairment favor fibrosis development, leading to chronic kidney disease progression. Sulforaphane (SFN), an isothiocyanate derived from green cruciferous vegetables, might improve mitochondrial functions and lipid metabolism; however, its role in UUO has been poorly explored. Therefore, we aimed to determine the protective effect of SFN related to mitochondria and lipid metabolism in UUO. Our results showed that in UUO, SFN decreased renal damage, attributed to increased mitochondrial biogenesis. We showed that SFN augmented peroxisome proliferator-activated receptor γ co-activator 1α (PGC-1α) and nuclear respiratory factor 1 (NRF1). The increase in biogenesis augmented the mitochondrial mass marker voltage-dependent anion channel (VDAC) and improved mitochondrial structure, as well as complex III, aconitase 2 (ACO2), and citrate synthase activities in UUO. In addition, lipid metabolism was improved, observed by the downregulation of cluster of differentiation 36 (CD36), sterol regulatory-element binding protein 1 (SREBP1), fatty acid synthase (FASN), and diacylglycerol O-acyltransferase 1 (DGAT1), which reduces triglyceride (TG) accumulation. Finally, restoring the mitochondrial structure reduced excessive fission by decreasing the fission protein dynamin-related protein-1 (DRP1). Autophagy flux was further restored by reducing beclin and sequestosome (p62) and increasing B-cell lymphoma 2 (Bcl2) and the ratio of microtubule-associated proteins 1A/1B light chain 3 II and I (LC3II/LC3I). These results reveal that SFN confers protection against UUO-induced kidney injury by targeting mitochondrial biogenesis, which also improves lipid metabolism.

3. INTRODUCCIÓN

La enfermedad renal crónica (ERC) tiene una prevalencia del 9.1% a nivel mundial con más de 1.7 millones de muertes al año atribuidas a esta enfermedad (Carney, 2020; Ruiz-Ortega et al., 2020). Muchas causas conducen al desarrollo de ERC, entre ellas la diabetes, la hipertensión, la obesidad y la obstrucción del tracto urinario, entre otras. La mayoría de las ERC convergen en que la disfunción mitocondrial en una de las principales características relacionadas con la génesis y progresión de esta patología (Bhargava & Schnellmann, 2017; Bhatia & Choi, 2019). Lo anterior se debe a que el riñón es el segundo órgano con mayor demanda energética requerida para llevar a cabo los mecanismos de reabsorción en el túbulo proximal (TP) (Galvan et al., 2017). La disfunción mitocondrial está asociada con la generación de estrés oxidante, periodos sostenidos de inflamación, la acumulación y síntesis de lípidos, muerte celular y fibrosis (Avila-Rojas et al., 2020; Fedorova et al., 2013; Forbes & Thorburn, 2018; Prieto-Carrasco et al., 2021).

El modelo de obstrucción ureteral unilateral (OUU) es un modelo comúnmente utilizado para estudiar el daño renal por obstrucción, ya que se reproduce la nefropatía obstructiva observada en la clínica en un perido de tiempo relativamente corto (Chevalier, 2004; Martínez-Klimova et al., 2019). Además, en este modelo se puede observar el desarrollo de la ERC y su transición a fibrosis en un periodo corto de tiempo (Chevalier, 2008; Martínez-Klimova et al., 2019; Ucero et al., 2010).

En el modelo de OUU se ha encontrado que las alteraciones mitocondriales favorecen el desarrollo de fibrosis (Cheng et al., 2016; Jiménez-Uribe et al., 2021; Ling et al., 2019). Estas alteraciones en la mitocondria incluyen la generación de estrés oxidante, la disminución de la bioenergética, así como la pérdida de la homeostasis mitocondrial, relacionado con el aumento de los marcadores de inflamación y de fibrosis (Ai et al., 2015; Guo et al., 2017; Jiménez-Uribe et al., 2021; Li et al., 2020). La fibrosis comprende la deposición de matriz extracelular y la acumulación de fibroblastos, principalmente miofibroblastos, causando la pérdida progresiva de las células epiteliales que no permite al riñón restaurar su función (Liu,

2006). En otros modelos de daño renal, se ha informado que la disminución en la biogénesis mitocondrial es un factor clave en la evolución de la ERC y de su transición a fibrosis (Aparicio-Trejo et al., 2019a; Briones-Herrera et al., 2020). Aunado a lo anterior, se ha informado que las alteraciones en el metabolismo lipídico se encuentran presentes desde el día uno posterior a la obstrucción, caracterizado por la deposición de lípidos y la disfunción en la β-oxidación que en conjunto contribuyen al proceso fibrótico (Kang et al., 2015; Okamura et al., 2009).

El sulforafano (SFN) es un isotiocianato derivado de alimentos crucíferos, entre los que se encuentran el brócoli, la coliflor y la col (Li, 2012). El SFN tiene propiedades anticancerígenas, anti-inflamatorias y es un potente antioxidante (Guerrero-Beltrán et al., 2012; Keum et al., 2004). Como antioxidante, el SFN es reconocido por ser un inductor del factor 2 relacionado con el factor nuclear eritroide 2 (Nrf2), desencadenando la respuesta antioxidante (Li et al., 2020). Adicionalmente, el SFN ha sido descrito como un inductor de la biogénesis mitocondrial, pues potencía los niveles del coactivador del receptor gamma 1-alfa activado por el proliferador de peroxisomas (PGC-1α), así como de los factores nucleares respiratorios 1 (NRF1) y 2 (NRF2) (Briones-Herrera et al., 2020; Li et al., 2020). En modelos de enfermedades renales, se ha informado que el SFN es capaz de atenuar el daño inducido por nefrotóxicos como el ácido maleico y el arsénico; en nefropatía inducida por el uso de agentes de contraste y en enfermedades renales crónicas que incluyen a la nefropatía diabética y al daño por OUU (Briones-Herrera et al., 2018, 2020; Chung et al., 2012; Thangapandiyan et al., 2019; Zhao et al., 2016). En el modelo de OUU, se informó que el uso del SFN disminuye la inflamación y la fibrosis al promover la activación de Nrf2, lo cual disminuye el estrés oxidante mitocondrial, sugiriendo que el SFN podría tener un papel importante en la restauración de la homeostasis mitocondrial (Chung et al., 2012). Adicionalmente, el SFN mejora el metabolismo de los lípidos, evitando su acumulación en modelos de nefropatía diabética (Li et al., 2020). Aunque se ha sugerido un papel mitocondrial del SFN en el modelo de OUU, no está claro si este antioxidante disminuye la lesión renal mediante la modulación de la homeostasis mitocondrial a través de la inducción de

la biogénesis mitocondrial. Aún más, no se ha explorado el papel de SFN en el metabolismo de los lípidos durante la obstrucción. Por lo tanto, planteamos la hipótesis de que SFN podría disminuir el daño renal al promover la biogénesis mitocondrial, mejorar el sistema de transporte de electrones (STE) e incluso regular la mitofagia, la autofagia y el metabolismo de los lípidos en el modelo de OUU.

3.1. Fisiopatología del riñón

El riñon es el segundo órgano con mayor demanda energética después del corazón y recibe aproximadamente 25% del gasto cardiaco mediante la arteria renal (Bhargava & Schnellmann, 2017). La unidad funcional del riñón es la nefrona. Un adulto posee posee alrededor de 2 millones de nefronas en cada riñón, siendo ésta la encargada del filtrado, por lo que se relaciona con los capilares provenientes de la arteria aferente, que forman un ovillo llamado glomérulo y la relación se da a través de la cápsula glomerular. La nefrona posee otros segmentos morfológios llamados glomérulo, túbulo contorneado proximal, asa de Henle, túbulo contorneado distal y túbulo colector, los cuales llevan a cabo funciones de filtración, reabsorción y secreción (Matovinović, 2009). El glomérulo está formado de tres membranas que forman la barrera de filtración glomerular y es el segmento de la nefrona que lleva a cabo la filtración del plasma sanguíneo en el cual se obtiene el ultrafiltrado (Nielsen et al., 2012). La primera membrana es un epitelio fenestrado constituido por células que forman poros de un diámetro de 70-100 nm cuya función es evitar el paso de células que rebasen este tamaño como las células sanguíneas y las que posean carga negativa (Fogo et al., 2014). La segunda membrana tiene como función evitar el paso de moléculas cargadas negativamente y la tercera y última membrana forma las prolongaciones de los podocitos conocidas como pedicelos, los cuales se entrelazan entre sí y se enrollan alrededor de los capilares glomerulares y forman ranuras de filtración de 25-60 nm (Fogo et al., 2014; Nielsen et al., 2012). En el túbulo proximal (TP) se lleva a cabo la mayor parte de los procesos de reabsorción, proceso en el cual el sodio, es un factor importante actuando como un cotransportador. La reabsorción se refiere al movimiento de solutos (principalmente por ósmosis). desde el lumen tubular al plasma. En el TP se

reabsorbe principalmente glucosa, amino ácidos y sales minerales (Figura 1). Además, el TP se constituye de dos regiones, una contorneada y una recta, siendo ésta última la que se dirige a la médula. Los TP desempeñan un papel destacado en la filtración de la orina, pues reabsorben dos tercios del volumen de filtrado y recuperan muchos compuestos provenientes de la orina (Stormark et al., 2007).

Procesos de reabsorción en la nefrona
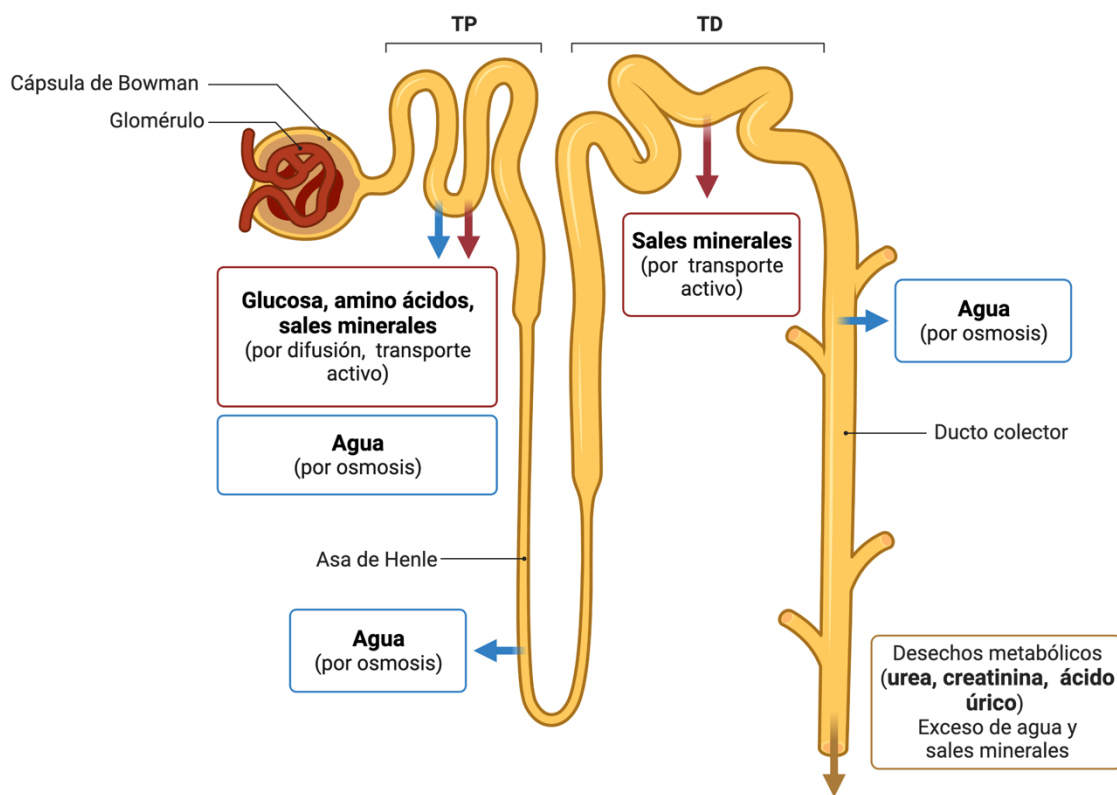
Figura 1. Procesos de reabsorción de la nefrona. Se muestran las porciones en las que se divide la nefrona y los procesos que se lleven a cabo en cada región. Las flechas representan a la absorción, de las cuales las flechas azules muestran la reabsorción por ósmosis y las flechas rojas por transporte activo. La flecha dorada indica la salida del filtrado. TP: túbulo proximal, TD:túbulo distal. Imagen modificada de Biorender.

En el asa de Henle se reabsorbe principalmente agua, mientras que el túbulo distal (TD) es impermeable al agua y en el que se lleva a cabo la reabsorción de sales minerales por transporte activo. El TD también posee una sección cortorneada en

la que se realiza la reabsorción del calcio para impulsar la actividad de la bomba Ca^{2+}-ATPasa. En la orina se eliminan principalmente desechos provenientes del metabolismo como urea, creatinina y ácido úrico, el exceso de agua y sales minerales.

3.2. Enfermedad renal crónica

Aproximadamente el 10% de la población a nivel mundial padece ERC, equivalente a 843.6 millones de personas, con una mayor prevalencia en la población de edad avanzada, mujeres y con factores de riesgo como hipertensión y diabetes (Kovesdy, 2022). La ERC es considerada una de las causas de muerte a nivel mundial. La mortalidad global atribuida a la ERC para todas las causas y todas las edades incrementó un 41.5% desde el año 2013 al 2017, ocupando el lugar 12 en mortalidad; sin embargo, se ha estipulado que para el año 2040 la ERC pasará a ser la quinta causa de muerte a nivel mundial (Foreman et al., 2018). De acuerdo a la kidney disease improving global outcomes (KDIGO, por sus siglas en inglés), la ERC se define como la disminución en la tasa de filtración glomerular (TGF) (<60 ml/min/1.73 m^2) y la presencia de albuminuria por un periodo mayor de 3 meses (Levey & Coresh, 2012). Ambos son los factores establecidos para evaluar la función excretora renal y la disfunción de la barrera renal, respectivamente y los cuales se utilizan para clasificar a la ERC en cinco estadíos (o grados) (Tabla 1).

Tabla 1. Clasificación de la enfermedad renal crónica

			Categorías de albuminuria persistente				
			A1 Normal a moderadamnete incrementada < 30 mg/g < 3 mg/mmol	A2 Moderadamnete incrementada 30-300 mg/g 3-30 mg/mmol	A3 Severamente incrementada > 300 mg/g > 30 mg/mmol		
Categorías de la TFG (ml/min/1.73 m²)	**G1 Normal o alto >90**						Bajo riesgo
	G2 Ligeramente disminuida	60-89					Riesgo moderadamente incrementado
	G3a Ligera a moderadamente disminuida	45-59					Alto riesgo
	G3b Moderada a severamente disminuida	30-44					Riesgo muy alto
	G4 severamente disminuida	15-29					
	G5 Falla renal	<15					

Modificada de Romagnani, et al. (Romagnani et al., 2017). Abreviaturas: G=grado, A=albuminuria

La ERC puede resultar de varios episodios agudos, consecutivos o no, que causan una disminución en el número de nefronas, las unidades funcionales del riñón. Aunque durante los primeros insultos agudos, las nefronas remanentes son capaces de recompensar la pérdida de nefronas, cambios hemodinámicos, vasculares e inflamatorios conllevan a una mayor pérdida de éstas, lo cual produce cambios a largo plazo, causando la pérdida progesiva de la función renal (Meguid El Nahas & Bello, 2005).

La mitocondria es el mayor organelo productor de energía de la célula y el riñón es el segundo órgano con mayor demanda energética en el TP, para lo cual un mayor número de mitocondrias es requerido (Forbes, 2016). Hoy en día es ampliamente aceptado que la función renal depende principalmente de la mitocondria y de su homeostasis, y que la disfunción mitocondrial desencadena los procesos patológicos que favorecen la progresión de la ERC. Estos procesos patológicos comprenden el estrés oxidante, la inflamación, la muerte celular, el proceso fibrótico y la transición epitelio-mesenquima (Hallan & Sharma, 2016). Muchos autores han sugerido que las alteraciones mitocondriales son relevantes en la ERC y que de éstas depende el curso de la enfermedad; así el uso de marcadores mitocondriales podría ser una excelente estrategia para entender la génesis y la progresión de la ERC, así como el proceso fibrótico (Braga et al., 2022; Irazabal et al., 2022; Zhang et al., 2021).

3.2.1 Alteraciones mitocondriales en la enfermedad renal crónica

Los principales factores que causan la ERC son la diabetes y la hipertensión; sin embargo, otras causas incluyen varios episodios agudos inducidos por periodos de isquemia, los nefrotóxicos, la sepsis, la nefropatía obstructiva, entre otros (Webster et al., 2017). Todos ellos desencadenan cambios hemodinámicos y procesos de hipertrofia en las nefronas, promoviendo la sobreproducción de especies reactivas del oxígeno (ERO) y la subsecuente generación de estrés oxidante; la reprogramación metabólica, la inflamación, la muerte celular y el desarrollo de fibrosis (Irazabal et al., 2022; Ruiz-Ortega et al., 2020). Además, la pérdida progesiva en el número de nefronas induce hipertrofia en las nefronas remanentes

debido al aumento en su masa y en la sobrecarga de trabajo en la reabsorción de solutos, principalmente sodio, lo cual promueve un incremento en los requerimientos de adenosin trifosfato (ATP) (Schnaper, 2014). Entonces, la demanda de ATP aumenta significativamente desencadenando disfunción de la mitocondria, característico de las ERC (Hallan & Sharma, 2016). Aunque los mecanismos que promueven el desarrollo de la ERC no son siempre los mismos, hay un consenso en que el daño mitocondrial juega un papel esencial en el desarrollo y evolución de la ERC, y su posterior progresion a enfermedad renal en estado terminal (Forbes & Thorburn, 2018; Jiang et al., 2019).

La producción de ATP en el riñón es sostenida principalmente por la oxidación de los ácidos grasos de cadena larga en la mitocondria en un proceso llamado β-oxidación (Bhargava & Schnellmann, 2017). Por lo anterior, la disminución de la β-oxidación debido a las alteraciones mitocondriales en la ERC desencadena la acumulación de lípidos y, en consecuencia, la generación de estrés oxidante y la activación de procesos inflamatorios y fibróticos (Herman-Edelstein et al., 2014; Jiménez-Uribe et al., 2021).

De hecho, varios autores han señalado a la reprogramación metabólica como un proceso de "rescate" en el que se intenta sostener la cantidad de ATP, favoreciendo la glicólisis sobre la fosforilación oxidativa (Li et al., 2021; Martínez-Klimova et al., 2020). Aunado a lo anterior, se han descrito alteraciones en el ciclo de Krebs, induciendo cambios en la generación de metabolitos, así como en el soporte de la cadena de transporte de electrones y, por lo tanto, en la fosforilación oxidativa. Por otro lado, la pérdida de la homeostasis mitocondrial es un proceso escencial de la ERC y mecanismos como la dinámica, la biogénesis y la mitofagia están desregulados (Aparicio-Trejo et al., 2017; Jiménez-Uribe et al., 2021; Ling et al., 2019). Todas estas alteraciones van acompañadas de la generación de ERO mitocondriales (EROmt) que favorecen aun más la disfunción mitocondrial durante la ERC. En la Figura 1 se presenta un esquema en el que se observan las alteaciones mitocondriales comunmente observadas durante la ERC.
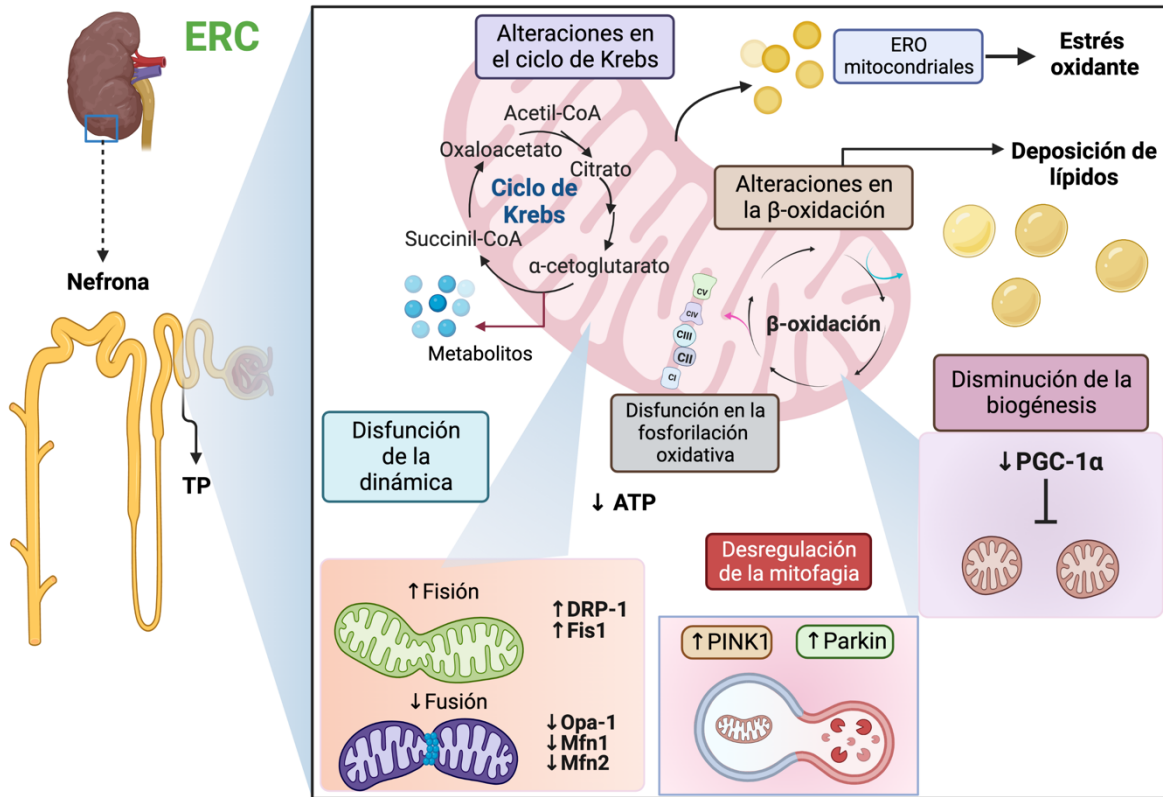
Figura 2. Alteraciones mitocondriales en el túbulo proximal (TP) de la nefrona durante la enfermedad renal crónica (ERC). El aumento en los marcadores de fisión: fisión 1 (FIS1) y de la proteína relacionada con la dinamina 1 (DRP1), y una disminución en los marcadores de fusión: la proteína de atrofia óptica 1 (Opa-1), mitofusina 1 (Mfn 1) y mitofusina 2 (Mfn2) son característicos de la disfunción de dinámica mitocondrial. Además, las alteraciones en el ciclo de Krebs y en la β-oxidación promueve el aumento o disminución en los metabolitos y a la deposición de lípidos, respectivamente. Ambos contribuyen a la disfunción de la fosforilación oxidativa, generando especies reactivas del oxígeno (ERO) mitocondriales. La desregulación de la mitofagia evita la eliminación de mitocondrias dañadas y la disminución del receptor gamma activado por el proliferador de peroxisomas coactivator-1 alpha (PGC-1α) previene la biogénesis mitocondrial, reduciendo la producción de adenosin trifosfato (ATP). PINK1: quinasa 1 inducida por fosfatidilinositol-3,4,5-trisfosfato 3-fosfatasa, Parkin: E3 ubiquitina-proteína ligasa parkin. TP: túbulo proximal. Imagen creada con Biorender.

3.2.2 Alteraciones en la biogénesis y la dinámica mitocondrial

Además de la bioenergética, la homeostasis de la mitocondria depende de la coordinación entre la dinámica mitocondrial que incluye a los procesos de fusión y fisión, así como de la biogénesis mitocondrial (Liesa & Shirihai, 2013). La fisión

consiste en la división de una mitocondria, o una parte de ella, y sucede cuando hay algún tipo de daño. Por su parte, la fusión consiste en la unión de dos mitocondrias para potenciar los requerimientos necesarios de ATP. La fisión y la fusión son reguladas por proteínas que se localizan en la mitocondria: la proteína relacionada con la dinamina 1 (DRP-1) y proteína de fisión 1 (FIS1) para la fisión y la proteína de atrofia óptica 1 (OPA1), mitofusina (Mfn) 1 y 2 para la fusión (Brooks et al., 2009; Liesa & Shirihai, 2013). En condiciones normales, existe un balance en ambos procesos y cualquier alteración en ellos o la sobreactivación de uno sobre el otro, induce anormalidades que impactan en la estructura y la función mitocondrial (Avila-Rojas et al., 2020; Fontecha-Barriuso et al., 2020; Reyes-Fermín et al., 2019). En la ERC, se ha descrito que la fisión está altamente regulada sobre la fusión mitocondrial, debido a que hay un aumento en los niveles de DRP-1 y FIS1, y una disminución en OPA1, Mfn1 y Mfn2, causando la sobreproducción de ERO y la reducción en el potencial de membrana mitocondrial ($\Delta\Psi$), lo cual resulta en mitocondrias aberrantes y disfuncionales. Además, los altos niveles de DRP-1 inducen apoptosis y la alta regulación de los marcadores de fibrosis, sugiriendo que la alta regulación del proceso de fisión contribuye al proceso fibrótico (Li et al., 2020).

Existe un consenso sobre que las alteraciones en estas proteínas conducen a la pérdida de la homeostasis mitocondrial. Además, los estudios de microscopía electrónica de transmisión (MET) realizadas en las mitocondrias revelan que en la ERC hay un aumento en la fisión debido a que las mitocondrias se observan alargadas y por lo tanto, son disfuncionales (Chen et al., 2013; Wang et al., 2020). La pérdida de la dinámica mitocondrial también se hace evidente por los bajos niveles de ATP, evaluados por el consumo de oxígeno durante la fosforilación oxidativa (Wang et al., 2020).

La masa mitocondrial es regulada por el receptor gamma activado por el proliferador de peroxisomas coactivator-1 alpha (PGC-1α), el cual controla el proceso de biogénesis mediante la transcripción de los factores nucleares de respiratorios

nucleares (NRF) 1 (NRF1) y 2 (NRF2) (Irrcher et al., 2009). Además, PGC-1α regula la expresión del factor de transcripción mitocondrial A (TFAM) para aumentar el número de copias del ácido desoxirribonucleico mitocondrial. La activación de PGC-1α es regulada por la proteína adenosin monofosfato quinasa (AMPK), la cual detecta los bajos niveles de ATP, induciendo su activación y posteriormente la fosforilación de PGC-1α para promover la biogénesis mitocondrial y aumentar la producción de ATP (Irrcher et al., 2009). Sin embargo, se han documentado bajos niveles de ARNm de PGC-1α y de AMPK durante la ERC (Hallan & Sharma, 2016). Además, se ha observado una disminución en los niveles de TFAM, NRF1 y NRF2, sugiriendo una disminución en la biogénesis (Jiménez-Uribe et al., 2021). Los bajos niveles de estas proteínas podrían deberse al exceso de estrés oxidante en la célula (Nishikawa et al., 2000) debido a que el estrés oxidante reduce los niveles de AMPK, desactivándola y promoviendo una disminución en la masa y en el metabolismo mitocondrial (Ren et al., 2021).

Aunque las proteínas que participan en la biogénesis mitocondrial no son propiamente de la mitocondria, excepto por TFAM, éstas son necesarias para ejercer un control de calidad sobre la misma, así su desregulación podría considerarse un marcador mitocondrial. Lo anterior podría explicarse debido a que comúnmente en la ERC, los bajos niveles de PGC-1α contribuyen a la acumulación de lípidos pues estas proteínas regulan genes que participan en la β-oxidación (Briones-Herrera et al., 2018). Aunado a lo anterior, la desregulación de PGC-1α disminuye los niveles de la sirtuina 3 (SIRT3), una desacetilasa localizada en la mitocondria que está involucrada en la biogénesis, la regulación del metabolismo mitocondrial y la fibrosis (Zhang et al., 2021). Además, la deleción de SIRT3 en la nefropatía diabética está relacionada con la reprogramación metabólica hacia la glicólisis debido a que la deficiencia de SIRT3 induce la translocación de la piruvato cinasa M2 al núcleo para promover la expresión de enzimás glicolíticas (Srivastava et al., 2018). Además, la SIRT3 regula la vía del factor de crecimiento transformante β1 (TGF-β1), impidiendo su regulación, lo cual ha sido demostrado debido a que el bloqueo de SIRT3 induce fibrosis (Chen et al., 2015). De acuerdo a lo anterior,

SIRT3 participa en la desacetilación de algunas proteínas mitocondriales y su deleción está relacionada con el aumento en los marcadores de fibrosis (Zhang et al., 2021). Por lo tanto, la desregulación de biogénesis y la dinámica mitocondrial son un indicador de la pérdida de la homeostasis y alteraciones en el metabolismo mitocondrial, debido a las alteraciones en las vías metabólicas mitocondriales, contribuyendo al desarrollo de fibrosis.

3.2.3. Alteraciones en el metabolismo lipídico en la ERC

Las alteraciones en el metabolismo de lípidos han sido reportadas en la ERC, como el caso de la alta excreción de palmitato a través de la orina de pacientes no diabéticos (Hallan & Sharma, 2016). Además, se ha informado la acumulación de triglicéridos en el modelo de OUU desde el día uno después de la obstrucción (Tan et al., 2020). Ciertamente, uno de los mecanismos que promueven las alteraciones en el metabolismo de los lípidos es la disfunción en la β-oxidación, la cual ha sido descrita durante la ERC. Adicionalmente, se ha demostrado que las enzimas que participan en este proceso están disminuidas (Aparicio-Trejo, Rojas-Morales, et al., 2020; Opazo-Ríos et al., 2020). Por ejemplo, un análisis transcriptómico reveló que la enzima acil-CoA deshidrogenasa 10 está disminuida en pacientes con nefropatía diabética (Tan et al., 2020). Además, en el modelo de nefrectomía 5/6 [el cual consiste en la ablación de un riñón y ligadura de suficientes ramas vasculares (dependientes de la arteria renal) del otro, logrando la inutilización por infarto de las 2/3 partes (o de la parte que se pretenda) del riñón remanente], la enzima acetil deshidrogenasa de cadena media presentó bajos niveles 28 días después de la nefrectomía, comparados con el grupo sham (Fedorova et al., 2013). En un estudio que evaluó la disfunción de la β-oxidación curso temporal en este modelo se describió que ésta disminuye desde el día dos hasta el día 28 después de la nefrectomía, sugiriendo que la disfunción empieza desde tiempos tempranos (Aparicio-Trejo, Rojas-Morales, et al., 2020; Prieto-Carrasco et al., 2021). Lo anterior podría atribuirse a la desregulación de las enzimas carnitina palmotoil transferasa 1 (CPT1) y 2 que permiten la entrada de los ácidos grasos a la membrana mitocondrial externa y a la membrana mitocondrial interna, respectivamente (Feingold et al., 2008; Idrovo et al., 2012; S. M. S. Moosavi et al.,

2010; Prieto-Carrasco et al., 2021). Por lo tanto, la disminución de estas enzimas impide la correcta oxidación de los ácidos grasos, lo cual podría inducir su acumulación. En concordancia con esos datos, en un estudio realizado por Afshinnia y colaboradores (Afshinnia et al., 2018), los niveles de ácidos grasos libres de cadena larga estuvieron elevados, mientras que los niveles de CPT1 fueron bajos. Importantemente, los bajos niveles de la isoforma A de CPT1 también se asociaron con el desarrollo de fibrosis en el modelo de OUU, en la ERC inducida por adenina y en la nefropatía inducida por ácido fólico (Miguel et al., 2021). En contraste, la sobreexpresión de esta isoforma disminuyó la inflamación y atenuó los niveles de TGF-β1 (Miguel et al., 2021). La fibrosis inducida por las alteraciones en la β-oxidación se deben principalmente a la acumulación de lípidos en forma de "gotas lipídicas", las cuales generan lipotoxicidad (Kang et al., 2015; Kume et al., 2007; Prieto-Carrasco et al., 2021). La fibrosis inducida por la lipotoxicidad también se debe a la sobreexpresión del receptor CD36 que se encarga del consumo de ácidos grasos (Souza et al., 2016). Por ejemplo, en el modelo de OUU los niveles de CD36 aumentaron al día diez después de la obstrucción (Souza et al., 2016), relacionado con la acumulación de lípidos en los TP de los riñones obstruídos y los altos niveles de α-SMA, TGF-β1 y colágeno IV (Col IV), comparados con los no obstruídos (Jiménez-Uribe et al., 2021). Su deleción, por su parte, dismininuyó la acumulación de miofibroblastos intersticiales (Okamura et al., 2009). La acumulación de lípidos y la sobreexpresión de CD36 también es evidente en los riñones de pacientes que sufren nefropatía diabética, causando daño renal e inflamación (Yang et al., 2018).

Considerando la inflamación, su alta regulación inducida por CD36 podría ser atribuida a la estimulación del receptor mediada por la interleucina-1 beta (IL-1β). Estos datos sugieren que CD36 podría ser un candidato para el desarrollo de nuevos tratamientos en los pacientes en los que se evidencien los altos niveles de lípidos.

Debido a que la disfunción en la β-oxidación está relacionada con la depleción de ATP en el TP, energía requerida para transportar el 67% del filtrado glomerular, las

células epiteliales de esta región de la nefrona son más suceptibles a cambios en los niveles de ATP y su acumulación se ha relacionado con la reprogramación metabólica, promoviendo la síntesis de lípidos (Aparicio-Trejo, Avila-Rojas, et al., 2020; Y. Li et al., 2021; Simon & Hertig, 2015). Además, periodos crónicos de isquemia o los altos niveles de glucosa activan al factor inducible por hipoxia 1-alfa (HIF-1α), favoreciendo aun más el flujo glicolítico (Aranda-Rivera et al., 2021; Bhargava & Schnellmann, 2017). Importantemente, la activación de HIF-1αtambién daña a la mitocondria a través de la reducción de la piruvato deshidrogenasa y la disminución del potencial de membrana. Por lo tanto, las alteraciones en la β-oxidación promoviendo la acumulación de lípidos junto con la alta regulación de factores que favorecen el proceso glicolítico son mecanismos necesarios para promover la ERC.

Las alteraciones en la β-oxidación pueden traer como resultado la síntesis de ácidos grasos y de lípidos *de novo*. Alteraciones en las enzimas como la síntasa de los ácidos grasos (FAS) y acetil coA carboxilasa (ACC), enzima que se encarga de la producción de palmitato, se han encontrado sobreexpresadas en modelos de ERC (Gai et al., 2019; Guebre-Egziabher et al., 2013). Se ha descrito que Nrf2 es un regulador importante del metabolismo de lípidos debido a que éste es capaz de inducir la activación de CPT1 y inducir la fosforilación de ACC, causando su inactivación (Li et al., 2020). Además, Nrf2 fue capaz de regular la expresión de CD36 (Ishii et al., 2004). Por lo tanto, la activación de Nrf2 en la ERC podría ser una buena estrategia para la regulación del metabolismo lipídico.

4. Objetivo general

Determinar si el efecto protector del sulforafano es mediante la promoción de la biogénesis mitocondrial en el modelo de OUU

4.1 Objetivos particulares

En el modelo de OUU:

1. Determinar si el sulforafano disminuye los marcadores de daño renal y de fibrosis.

2. Evaluar si el sulforafano induce biogénesis y el aumento de los marcadores de masa mitocondrial.

3. Determinar si las alteraciones ultraestructurales de la mitocondria mejoran con el sulforafano.

4. Evaluar las alteraciones en la síntesis de lípidos.

5. Determinar si el mejoramiento de la biogénesis mitocondrial con el sulforafano, disminuye la síntesis y acumulación de lípidos.

6. Evaluar el mejoramiento de la dinámica mitocondrial y la autofagia por el sulforafano.

5. ANTECEDENTES

5.1 Nefropatía obstructiva y el modelo de obstrucción unilateral del uréter

La nefropatía obstructiva es un problema significante de salud a nivel mundial que afecta predominantemente a neonatos y niños, así como adultos mayores de 65 años. Esta enfermedad se caracteriza por un bloqueo en el flujo de la orina que causa hidronefrosis y que en última instancia conduce a falla renal (Chevalier, 2008). Además, dada la naturaleza silenciosa de la enfermedad, la nefropatía obstructiva favorece el desarrollo de la ERC (Girardi & Martin, 2015). El modelo de OUU es un modelo *in vivo* que mimetiza fibrosis renal asociada con la nefropatía obstructiva crónica, el cual puede ser desarrollado en un periodo corto de tiempo (Chevalier et al., 2009). Este modelo consiste en la ligación del uréter izquierdo con un hilo de seda y a este riñón del uréter ligado se le denomina riñón obstruido, mientras contralateral no sufre ninguna manipulación y en algunas ocasiones es utilizado como control (Martínez-Klimova et al., 2019).

En la obstrucción, el flujo estacionario de orina provoca el aumento de la presión hidrostática, que inicialmente dilata el túbulo colector. Luego, esta presión se transmite de regreso a los túbulos distal y proximal. El aumento de la presión del TP tiene dos efectos: la disminución de la tasa de filtración glomerular (TFG) y el daño por estiramiento mecánico en las células epiteliales tubulares (Figura 3).
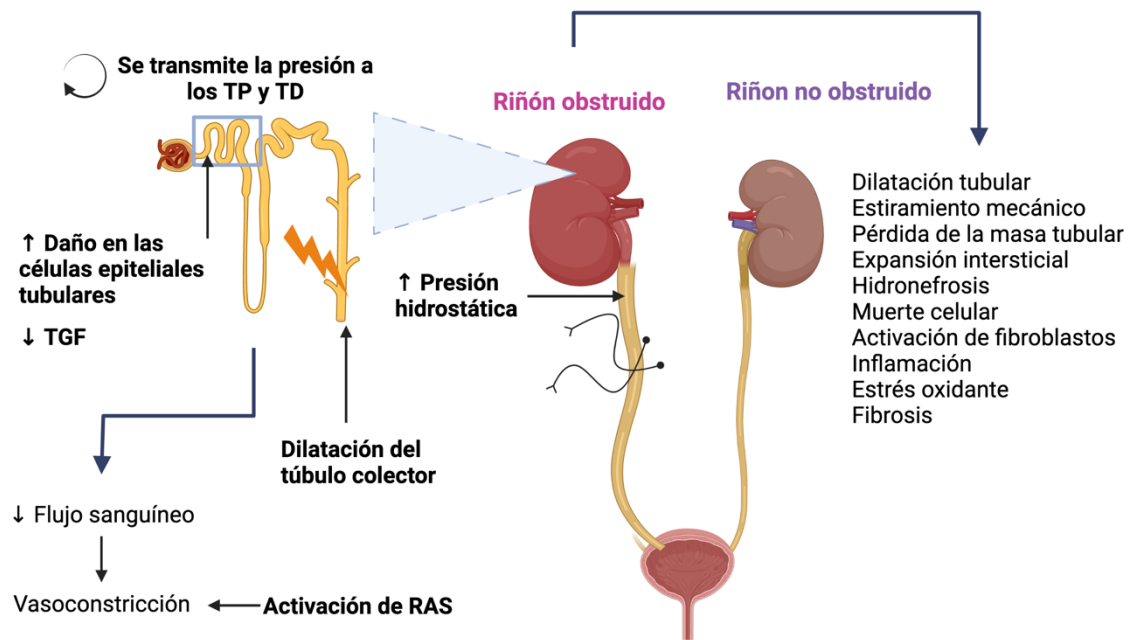
Figura 3. Mecanismos inducidos durante la obstrucción unilateral del uréter (OUU). El estancamiento de la orina causa la dilatación del túbulo colector lo cual aumenta la presión hidrostática que se transmite de regreso a los túbulos proximales (TP) y distales (TD). En el TP se genera daño a las células epiteliales y hay una caída de la tasa de filtración glomerular (TFG). El aumento de la presión hidrostática es debido a la activación del sistema renina angiotensina (RAS) lo cual causa vasoconstricción, mientras que la caída del flujo sanguíneo en los otros segmentos tambien genera vasoconstricción. Figura creada con Biorender.

En las células epiteliales, el aumento de la presión hidrostática desencadena la acivación del sistema renina angiotensina (RAS), mediado por la la sobreproducción de angiotensina II (Ang II). Ang II es secretada por el riñón bajo condiciones de aumento de presión arterial o cuando hay unadisminución de sodio . Ang II activa a las nicotinamida adenina dinucleótido fosfato (NADPH) oxidasas (NOXs), lo cual induce la producción de ERO. La producción de ERO genera estrés oxidante e inflamación que causa muerte celular por apoptosis o necrosis (Ucero et al., 2010). Estos mecanismos activan a los miofibroblastos desde fibroblastos residentes del riñón que se encargan de reemplazar la pérdida de las células epiteliales a través

de la producción de matriz extracelular (MEC), desencadenando la fibrosis progresiva (LeBleu et al., 2013; Xia et al., 2018). Los mecanismos que se han informado que promueven el desarrollo de la ERC en el modelo de obstrucción son el estrés oxidante, la inflamación, la disfunción mitocondrial, la muerte celular, la fibrosis (Figura 3).

6. JUSTIFICACIÓN

En el modelo de OUU, la disfunción mitocondrial participa en la génesis y progresión de la enfermedad. Por lo tanto, determinar las alteraciones mitocondriales y cómo éstas inducen la progresión de la ERC ha sido el objetivo de muchos grupos de trabajo, incluido el nuestro. De acuerdo con recientes estudios, la disminución en la biogénesis promueve la disfunción mitocondrial llevando a cabo los procesos inflamatorios, de estrés oxidante y fibróticos. Aun más, las alteraciones en el metabolismo de los lípidos han sido previamente informadas y se encuentran estrechamente relacionadas con la disminución de las proteínas de la biogénesis como PGC-1α, NRF1 y NRF2. En este sentido, el uso de compuestos que potencien la biogénesis mitocondrial resulta ser una estrategia que podría atenuar el daño renal causado por la obstrucción. Entre estos compuestos se encuentra el SFN, que es un un inductor de PGC-1α. En el presente trabajo, se evaluó el efecto del SFN sobre la biogénesis y si el mejoramiento de este proceso regula el metabolismo de los lípidos, evitando su acumulación en el riñón. La potenciación de la biogénesis reducirá el daño renal, la inflamación y la fibrosis.

7. HIPÓTESIS

El sulforafano protegerá del daño renal causado por la OUU al estimular la biogénesis mitocondrial

8. METODOLOGÍA

8.1 Reactivos

El D-/L-SFN se obtuvo de los laboratorios LKT (St. Paul, MN, EUA); el pentobarbital sódico se adquirió de Sedalphorte®, adquirido de Salud y Bienestar Animal S.A. de C.V. (CDMX, Mexico); el D-manitol, la sacarosa, el EDTA, el HEPES, la glicina, el BSA, el Tris, el NaCl, el EGTA, el NaF, el Na_3VO_4, el PMSF, el deoxicolato de sodio, el docecil sulfato de sodio (SDS), la acrilamida, el ácido 5-tio-2-nitrobenzoico (TNB), la decil ubiquinona (DUB), el NADH, la antimicina A, el KCN, la azida sódica se adquirieron de Sigma-Aldrich (St. Louis, MO, EUA); el coctel de inhibidor de proteasas se adquirió de Roche Applied Science (Mannheim, Alemania); los anticuerpos secundarios fluorescentes 680RD, 926-68074 800RD, 926-32214; 680RD, 926-68073; 800RD, 926-32212; 800CW, 926-32213 fueron adquiridos de LI-COR Inc. (Lincoln, NE, EUA). Fluoruro de polivinilideno (PVDF) (Merck Millipore, Massachusetts, EUA); Estuche comercial para triglicéridos (TGs) (Triglycerides, Sekisui Diagnostics, Burlington, MA, EUA),

8.2 Estrategia experimental

El Comité Institucional para el Cuidado y Uso de Animales de Laboratorio (CICUAL) aprobó el protocolo experimental en la "Facultad de Química de la Universidad Nacional Autónoma de México" (FQ/CICUAL/441/21). La investigación fue realizada de acuerdo a las guías de la Norma Oficial Mexicana (NOM-062-ZOO-1999). En total, 46 ratas macho Wistar fueron utilizadas con un peso inicial de 200-250 g, divididas en cuatro grupos: (1) ratas sham operadas, en las cuales la cirugía fue simulada sin la ligación del uréter; (2) ratas con obstrucción unilateral del uréter (OUU); (3) ratas con obstrucción unilateral del uréter administradas con sulforafano (OUU+SFN) y (4) ratas control que no sufrieron manipulación quirúrgica pero fueron tratadas con SFN. La cirugía de OUU se realizó por doble ligación del uréter izquierdo con hilo de sutura 3-0 y 2 cm abajo del riñón. El SFN se administró de forma intraperitoneal (i.p) empleando una dosis de 1 mg/kg. La dosis se SFN se seleccionó de acuerdo con estudios previos de nuestro grupo informados en el daño

renal inducido maleato y cisplatino (Briones-Herrera et al., 2018, 2020; Guerrero-Beltrán et al., 2010). El SFN se administró por cinco días, iniciando el segundo día después de la cirugía y finalizando un día antes del sacrificio (Figura 4). De la misma manera, el grupo de ratas que no sufrió manipulación quirúrgica fue tratado con SFN bajo el mismo esquema que el grupo de OUU+SFN. Las ratas fueron mantenidas en un ambiente de temperatura controlada, con ciclos de luz-oscuridad de 12 h y agua y alimento *ad libitum*. Ningún animal murió durante ni después de las cirugías. La eutanasia de los animales se llevó a cabo siete días después de la obstrucción utilizando pentobarbital sódico una dosis de 120 mg/kg. La disposición de residuos biológicos se realizó de acuerdo a la NOM-087-SEMARNAT-SSA1-2002. La distribución de los animales fue como sigue: para ensayos de inmunoblot y las actividades de los complejos del sistema de transporte de electrones (STE) y del ciclo de Krebs se utilizaron n=3-5 animales por grupo. Para los inmunoblots de proteínas mitocondriales y del metabolismo de los lípidos, una n=3 fue empleada. Para la determinación de triglicéridos (TG) se utilizaron una n=3-4 animales por grupo. Para los estudios de microscopías (histológicas y electrónicas) una n=3-4 por grupo. Algunos animales fueron excluidos por presentar datos atípicos. El número exacto de animales se indica en el pie de figura de cada experimento en la sección de resultados.
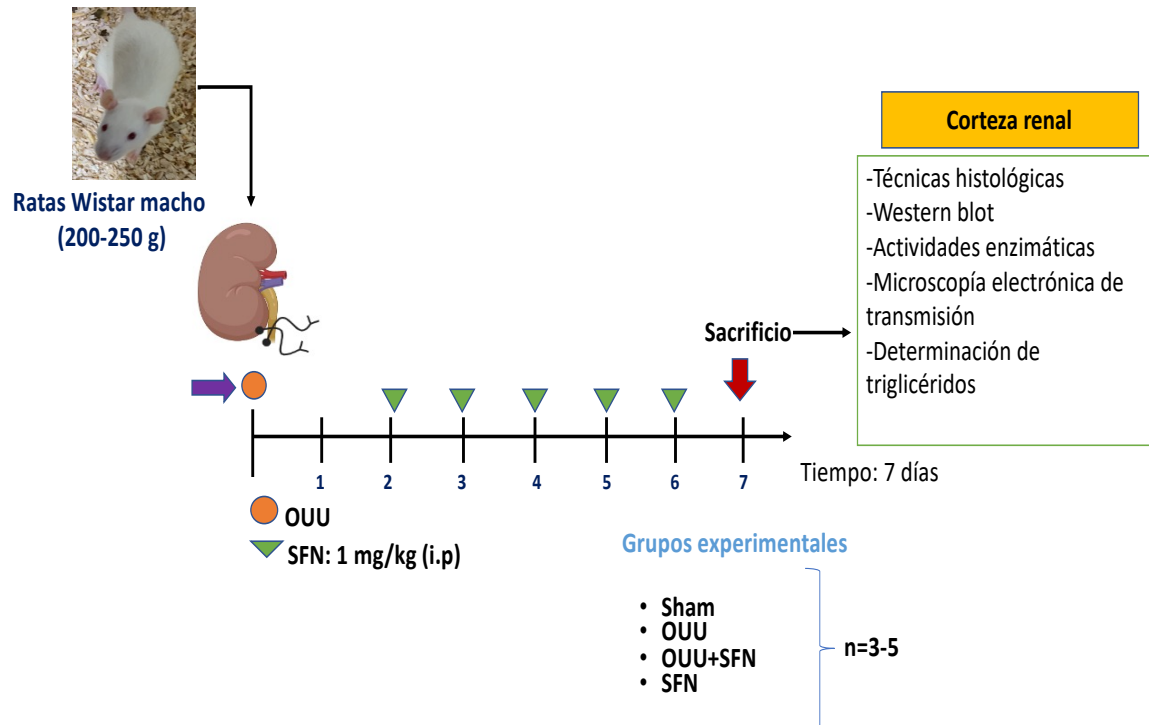
Figura 4. Diseño experimental. Un total de 46 ratas macho Wistar se dividieron en cuatro grupos: (1) Sham, en el cual la cirugía fue simulada sin ligación del uréter, (2) obstrucción unilateral del uréter (OUU), con doble ligación del uréter izquierdo, (3) OUU tratado con sulforafano (SFN) a una dosis de 1 mg/kg intraperitoneal (i.p.) (OUU+SFN) y (4) SFN, grupo que no tuvo ninguna manipulación quirúrgica pero fue administrado con SFN. El número para cada experimento fue de 3-5 por grupo (n=3-5). El número exacto de animales se especifica en el pie de figura de cada ensayo experimental.

8.2 Histología renal

Siete días después de la OUU, las ratas fueron eutanizadas y se obtuvo el riñón izquierdo que fue disectado longitudinalmente. Una mitad del riñón fue fijada por inmersión en 2-metilbutano a 0ºC, cubierto con solución crioprotectora y montados en portaobjetos. En seguida, los riñones fueron cortados en secciones seriadas de 8 µm en un criostato a -20°C (CM-1520; Leica Microsystems, Nussloch, Alemania) y después montados en cubreobjetos de vidrio para teñir. La morfología renal se evaluó con la tinción de hematoxilina y eosina (H&E) y la acumulación de lípidos con la tinción de rojo Nilo (Stuhr et al., 2022). Para esta última, las secciones fueron lavadas con PBS a pH 7.4 e incubadas 10 min en oscuridad con 2.5 µg/mL de rojo Nilo. El rojo Nilo se disolvió en PBS con 1% de acetona utilizando Vectashield® como medio de montaje. Las fotomicrografías fueron tomadas utilizando un lector

multimodo de imágenes celulares Cytation 5 (BioTek Instruments, Inc., Winooski, VT, USA). La cuantificación del rojo Nilo se realizó utilizando Fiji (Schindelin et al., 2012) por el software ImageJ (National Institutes of Health, Bethesda, MD, USA, https://imagej.nih.gov/ij/index.htm, consultado el 20 de julio de 2022) (Stuhr et al., 2022).

8.3 Aislamiento de mitocondrias renales

Las mitocondrias renales se aislaron de acuerdo a reportes previos de nuestro grupo (Aparicio-Trejo et al., 2019b). Brevemente, después de ser disectados, los riñones fueron cortados transversalmente en pequeños pedazos y enfriados por inmersión en amortiguador de aislamiento (D-manitol 225 mM, sacarosa 75 mM, EDTA 1 mM, HEPES 5 mM, BSA 0.1%, pH 7.4) a 4ºC y homogenizados empleando una trituradora de tejidos Potter Elvehjem de vidrio/teflón. Entonces, las mitocondrias fueron aisladas por centrifugación diferencial y los pellets se resuspendieron en 180 µL de amortiguador de aislamiento libre de BSA.

8.4 Extracción de proteínas

Para la extracción de proteínas totales, se pesó 100 mg de tejido renal y se homogenizó en 1 mL de amortiguador de radioinmuniprecipitación (RIPA): Tris-HCl 40 mM, NaCl 150 mM, EDTA 2 mM, EGTA 1 mM, NaF 5 mM, Na_3VO_4, PMSF 1 mM, deoxicolato de sodio al 0.5%, docecil sulfato de sodio (SDS) 0.1% a pH 7.6, suplementado con coctel de inhibidor de proteasas. El tejido fue homogenizado con ayuda de un politrón y centrifugado a 15 000 g por 10 min a 4ºC, y los sobrenadantes fueron recuperados. Para la cuantificación de la proteína total se empleó el método de Lowry de acuerdo a las instrucciones del fabricante (Waterborg & Matthews, 1984).

8.5 Western blot

Un total de 20-40 μg de proteínas fueron desnaturalizadas con amortiguador Laemli sample 6X (Tris-HCl 60 mM, SDS 2%, glicerol 10%, β-mercaptoethanol al 5%, azul de bromofenol al 0.01%, pH 6.8) y calentadas por 5 min. Las muestras se cargaron

en geles de SDS-poliacrilamida para la electroforesis. Posteriormente, las proteínas se transfirieron a membranas de PVDF que se bloquearon con leche sin grasa al 5% en TBS-tween al 0.1% durante 1 hora a temperatura ambiente. Las membranas fueron incubadas con las diluciones recomendadas de los anticuerpos que se presentan en la Tabla 2 toda la noche en agitación constante. Posteriormente, las membranas se incubaron con los anticuerpos secundarios acoplados a fluorescencia a una dilución de 1:15,000 durante 1 h 30 min a temperatura ambiente en oscuridad. Las bandas de las proteínas se detectaron usando fluorescencia en un escaner llamado Odyssey Sa (LI-COR Biosciences, Lincoln, NE, USA). La densidad de las bandas de las proteínas se analizó con el programa de acceso libre ImageJ studio. La cuantificación de las proteínas se expresó como unidades arbitrarias y se representó como cociente de las densidades de las proteínas de interés/control de carga. En algunos casos, una membrana fue utilizada para detectar más de una proteína. Para esto, las membranas fueron lavadas con solución desnudadora (glicina 100 mM, SDS 0.5% pH 2.5) durante 15 min en agitación constante y después se lavaron tres veces con TBS-T 0.1%. Después, las membranas fueron bloqueadas e incubadas con el anticuerpo correspondiente como se indicó anteriormente.

Tabla 2. Lista de anticuerpos utilizados

Anticuerpos	Nombre	Especie	# Catálogo	Casa comercial	Dilución
Anti-KIM1	Molécula de daño renal 1	Cabra	AF3689	R&D Systems	1:5000
Anti-IL-1β	Interleucina-1 beta	Hámster	503502	BioLegend	1:5000
Anti-α-SMA	Alfa-actina de músculo liso	Conejo	GTX10034	Genetex	1:2000
Anti-Col IV	Colágeno IV	Ratón	SAB4200500	Sigma aldrich	1:1000
Anti-PGC-1α	Coactivador gamma del receptor	Conejo	AB3242	Sigma aldrich	1:2000

	activado por el proliferador de peroxisomas (PGC)-1alfa				
Anti-NRF1	Factor nuclear respiratorio 1	Conejo	46743	Cell Signaling Technology	1:2000
Anti-VDAC	Canal de aniones dependiente de voltaje	Conejo	V2139	Sigma aldrich	1:2000
Anti-ANT	Translocator de nucleótidos de adenine	Conejo	Ab102032	Abcam	1:3000
Anti-ACO2	Aconitasa 2	Conejo	SC-130677	Santa Cruz Biotechnology	1:3000
Anti-OXPHOS	Cóctel de anticuerpos de fosforilación oxidativa total (OXPHOS) de roedores	Ratón	ab110413	Abcam	1:10000
Anti-DRP1	Proteína relacionada a dinamina 1	Conejo	sc-32898	Santa Cruz Biotechnology	1:2000
Anti-OPA1	Proteína de atrofia óptica 1	Cabra	Sc-30573	Santa Cruz Biotechnology	1:3000
Anti-MFN2	Mitofusina 2	Conejo	9482S	Cell Signaling Technology	1:2000
Anti-PINK1	Cinasa 1 inducida por PTEN	Conejo	Ab23707	Abcam	1:3000
Anti-Parkin	Parkin	Conejo	Ab15954	Abcam	1:2000
Anti-beclin	Beclina	Ratón	MAB5295	R&D Systems	1:3000
Anti-Bcl2	Linfoma de células B 2	Conejo	14-6992-82	Thermo fisher scientific	1:2000
Anti-p62	Secuetrosoma	Conejo	P0067	Sigma Aldrich	1:3000
Anti-LC3	Proteínas asociadas a microtúbulos	Conejo	L7543	Sigma Aldrich	1:3000

	1A/1B cadena ligera 3				
Anti-CD36	Clúster de diferenciación 36	Conejo	GTX55559	Genetex	1:1000
Anti-PPAR-α	Receptor alfa activado por el proliferador de peroxisomas	Conejo	Ab24509	Abcam	1:2000
Anti-CPT1	Carnitina palmitoiltransferasa 1	Conejo	Ab234111	Abcam	1:2000
Anti-FASN	Sintasa de los ácidos grasos	Conejo	GTX109833	Genetex	1:1000
Anti-DGAT1	Diacilglicerol O-aciltransferasa 1	Conejo	GTX48577	Genetex	1:1000
Anti-SREBP1	Proteína de unión al elemento regulador de esteroles 1	Conejo	GTX79299	Genetex	1:1000
Anti-GAPDH	Gliceraldehído 3-fosfato deshidrogenasa	Ratón	Ab8245	Abcam	1:5000

8.6 Actividades del ciclo de los ácidos tricarboxílicos (ciclo de Krebs)

Las actividades de la aconitasa 2 (ACO2) y citrato sintasa fueron evaluadas para determinar el efecto del SFN sobre el ciclo de Krebs. La actividad de la ACO2 fue evaluada en mitocondrias aisladas las cuales fueron obtenidas inmediatamente después del sacrificio. La actividad corresponde a la tasa de formación del producto intermediario cis-aconitato que se forma durante la reacción a 240 nm, como previamente lo describió Negrete-Guzmán (Negrette-Guzmán et al., 2015). La actividad de la citrato sintasa fue determinada al registrar en incremento de la absorbancia del aducto del TNB a 412 nm (Vela-Guajardo et al., 2017). Ambas

actividades fueron expresadas como nmol por minuto por miligramo de proteína (nmol/min/mg de proteína).

8.7 Actividades de los complejos mitocondriales del sistema de transporte de electrones

Las actividades de los complejos mitocondriales I (CI, NADH), II (CII, succinato deshidrogenasa), III (CIII, ubiquinol-citocromo c oxidorreductasa) y CIV (citocromo c oxidasa) se evaluaron espectrofotométricamente usando 20 μg de proteína total a 37ºC usando un Lector de microplacas Synergy-Biotek (Biotek Instruments, Winooski, VT, EUA.) como se informó anteriormente (Briones-Herrera et al., 2018). Brevemente, se rastreó al CI reduciendo la DUB a DUB reducida (DUBH$_2$) en una reacción acoplada con la reducción de DCPIP. Así, la actividad de CI fue proporcional a la desaparición de DCPIP oxidado a 600 nm en presencia de NADH 10 mM, antimicina A 2.5 μM y KCN 5 mM. Se restó la reacción no específica agregando rotenona 2.5 μM en un ensayo paralelo. La actividad de CII se evaluó de manera similar a la de CI, pero la reacción se realizó en presencia de succinato 400 mM, rotenona 2.5 μM y antimicina A 2.5 μM. La reacción no específica se obtuvo agregando malonato 2.5 μM. La actividad de CIII se determinó siguiendo la generación de la forma reducida de citocromo c a 550 nm empleando DUBH$_2$ 0.312 mM, en presencia de KCN 5 mM, rotenona 2.5 μM y citocromo c oxidado 1 mM. La reducción no específica del citocromo c se obtuvo mediante la adición de antimicina A 2.5 μM. La actividad de CIV se evaluó siguiendo la oxidación del citocromo c a 565 nm en presencia de KCN 5 mM, antimicina A 1 M y citocromo c reducido 1 mM. La oxidación no específica del citocromo c se determinó añadiendo azida sódica 1M. Todas las actividades se expresaron como nmol por minuto por miligramo de proteína (nmol/min/mg de proteína).

8.8 Determinación de triglicéridos en la corteza renal

La extracción de TGs intrarrenales fue levemente modificada del método de Folch (Folch et al., 1957). Cuidadosamente, 20-40 mg de corteza renal fueron homogenizadas en amortiguador de fosfatos (PBS) 1X frío y se determinó la

concentración de la proteína. Después, 1.5 mL de una mezcla cloroformo:metanol 2:1 se añadió a los homogenados y fueron centrifugados a 2050 x g durante 10 min a 4ºC. La fase orgánica fue separada, se secó y se disolvió con 200 µL de Tritón X-100 al 5%. Los TGs fueron determinados de acuerdo a las instrucciones del fabricante utilizando una curva estándar de glicerol y evaluados por ensayos coloriméticos en un lector multimodo híbrido (Sinergy H1, Biotek-Agilent, Santa Clara, CA, EUA). Los resultados fueron corregidos por miligramo de proteína.

8.9. Microscopía electrónica de transmisión (MET)

Se fijaron cubos de riñón de aproximadamente 1 mm^3 en glutaraldehído al 2.5% durante 1.5 h, se lavaron con amortiguador de fosfatos a pH 7,2 y se fijaron posteriormente con tetróxido de osmio al 0.5% durante 1 h. Posteriormente, los cubos se lavaron y se deshidrataron en series ascendentes de alcohol, se sumergieron en óxido de propileno durante 10 min y se incluyeron previamente en una mezcla de óxido de propileno/resina Epon 1:1 durante la noche. Finalmente, las piezas de tejido se embebieron en resina Epon a 60°C durante 24 h, y los bloques resultantes se utilizaron para obtener cortes semifinos de 300 nm de espesor teñidos con azul de toluidina para comprobar la presencia de la región de interés. Finalmente, se obtuvieron secciones ultrafinas seriadas de 60-90 nm de espesor y se contrastaron con acetato de uranilo al 4% durante 20 min y citrato de plomo al 1% durante 10 min. Las muestras se examinaron utilizando un microscopio electrónico de transmisión (JEM-1400 Plus, JEOL, Boston, MA, EUA).

8.10 Análisis estadísticos

Los datos se informaron como la media ± error estándar de la media (SEM). Los datos presentaron una distribución normal y se probaron mediante un análisis de varianza (ANOVA) de una vía con post-test de Tukey para comparar más de dos grupos. Un valor de p inferior a 0.05 se consideró estadísticamente significativo. El análisis de datos se realizó con Graph Pad Prism 7 (San Diego, CA, EUA).

9. RESULTADOS

9.1 Efecto del sulforafano sobre el daño renal en la obstrucción unilateral del uréter

Para determinar el daño renal causado por la OUU y su mejora con el SFN, evaluamos los niveles de la molécula de daño renal 1 (KIM-1) y la IL-1β. Se encontró que los niveles de ambas moléculas aumentan en el grupo de OUU. En el grupo de OUU tratado con SFN (OUU+SFN), los niveles de ambas proteínas no aumentan, mostrando una diferencia significativa entre el grupo de OUU y el grupo de OUU+SFN (Figura 5A, B). Se determinó además el efecto del SFN sobre la fibrosis renal y se encontró que los niveles de la actina de músculo liso alfa (α-SMA) y de colágeno IV (Col IV) incrementaron en el grupo de OUU y el tratamiento con SFN los disminuye (Figura 5C, D). En conjunto, estos datos revelan que el SFN protege en contra del daño renal y la fibrosis en el modelo de OUU.

Por su parte, la histología renal H&E reveló que la OUU desencadena la pérdida de la estructura tubular, caracterizada por la pérdida de células epiteliales, dilatación tubular, infiltración de leucocitos y presencia de tejido conectivo entre los túbulos, que disminuyeron debido al tratamiento con SFN. Ambos grupos OUU y OUU+SFN presentaron infiltración de leucocitos (Figura 5E). Por lo tanto, nuestros resultados sugieren que el SFN disminuye significativamente el daño renal en este modelo.
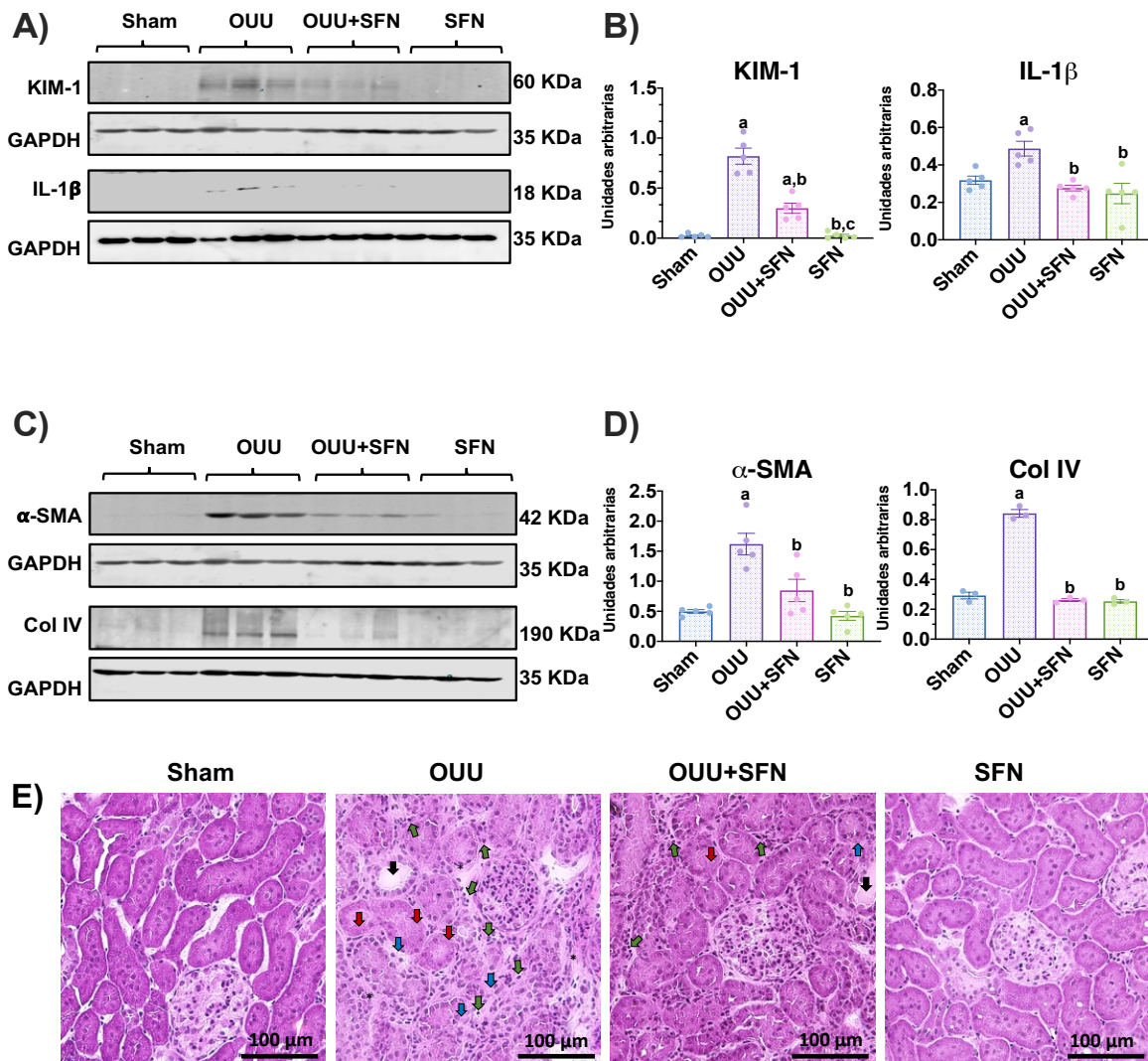
Figura 5. El sulforafano (SFN) disminuye el daño renal inducido por la obstrucción unilateral del uréter (OUU) durane siete días. A) El daño renal se determinó a través de los niveles de la proteína de daño renal (KIM-1). Los niveles de esta proteína aumentan significativamente en el grupo de OUU con respecto a los sham. e interleucina-1 beta (IL-1β). (C) Inmunoblot representativo y (D) análisis densitométrico de los marcadores fibróticos alfa-actina del músculo liso (α-SMA) y colágeno IV (Col IV). Se Los resultados son presentados como el error estándar de la media (± SEM, por sus siglas en inglés), n=5, usando un análisis de varianza (ANOVA) de una vía. Gliceraldehido fosfato deshidrogenasa (GAPDH) fue empleado como control de carga. Las diferencias estadísticas se determinaron mediante comparaciones múltiples, empleando la prueba de Tukey. [a] $p < 0.05$ vs control, [b] $p < 0.05$ vs OUU, [c] $p < 0.05$ vs OUU+SFN. E) Tinción representativa de hematoxilina y eosina (H&E) de la corteza renal. La tinción H&E reveló que la OUU indujo la pérdida de estructura tubular, caracterizada por la pérdida de células epiteliales (flechas rojas), dilatación tubular (flechas negras) y necrosis (flechas azules). La OUU también induce infiltración de polimorfonucleares y linfocitos

(flechas verdes) y la presencia de tejido conectivo entre los túbulos (asteriscos). El tratamiento con SFN disminuyó parcialmente la lesión renal a pesar de algunas áreas necróticas y se observó infiltración de leucocitos. Barra de escala = 100 μm. n = 3 para Sham y SFN; n = 4 para OUU y OUU+SFN. Sham: cirugía simulada sin ligadura del uréter; OUU: obstrucción ureteral unilateral con doble ligadura del uréter izquierdo durante siete días; OUU+SFN: OUU tratado con SFN (1 mg/kg, intraperitoneal) y SFN administrado con SFN (1 mg/kg, intraperitoneal).

9.2 Efecto del sulforafano sobre la biogénesis y la masa mitocondrial en el modelo de OUU

Debido a que la biogénesis mitocondrial es regulada por el coactivador gamma del receptor activado por el proliferador de peroxisomas (PGC)-1alfa (PGC-1**α**), mediante la transcripción del factor nuclear de respiratorio nuclear 1 (NRF1), se evaluaron ambas proteínas. Los resultados indicaron que los niveles de PGC-1**α** y de NRF1 disminuyeron significativamente en el grupo de OUU, mientras que el SFN previene su disminución de manera significativa (Figuras 6A,B). Para determinar si el aumento en la biogénesis mitocondrial tenía un efecto sobre la masa mitocondrial, se evaluaron los niveles de la proteína del canal de aniones dependiente de voltaje (VDAC) y del traslocador de nucleótidos de adenina (ANT). Los datos obtenidos revelaron que ambas proteínas disminuyeron en el grupo de OUU (Figuras 6C,D), mientras que en el grupo de OUU+SFN, solo los niveles de VDAC aumentaron pero no los de ANT (Figuras 6C,D). También encontramos que el grupo de SFN se comporta de manera similar al grupo Sham para todas las proteínas evaluadas. De este modo, los resultados sugieren que el SFN es capaz de promover la biogénesis mitocondrial, aumentando la masa mitocondrial en el modelo de OUU.
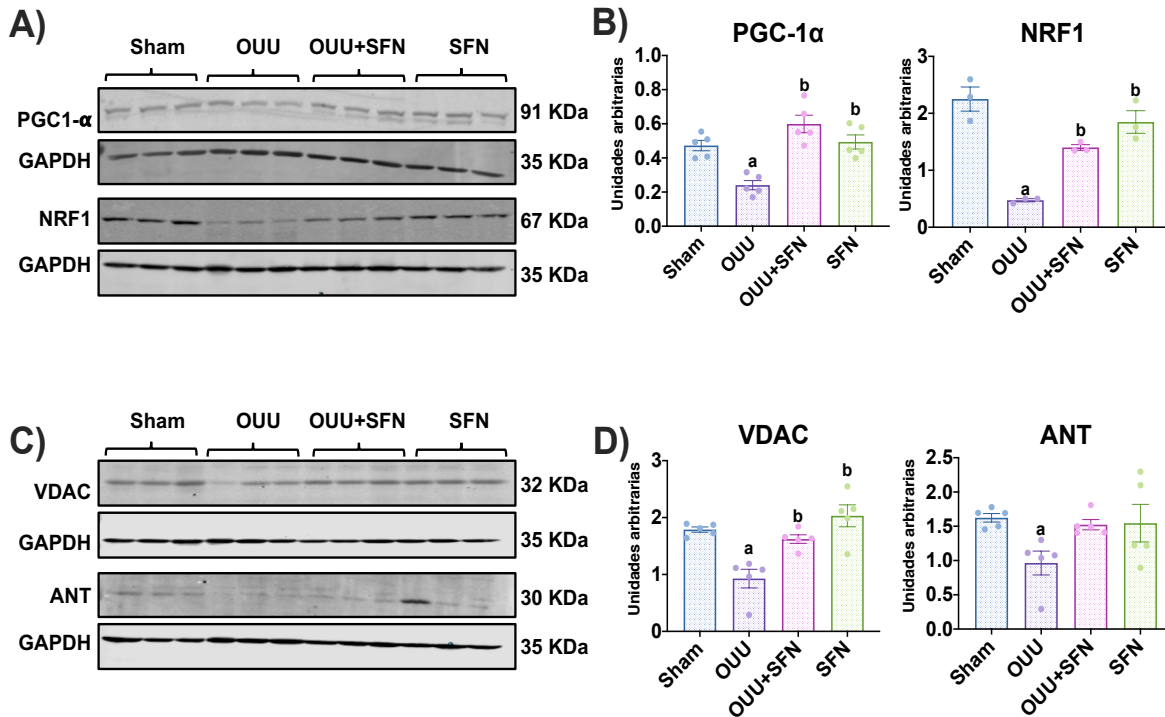
Figura 6. El sulforafano (SFN) induce la biogénesis mitocondrial y el aumento de la masa mitocondrial en el modelo de obstrucción ureteral unilateral (OUU). (A) Inmunoblot representativo y (B) análisis densitométrico de los marcadores de biogénesis mitocondrial, coactivador del receptor γ activado por el proliferador de peroxisomas 1α (PGC-1α) y factor respiratorio nuclear 1 (NRF1). n = 5 por grupo para PGC-1α y n = 3 por grupo para NRF1. (C) Inmunoblot representativo y (D) análisis densitométrico de marcadores de masa mitocondrial: canal de aniones dependientes de voltaje (VDAC) y translocador de nucleótidos de adenina (ANT), n = 5 por grupo. Los datos se presentan como el error estándar de la media (± SEM, por sus siglas en inglés) y se analizaron mediante un análisis de varianza (ANOVA) de una vía y las diferencias estadísticas se determinaron con comparaciones múltiples utilizando la prueba de Tukey. Se utilizó gliceraldehído 3-fosfato deshidrogenasa (GAPDH) como control de carga. a $p < 0,05$ frente a Sham, b $p < 0,05$ frente a OUU. Sham: cirugía simulada sin ligadura del uréter; OUU: obstrucción ureteral unilateral con doble ligadura del uréter izquierdo durante siete días; OUU+SFN: OUU tratado con SFN (1 mg/kg, intraperitoneal); y SFN: administrado con SFN (1 mg/kg, intraperitoneal).

9.3. El sulforafano restaura los niveles del sistema de transporte de electrones

La proteína PGC-1α es un potente factor de transcripción que regula la fosforilación oxidativa (OXPHOS); por lo tanto, la reducción de la biogénesis altera las proteínas de este proceso [28]. Por otro lado, el aumento de PGC-1α podría influir en la

OXPHOS, por lo que medimos los niveles de proteína de las subunidades CI-CIV y la adenosina trifosfato (ATP) sintasa (ATPasa). Se encontró que los niveles de succinato deshidrogenasa B (SDHB) del CII y la proteína ubiquinol-citocromo c reductasa core protein 2 (UQCRC2) del CIII disminuyeron en OUU en comparación con el grupo Sham (Figura 7A, C, D).

Por otro lado, el tratamiento con SFN aumentó los niveles de la proteína CIII-UQCRC2 en los grupos OUU+SFN y SFN en comparación con el grupo OUU (Figura 7B). Del mismo modo, los niveles de proteína CI-NADH: ubiquinona oxidorreductasa subunidad B8 (NDUFB8) y el CII-SDHB aumentaron en el grupo SFN en comparación con OUU (Figura 7B, C). No encontramos cambios para la proteína CIV citocromo c oxidasa (MTCO1) en ninguno de los grupos (Figura 7A,E). Curiosamente, observamos que la subunidad ATP sintasa-α (ATP5A) aumentó en la OUU, en comparación con el Sham, mientras que SFN lo disminuyó (Figura 7A, F). Estos resultados sugieren que SFN mejora la función OXPHOS en el modelo de OUU.
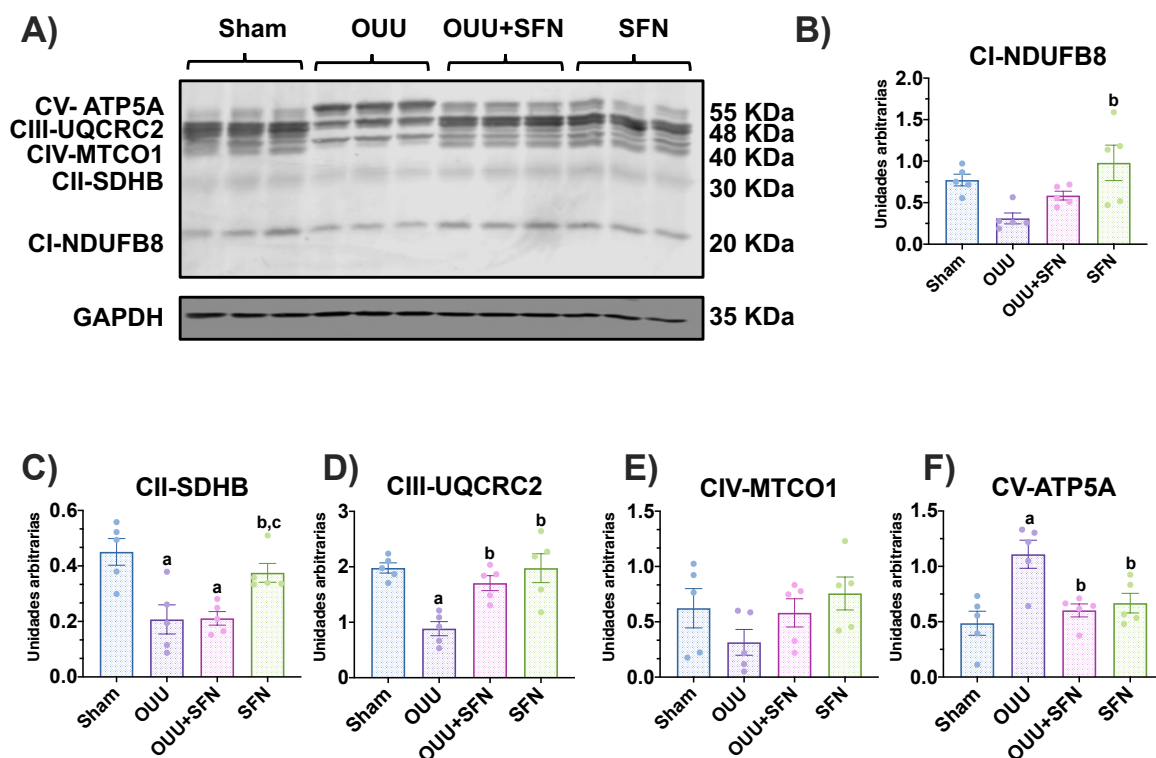
**Figura 7.** Efecto del sulforafano (SFN) sobre los niveles de subunidades de los complejos del sistema de transporte de electrones en el modelo de obstrucción

ureteral unilateral (OUU). (A) Inmunoblot representativo y análisis densitométricos de (B) la forma reducida de la subunidad B8 de la nicotinamida adenina dinucleótido ubiquinona oxidorreductasa (CI-NDUFB8), (C) la subunidad B del complejo hierro-azufre de la succinato deshidrogenasa (CII-SDHB), (D) proteína central 2 de ubiquinol-citocromo c reductasa (CIII-UQCRC2), (E) subunidad I de citocromo c oxidasa (CIV-MTCO1) y (F) subunidad de adenina trifosfato (ATP) sintasa-α (CV-ATP5A). Los datos son el error estándar de la media (± SEM, por sus siglas en inglés), n = 5 por grupo, usando un análisus de varianza (ANOVA) de una vía. Las diferencias estadísticas se determinaron con comparaciones múltiples utilizando la prueba de Tukey. Se usó gliceraldehído fosfato deshidrogenasa (GAPDH) como control de carga. a $p < 0,05$ frente a Sham, b $p < 0,05$ frente a OUU, c $p < 0,05$ frente a OUU+SFN. Sham: cirugía simulada sin ligadura del uréter; OUU: obstrucción ureteral unilateral con doble ligadura del uréter izquierdo durante siete días; OUU+SFN: OUU tratado con SFN (1 mg/kg, intraperitoneal); y SFN: administrado con SFN (1 mg/kg, intraperitoneal).

9.4 El sulforafano aumenta la actividad CIII en el modelo de OUU

Para determinar si el aumento de las proteínas OXPHOS mejora la ETS, evaluamos sus actividades. Encontramos que la actividad de CIII se redujo significativamente en el grupo de OUU en comparación con el grupo simulado, y el tratamiento con SFN indujo su aumento en los grupos de OUU+SFN y SFN (Figura 8C). Los resultados observados en esta actividad compleja fueron similares a los hallazgos para UQCRC2 de las proteínas OXPHOS. No se encontraron cambios significativos en las actividades de CI, CII y CIV (Figura 8A,B,D). Por lo tanto, la expresión de complejos concuerda con su actividad, donde el SFN aumentó al CIII en el grupo OUU+SFN en comparación con el grupo de obstrucción sin tratamiento.
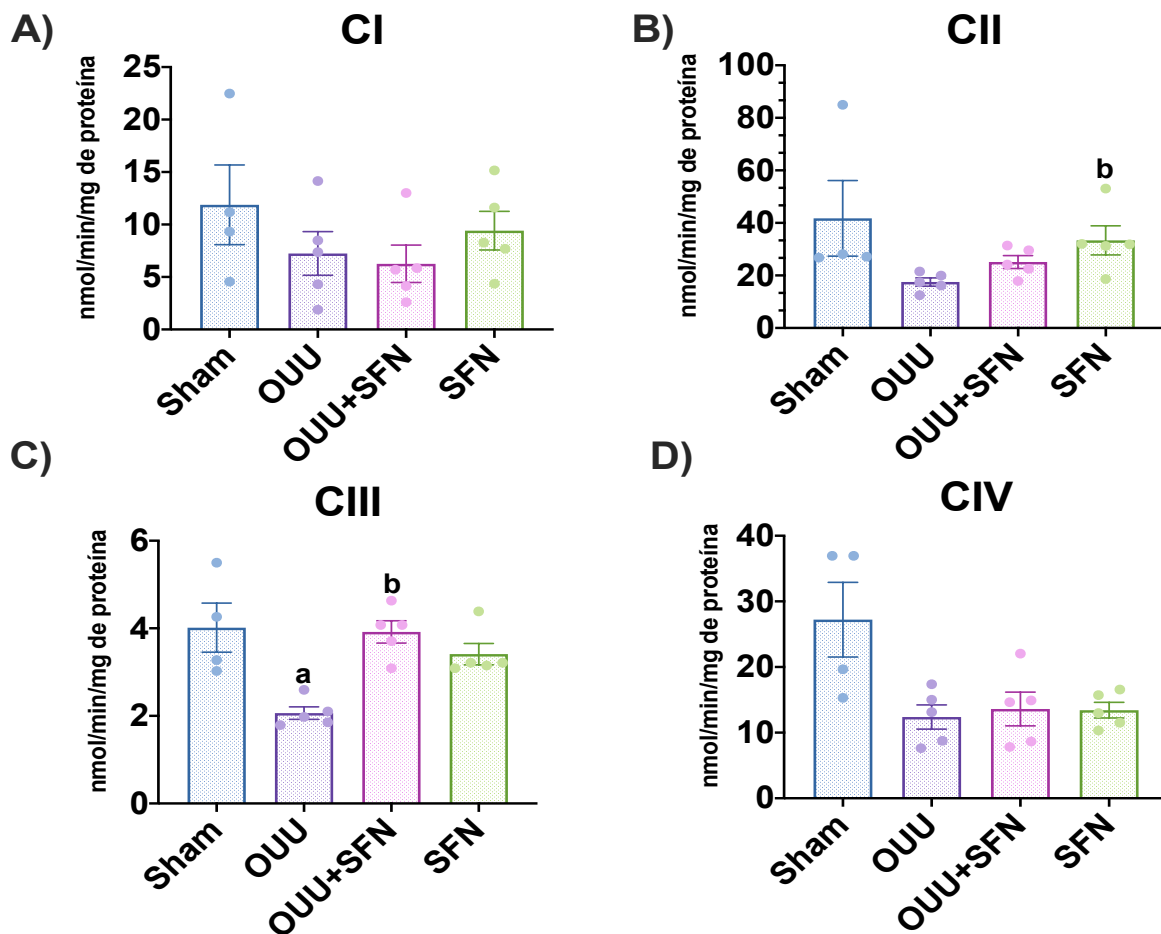
Figura 8. Efecto del sulforafano (SFN) sobre las actividades enzimáticas de los complejos del sistema de transporte de electrones (ETS) en el modelo de obstrucción ureteral unilateral (OUU). (A) Complejo I (CI), (B) complejo II (CII), (C) complejo III (CIII) y (D) complejo IV (CIV) se determinaron en la corteza renal total. Los datos son el error estándar de la media (± SEM, por sus siglas en inglés), n = 4 para el grupo falso y n = 5 para los grupos OUU, OUU+SFN y SFN. Los datos se analizaron mediante análisis de varianza (ANOVA) de una vía y las diferencias estadísticas se determinaron con comparaciones múltiples utilizando la prueba de Tukey. a $p < 0,05$ frente a Sham, b $p < 0,05$ frente a OUU. Sham: cirugía simulada sin ligadura del uréter; OUU: obstrucción ureteral unilateral con doble ligadura del uréter izquierdo durante siete días; OUU+SFN: OUU tratado con SFN (1 mg/kg, intraperitoneal) y el grupo SFN administrado con SFN (1 mg/kg, intraperitoneal).

9.5 El sulforafano aumenta los niveles de la aconitasa y su actividad y la actividad de la citrato sintasa en la OUU

Debido a que en el modelo de OUU se han reportado alteraciones en el ciclo de Krebs como uno de los factores que promueven la fibrosis en este modelo (H. Liu

et al., 2017), se evaluaron los niveles de la aconitasa 2 así como las actividades de las enzimas del ciclo de Krebs aconitasa y citrato sintasa. Se encontró que los niveles de la proteína ACO2 disminuyeron en el grupo de OUU en comparación con el grupo Sham (Figuras 9A,B). La disminución de ACO2 se asoció con el aumento de estrés oxidante, como se informó anteriormente (Aparicio-Trejo et al., 2019b; Cantu et al., 2009). El tratamiento con SFN no fue capaz de aumentar los niveles de esta proteína en el grupo de OUU pero sí presentó diferencia entre el grupo de OUU y el grupo tratado solo con SFN (Figura 9A,B). En relación a las actividades, se encontró que ambas disminuyen en el grupo de OUU pero solo esta disminución fue estadísticamente significativa para la actividad de la citrato sintasa (Figura 9D). Sin embargo, el SFN fue capaz de aumentar significativamente la actividad de ambas enzimas, sugiriendo una mejora en el ciclo de Krebs en el modelo de obstrucción.
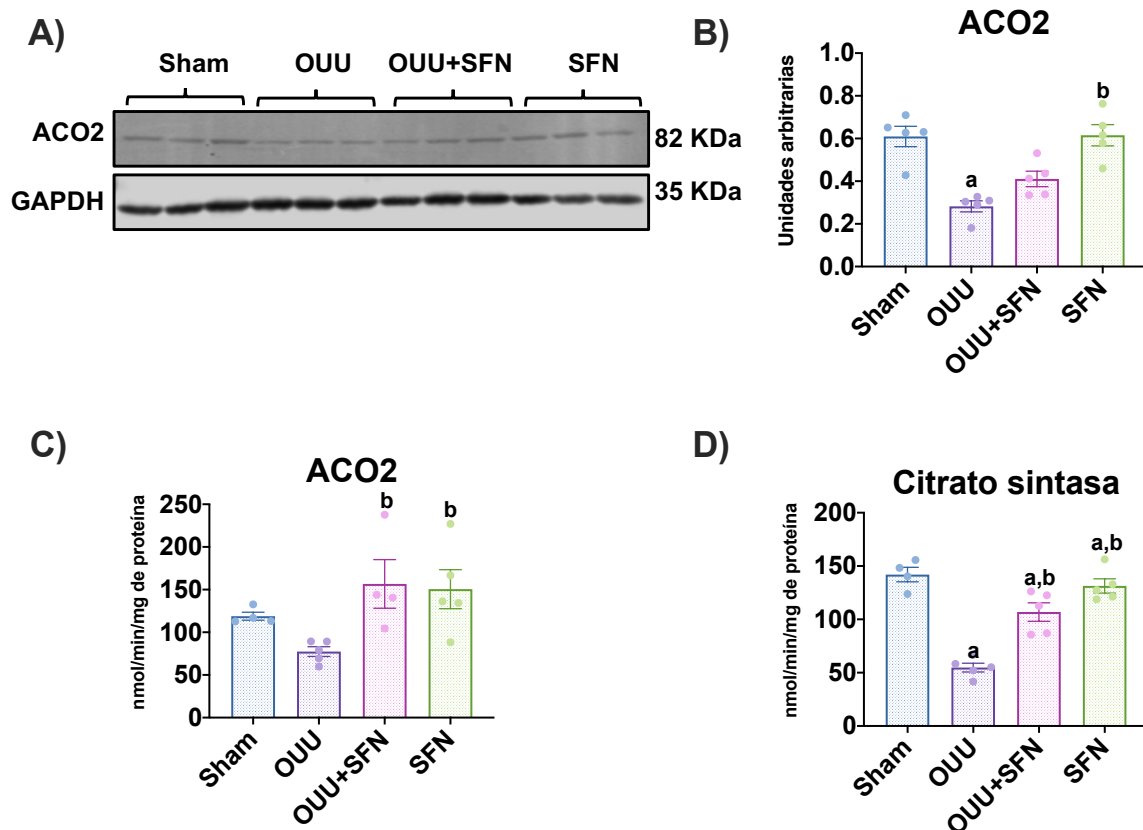
Figura 9. El sulforafano (SFN) aumenta la actividad de la aconitasa y de la citrato sintasa del ciclo de Krebs en la obstrucción unilateral del uréter (OUU). (A) Inmunoblot representativo y (B) análisis densitométrico de los niveles de aconitasa 2 (ACO2). Los datos son el error estándar de la media (± SEM, por sus

siglas en inglés), n = 5 por grupo. Los datos se analizaron mediante ANOVA de una vía y las diferencias estadísticas se determinaron mediante comparaciones múltiples mediante la prueba de Tukey. Se usó gliceraldehído fosfato deshidrogenasa (GAPDH) como control de carga. (C) Las actividades de ACO2 y (D) citrato sintasa de la corteza renal de los diferentes grupos experimentales se evaluaron en mitocondrias aisladas y homogeneizados totales, respectivamente. Los datos son la media ± SEM, n = 5 por grupo (excepto para el tratamiento simulado para ACO2 y citrato sintasa y OUU+SFN para ACO2, n = 4). Los datos se analizaron mediante ANOVA de una vía y las diferencias estadísticas se determinaron con comparaciones múltiples mediante la prueba de Tukey [a] p < 0,05 frente a Sham, [b] p < 0,05 frente a OUU. Sham: cirugía simulada sin ligadura del uréter; OUU: obstrucción ureteral unilateral con doble ligadura del uréter izquierdo durante siete días; OUU+SFN: OUU tratado con SFN (1 mg/kg, intraperitoneal) y SFN administrado con SFN (1 mg/kg, intraperitoneal).

9.6 El sulforafano media la absorción de ácidos grasos en el modelo de OUU

La disfunción mitocondrial en los modelos de ERC, incluida la OUU, también se ha asociado con el deterioro del metabolismo de los lípidos debido a la regulación positiva de la biosíntesis de lípidos y la regulación negativa de su degradación a través de la β-oxidación de ácidos grasos (AG), lo que induce la acumulación de lípidos en la corteza renal (Stadler et al., 2015). Además, el deterioro de la bioenergética conduce a la absorción de AG porque los riñones dependen en gran medida de la β-oxidación (Lewy et al., 1973). En informes anteriores se ha demostrado que la inducción de la biogénesis por SFN tiene un impacto en el metabolismo de los lípidos (Lei et al., 2019); por lo tanto, investigamos el efecto de SFN en la absorción, biosíntesis y utilización de AG en el riñón obstruido. Se encontró que los niveles de CD36, la proteína responsable de capturar e internalizar AG, aumentaron significativamente en el grupo OUU, y el tratamiento con SFN fue capaz de disminuirlo en el grupo OUU+SFN (Figura 10A, B). También evaluamos los niveles del receptor nuclear PPAR-α, involucrado en el metabolismo de los AG. Observamos que el receptor PPAR-α estaba regulado al alza en el modelo de OUU mientras que SFN lo disminuía (Figura 10A,B). También evaluamos los niveles de CPT1A, que cataliza el transporte de ácidos grasos de cadena larga a las mitocondrias para la β-oxidación, y no encontramos diferencias entre los grupos OUU y OUU+SFN; sin embargo, el SFN aumentó los niveles de CPT1A y en el

grupo tratado con SFN (Figura 10A,B). Por lo tanto, nuestros resultados sugieren que el SFN disminuye la captación de AG en la OUU.
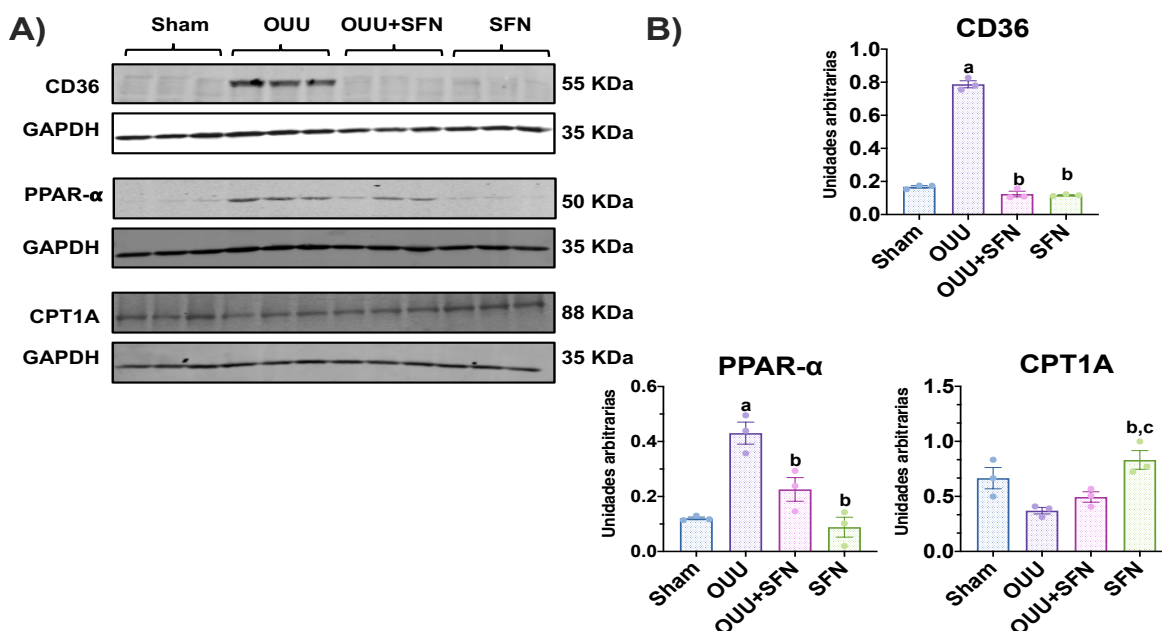

Figura 10. El sulforafano (SFN) evita la captación de ácidos grasos en el modelo de obstrucción ureteral unilateral (OUU). (A) Inmunoblot representativo y (B) análisis densitométrico del cluster de diferenciación 36 (CD36), del receptor alfa activado por el proliferador de peroxisomas (PPAR-α) y la carnitina palmitoil transferasa 1A (CPT1A). Los datos son el error estándar de la media (± SEM, por sus siglas en inglés), n = 3 por grupo. Los datos se analizaron mediante un análisis de varianza (ANOVA) de una vía y las diferencias estadísticas se determinaron mediante comparaciones múltiples mediante la prueba de Tukey. Se utilizó gliceraldehído 3-fosfato deshidrogenasa (GAPDH) como control de carga. [a] $p < 0,05$ frente a Sham, [b] $p < 0,05$ frente a OUU, [c] $p < 0,05$ frente a OUU+SFN. Sham: cirugía simulada sin ligadura del uréter; OUU: obstrucción ureteral unilateral con doble ligadura del uréter izquierdo durante siete días; OUU+SFN: OUU tratado con SFN (1 mg/kg, intraperitoneal); y SFN: administrado con SFN (1 mg/kg, intraperitoneal).

9.7 El sulforafano disminuye la deposición de lípidos en la OUU

Para determinar si el aumento de la captación de AG en la obstrucción desencadena la deposición de lípidos y su probable disminución después de la administración de SFN, determinamos la acumulación de lípidos en secciones de tejido a través de la tinción con rojo Nilo. Observamos que los lípidos tendían a acumularse en el grupo de obstrucción, pero parecían parcialmente prevenidos en el grupo OUU+SFN. La acumulación de lípidos se encontró principalmente en el epitelio del túbulo.

Curiosamente, el SFN por sí mismo también aumentó el contenido total de lípidos, pero no se observó acumulación en una estructura particular (Figura 11A,B).

A)

B)
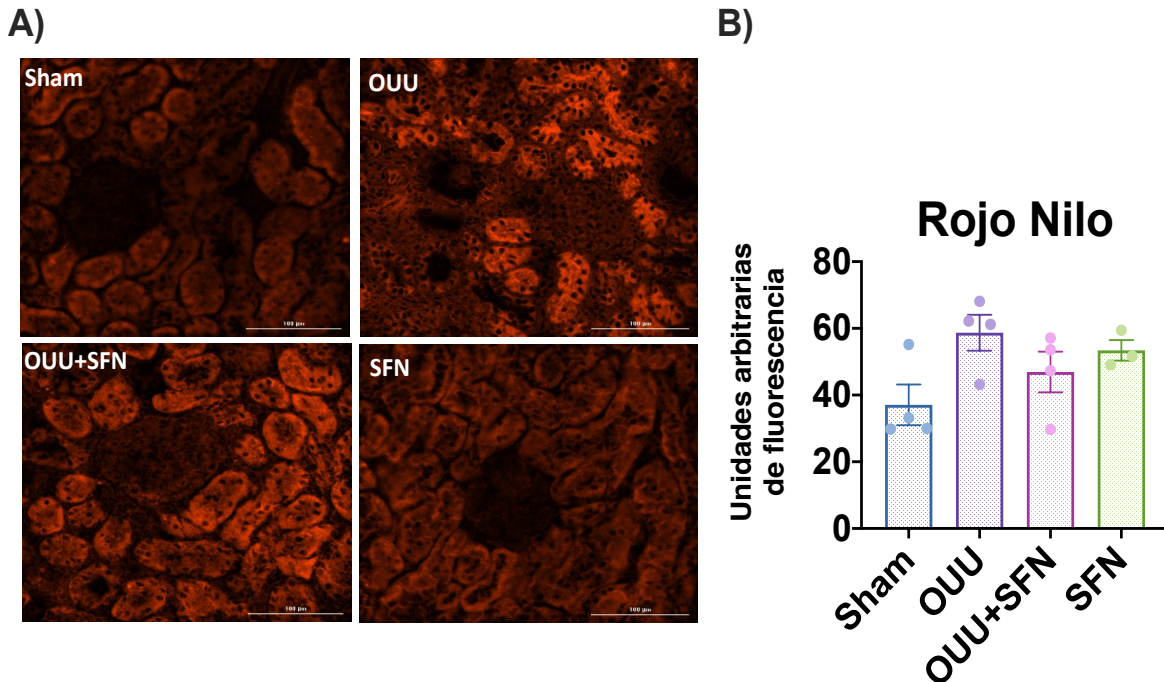
Figura 11. El sulforafano (SFN) afecta el depósito de lípidos en el modelo de obstrucción ureteral unilateral (OUU). (A) Micrografías representativas de la tinción con rojo Nilo y (B) cuantificación de la tinción con Nilered. La tinción con rojo Nilo mostró una mayor deposición de lípidos en el grupo de obstrucción ureteral unilateral (OUU) que en el grupo simulado, mientras que SFN disminuyó los lípidos en el grupo de OUU+SFN. n = 4 para simulación, OUU y OUU+SFN y n = 3 para SFN. Los datos se presentan como el error estándar de la media (± SEM, por sus siglas en inglés) y se analizaron mediante un análisis de varianza (ANOVA) de una vía y las diferencias estadísticas se determinaron con comparaciones múltiples utilizando la prueba de Tukey. Sham: cirugía simulada sin ligadura del uréter; OUU: obstrucción ureteral unilateral con doble ligadura del uréter izquierdo durante siete días; OUU+SFN: OUU tratado con SFN (1 mg/kg, intraperitoneal); y SFN: administrado con SFN (1 mg/kg, intraperitoneal).

9.8 El sulforafano disminuye la síntesis de lípidos

Adicionalmente, determinamos los niveles de proteína de las enzimas involucradas en el metabolismo de los lípidos en OUU y su posible mejora con el tratamiento con SFN. Encontramos que FASN, DGAT1 y SREBP1 aumentaron en el riñón obstruido en comparación con el grupo simulado. Por el contrario, en el grupo OUU+SFN, los

niveles de estas enzimas disminuyeron significativamente (Figura 12A,B). Finalmente, para dilucidar si la disminución de las enzimas involucradas en la lipogénesis disminuía los niveles de lípidos con el tratamiento con SFN, evaluamos la cantidad de TGs intrarrenales. Se encontró que los TGs aumentaron en el grupo de OUU mientras que SFN los disminuyó, lo que sugiere que SFN evita la acumulación de lípidos en la obstrucción (Figura 12C).
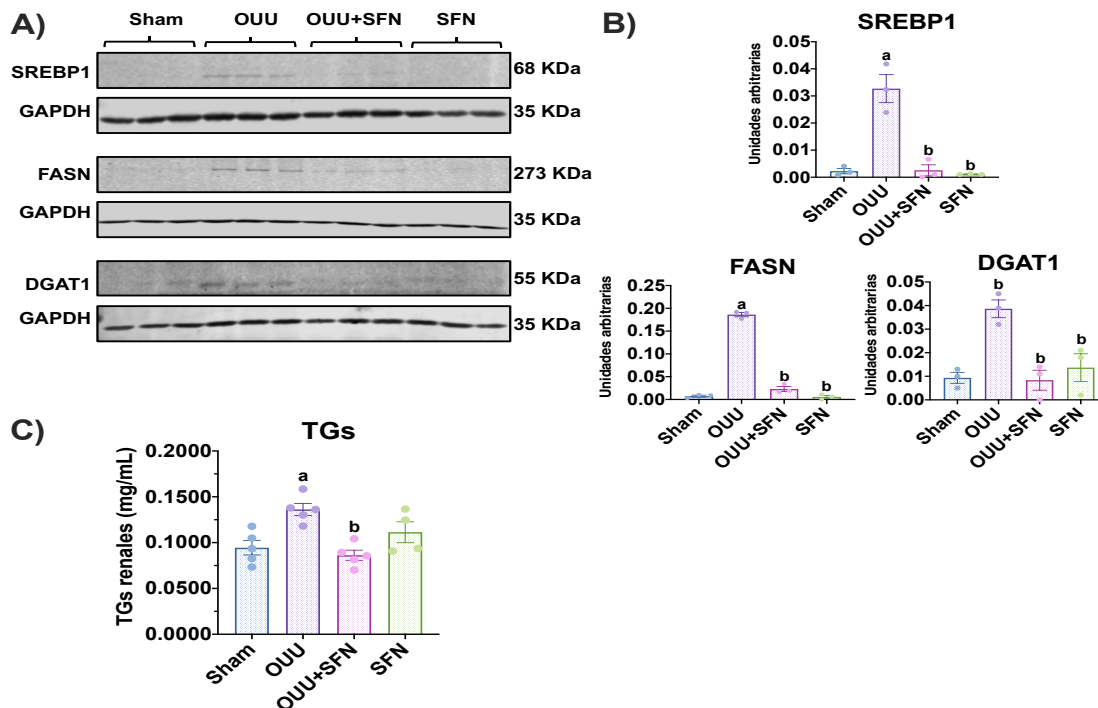
Figura 12. Efecto del sulforafano (SFN) sobre la síntesis de lípidos en el modelo de obstrucción ureteral unilateral (OUU). (A) Inmunoblot representativo y (B) análisis densitométrico de las proteínas de unión a elementos reguladores de esteroles (SREBP1), ácido graso sintasa (FASN) y diacilglicerol O-aciltransferasa 1 (DGAT1) en el grupo sham, OUU, OUU tratado con SFN (OUU+SFN), y un grupo tratado con SFN (SFN). Los datos son el error estándar de la media (± SEM, por sus siglas en inglés), n = 3 por grupo. Los datos se analizaron mediante un análisis de varianza (ANOVA) de una vía y las diferencias estadísticas se determinaron con comparaciones múltiples utilizando la prueba de Tukey. Se usó gliceraldehído fosfato deshidrogenasa (GAPDH) como control de carga. (C) Los triglicéridos intrarrenales (TGs) se determinaron en la corteza renal en todos los grupos experimentales. Los datos son la media ± SEM, n = 5 para los grupos sham, OUU y OUU+SFN y n = 4 para el grupo SFN. Los datos se analizaron mediante ANOVA de una vía y las diferencias estadísticas se determinaron con comparaciones múltiples utilizando la prueba de Tukey. [a] $p < 0,05$ frente a Sham, [b] $p < 0,05$ frente a OUU. Sham: cirugía simulada sin ligadura del uréter; OUU: obstrucción ureteral

unilateral con doble ligadura del uréter izquierdo durante siete días; OUU+SFN: OUU tratado con SFN (1 mg/kg, intraperitoneal); y SFN: administrado con SFN (1 mg/kg, intraperitoneal).

9.9 El sulforafano disminuye el proceso de fisión en el riñón obstruido

Para dilucidar si la restauración de la estructura mitocondrial y la bioenergética por SFN modula la dinámica mitocondrial, un proceso que involucra fisión y fusión, determinamos en mitocondrias aisladas los niveles de las proteínas involucradas en este proceso. Se observó que en el grupo de OUU, los niveles de la proteína de fisión DRP1 aumentaron en comparación con el grupo simulado, y el tratamiento SFN los disminuyó (Figura 13A, B). Además, las proteínas de fusión OPA1 y MFN2 disminuyeron en la fracción mitocondrial de OUU, los cuales no pudieron restaurarse con el tratamiento con SFN (Figura 13A,C). En conjunto, nuestros resultados indican que el SFN regula parcialmente la dinámica mitocondrial al disminuir la fisión mitocondrial en el riñón obstruido.
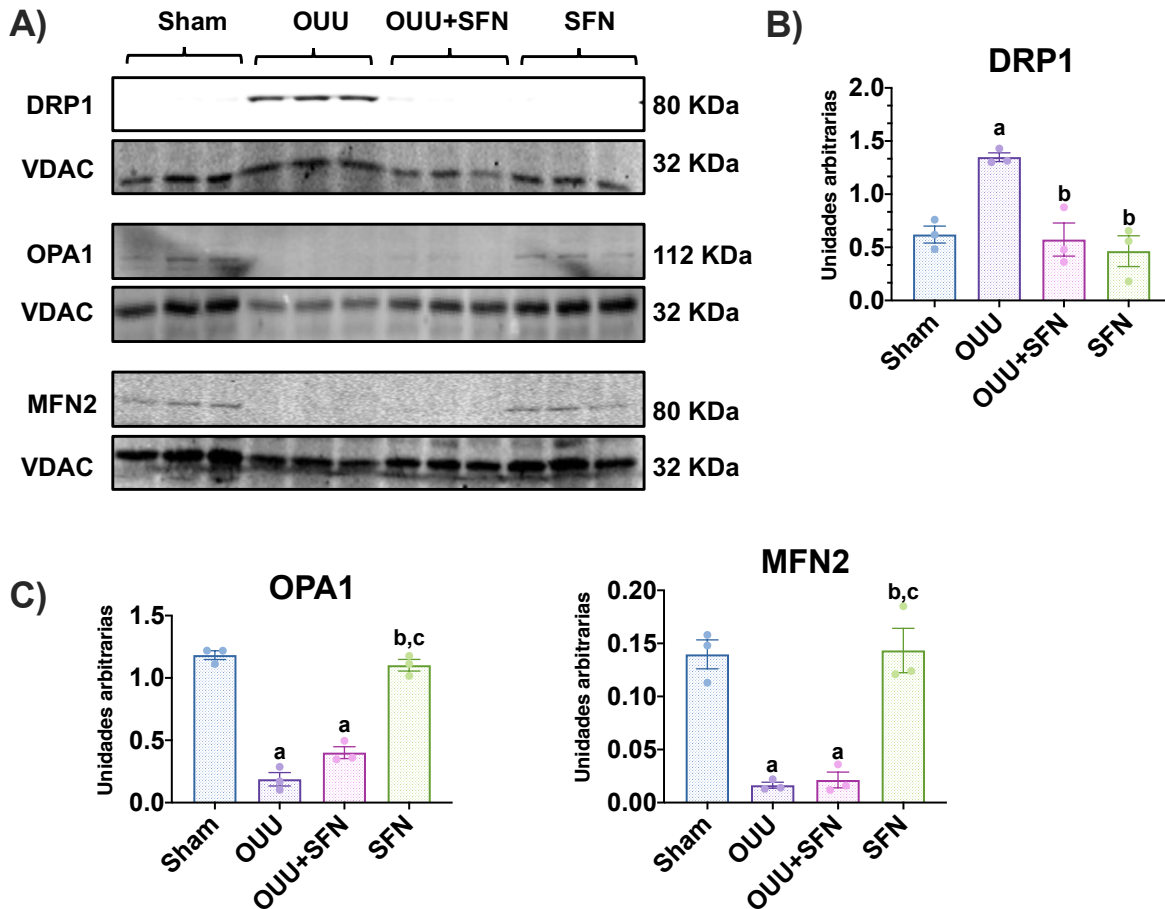
Figura 13. El sulforafano (SFN) disminuye el proceso de fisión en mitocondrias aisladas en el modelo de obstrucción ureteral unilateral (OUU). (A) Inmunoblot representativo y análisis densitométrico de los niveles de proteína de (B) la proteína de fisión relacionada con la dinamina-1 (DRP1) y (C) las proteínas de fusión atrofia óptica tipo 1 (OPA1) y mitofusina 2 (MFN2). Los datos son la media ± SEM, n = 3 por grupo. Los datos se presentan como el error estándar de la media (± SEM, por sus siglas en inglés) y se analizaron mediante un análisis de varianza (ANOVA) de una vía y las diferencias estadísticas se determinaron mediante comparaciones múltiples mediante la prueba de Tukey. Se utilizó al canal de aniones dependiente de voltaje (VDAC) como control de carga. [a] p < 0,05 frente a Sham, [b] p < 0,05 frente a OUU, [c] p < 0,05 frente a OUU+SFN. Sham: cirugía simulada sin ligadura del uréter; OUU: obstrucción ureteral unilateral con doble ligadura del uréter izquierdo durante siete días; OUU+SFN: OUU tratado con SFN (1 mg/kg, intraperitoneal); y SFN: administrado con SFN (1 mg/kg, intraperitoneal).

9.10 El flujo de autofagia es restaurado por sulforafano en el modelo de OUU

Las alteraciones en la dinámica mitocondrial, como el aumento de la fisión desencadenan la mitofagia, un proceso que elimina las mitocondrias dañadas; sin embargo, en las OUU, alteraciones en la mitofagia se informa comúnmente (Bhatia

& Choi, 2019; Jiménez-Uribe et al., 2021; S. Li et al., 2020). Nuestro objetivo fue investigar si la mejora de la ultraestructura mitocondrial, la bioenergética y la dinámica por SFN tuvo un enfecto sobre la mitofagia. Evaluamos en mitocondrias aisladas los niveles de PINK1 y E3 ubiquitina-proteína ligasa parkin (Parkin) y observamos que en el grupo de OUU, la proteína PINK1 aumentó significativamente en comparación con el grupo simulado pero no los niveles de Parkin. También encontramos que SFN no afectó a las proteínas de mitofagia PINK1 y Parkin (Figura 14A, B). Dado que la mitofagia mediada por PINK1/Parkin está muy relacionada con la macroautofagia, queríamos estudiar el efecto SFN en el proceso macroautofágico. Encontramos que los niveles de los marcadores de autofagia Beclin y p62 aumentaron en el grupo de OUU mientras que los niveles de Bcl2 disminuyeron (Figura 14C, D). En el riñón obstruído, el tratamiento con SFN redujo los niveles de Beclin y p62 y aumentó los niveles de Bcl2, lo que sugiere la restauración del flujo autofagico. Además, encontramos que la relación LC3-II/LC3-I disminuyó en el grupo OUU mientras que el SFN la aumentó significativamente (Figura 14C, D), lo que sugiere que el SFN restaura el flujo de autofagia. En conjunto, los resultados sugieren que SFN restauró el flujo de autofagia en el riñón obstruido.
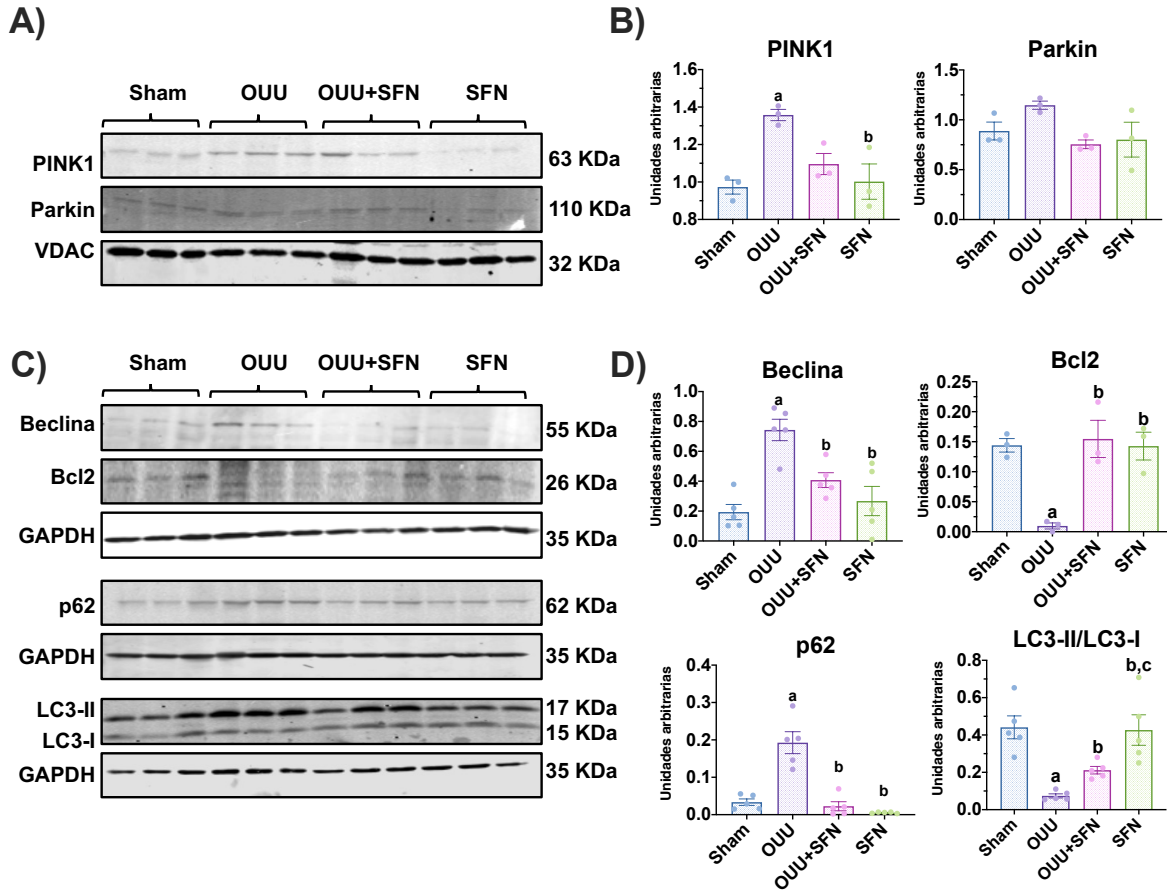
Figura 14. Efecto del sulforafano (SFN) sobre los niveles de proteínas de mitofagia y autofagia en el modelo de obstrucción ureteral unilateral (OUU). (A) Inmunoblot representativo y (B) análisis densitométrico de los niveles de marcadores de mitofagia fosfatasa y homólogo de tensina eliminados en la quinasa 1 inducida por el cromosoma 10 (PINK1) y Parkin en mitocondrias aisladas. El canal dependiente de aniones de voltaje (VDAC) se utilizó como control de carga. n = 3 por grupo. (C) Inmunoblot representativo y (D) análisis densitométrico de los marcadores de autofagia linfoma de células B 2 (Bcl2), secuestrosoma (p62) y el ratio de proteínas asociadas a microtúbulos 1A/1B cadena ligera 3 (LC3I/LC3II). Los datos son el error estándar de la media (± SEM, por sus siglas en inglés), n = 5 por grupo (excepto para Bcl2, n = 3 por grupo). Los datos se analizaron mediante un análisis de varianza (ANOVA) de una vía y las diferencias estadísticas se determinaron con comparaciones múltiples utilizando la prueba de Tukey. Se usó gliceraldehído fosfato deshidrogenasa (GAPDH) como control de carga. [a] $p < 0,05$ frente a Sham, [b] $p < 0,05$ frente a OUU, [c] $p < 0,05$ frente a OUU+SFN. Sham: cirugía simulada sin ligadura del uréter; OUU: obstrucción ureteral unilateral con doble ligadura del uréter izquierdo durante siete días; OUU+SFN: OUU tratado con SFN (1 mg/kg, intraperitoneal); y SFN: administrado con SFN (1 mg/kg, intraperitoneal).

9.11 SFN mejora el daño ultraestructural mitocondrial y restaura el flujo de autofagia en la OUU

La corteza renal fue analizada por microscopía electrónica de transmisión (MET) para observar los cambios en la distribución mitocondrial y la morfología inducida por la obstrucción de siete días y su probable restauración con el tratamiento SFN. Se revisaron las crestas mitocondriales, las membranas y la integridad de la matriz. En concordancia con reportes previos (Jiménez-Uribe et al., 2021), se observaron cambios en la morfología mitocondrial y daño mitocondrial en el grupo de OUU, ya que las mitocondrias cambiaron de una morfología grande y alargada en el riñón Sham (Figura 15A, B) a una morfología más pequeña y redonda en el riñón obstruido (Figura 15C,D). Además, el riñón obstruido mostró mitocondrias que habían perdido la continuidad de la doble membrana (Figura 15D, flecha roja). Por su parte, el grupo SFN mostró mitocondrias con morfología grande y alargada, similar al grupo control (Figura 15G,H).

También determinamos la restauración de la autofagia por MET para confirmar si el SFN efectivamente restableció el flujo de autofagia. Encontramos que en el riñón obstruído la presencia de cuerpos autofágicos sugestivos de mitofagia (asteriscos en la Figura 15C,I-L). El grupo OUU+SFN no presentó cuerpos autofágicos a pesar de que algunas mitocondrias exhibieron una morfología más redonda y baja electrodensidad (Figura 15E,F). Por lo tanto, con estos datos se hizo evidente la recuperación de la ultraestructura mitocondrial y el flujo de mitofagia por SFN.
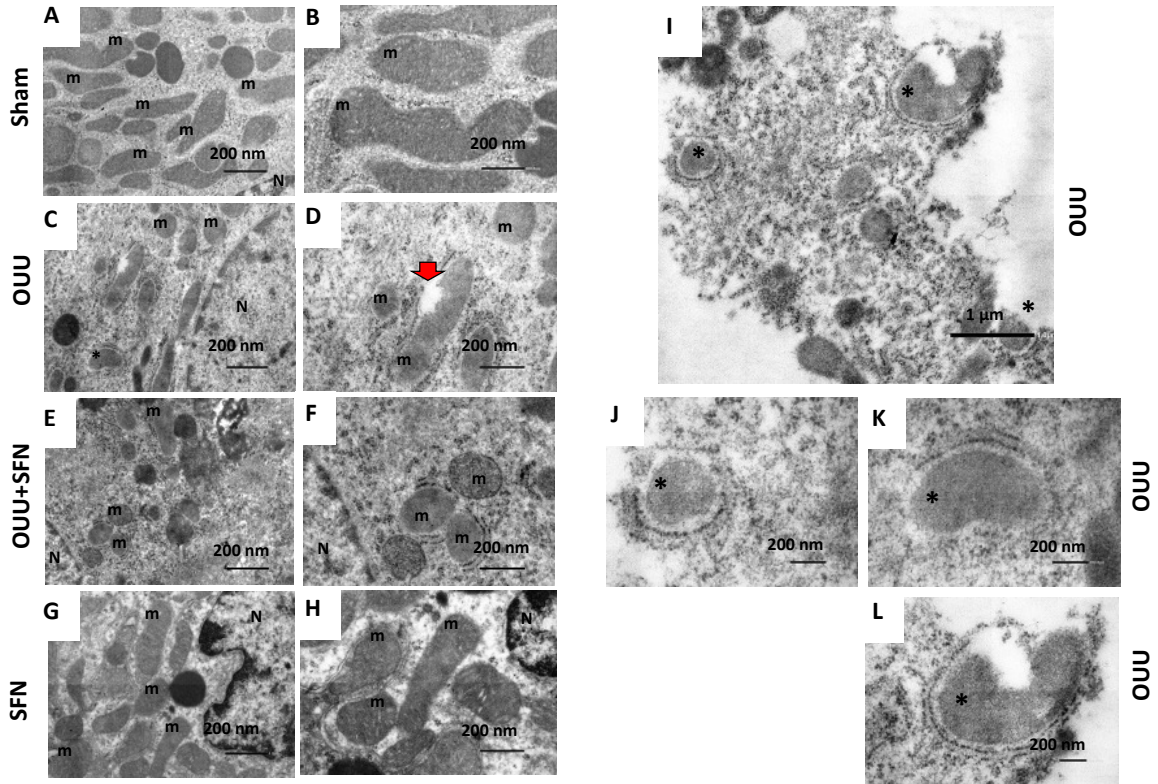
Figura 15. Morfología mitocondrial, autofagia y mitofagia. La corteza renal fue analizada por microscopía electrónica de transmisión para observar la distribución y morfología mitocondrial. (A,B) Sham. (C,D,I,–L), obstrucción unilateral del ureter (OUU). (E,F), OUU tratado con sulforafano (SFN) OUU+SFN. (G, H) SFN. m: mitocondrias; N: núcleo; asteriscos: cuerpos autofágicos; flecha roja: mitocondrias que han perdido la continuidad de la doble membrana. Las micrografías en la columna de la izquierda se tomaron a 10 000 × (barra de escala = 1 µm) y en la columna de la derecha a un aumento de 20 000 × (barra de escala = 500 nm). n = 3 para Sham y SFN y n = 4 para OUU y OUU+SFN. Sham: cirugía simulada sin ligadura del uréter; OUU: obstrucción ureteral unilateral con doble ligadura del uréter izquierdo durante siete días; OUU+SFN: OUU tratado con SFN (1 mg/kg, intraperitoneal); y SFN: administrado con SFN (1 mg/kg, intraperitoneal).

10. RESUMEN DE RESULTADOS

1. El SFN disminuye el daño renal y la fibrosis en el riñón obstruído.

2. El SFN induce la biogénesis mitocondrial, aumentando la masa mitocondrial.

3. El SFN induce la actividad del CIII del STE.

4. El aumento de la actividad del CIII estuvo relacionado con el aumento en los niveles de proteína de la subunidad UQCRC2 del CIII.

5. El SFN además aumentó los niveles de la subunidad SDHB del CII y disminuyó los niveles de la ATP5A del CV.

6. El SFN promovió las actividades de las enzimas del ciclo de Krebs aconitasa y citrato sintasa, pero no tuvo efecto sobre los niveles proteicos de la ACO2.

7. El SFN disminuyó los niveles de CD36 y de PPAR-α, pero no tuvo efecto sobre los niveles de CPT1.

8. El SFN disminuyó la deposición de lípidos.

9. La disminución de los lípidos se atribuyó a la regulación a la baja de las proteínas que llevan a cabo su síntesis.

10. El SFN diminuyó los niveles de DRP1 pero no de OPA1 ni de MFN2.

11. El SFN reguló la mitofagia/autofagia y mejoró la estructura mitocondrial.

11. DISCUSIÓN

En la OUU, la disfunción mitocondrial como la disminución en la biogénesis mitocondrial son mecanismos que conducen a la progresión de la ERC, por lo que son requeridos fármacos o productos naturales que tengan como blanco a la mitocondria (Jiménez-Uribe et al., 2021; Kang et al., 2015; Martínez-Klimova et al., 2020). En este trabajo se usó al SFN el cual ha demostrado que preserva la función mitocondrial al promover la biogénesis mitocondrial, la bioenergética y la activación de Nrf2 (Briones-Herrera et al., 2020; Guerrero-Beltrán et al., 2010; Mohammad et al., 2022). Los resultados obtenidos demuestran que el SFN protege en contra del daño renal inducido por la obstrucción al promover la biogénesis mitocondrial. La protección fue determinada al evaluar los niveles de KIM-1 y de IL-1β (Figura 5A,B), así como los niveles de α-SMA y de Col IV (Figura 5C,D). Además, la tinción de H&E reveló la reducción del daño renal mediada por la administración de SFN, aunque la infiltración de células inflamatorias como los leucocitos fue todavía evidente en el grupo de OUU tratado con SFN (Figura 5E). La presencia de células inflamatorias podría ser parcialmente explicada debido a que en el modelo de OUU la infiltración leucocitaria comienza 12 hrs después de la obstrucción y continúa durante el tiempo que el riñón se encuentre obstruído (Diamond et al., 1995; Ucero et al., 2014). En el presente trabajo, la administración del SFN comenzó el segundo día después de la cirugía (Figura 4), por lo que la inflamación podría ser una consecuencia de esas primeras horas de daño. Es posible que los efectos del SFN sobre la inflamación se potencíen después de siete días de su administración en el grupo de obstrucción, lo cual requiere estudios futuros. Interesantemente, los niveles de IL-1β, citocina que es liberada por las células inflamatorias, disminuyeron significativamente en el grupo con tratamiento comparados con los niveles del grupo de obstrucción, sugiriendo que la inflamación fue efectivamente atenuada por el SFN (Figura 5A,B). Nuestros hallazgos sobre la disminución del daño y la fibrosis inducidos por el SFN concuerdan con lo reportado por otros autores (Chung et al., 2012), quienes demostraron que el efecto protector del SFN estuvo relacionado con la diminución del estrés oxidante en la mitocondria mediados por la activación del

flujo autofágico, sugiriendo que el efecto protector de este antioxidante durante la OUU podría estar relacionado con la reestauración de la mitocondria.

La reducción en el proceso de biogénesis mitocondrial ha sido previamente relacionada con el proceso de fibrosis en las enfermedades renales (Bhargava & Schnellmann, 2017; Prieto-Carrasco et al., 2021) y se ha demostrado que el el SFN la previene al inducir los niveles de PGC-1α, el principal regulador de este proceso en modelos de daño renal agudo inducido por maleato y daño renal crónico inducido por streptozotocina (Briones-Herrera et al., 2020; Lei et al., 2019; Z. Li et al., 2020). El PGC-1α induce la biogénesis mitocondrial mediante la activación de NRF1 y NRF2 lo cual induce la transcripción de genes mitocondriales que regulan la fosforilación oxidativa, el ciclo de Krebs y el metabolismo de los ácidos grasos, entre otros (Fontecha-Barriuso et al., 2020; Uittenbogaard & Chiaramello, s. f.). Los resultados efectivamente revelaron que el SFN restaura tanto los niveles de PGC-1α como de NRF1 en el riñón obstruído (Figura 8A,B), lo cual condujo a un aumento en los niveles de la proteína mitocondrial VDAC, utilizada como un marcador de masa mitocondrial externa (Figura 6C,D). No se observaron cambios significativos en los niveles de ANT, proteína que se empleó como un marcador de masa mitocondrial interna en el grupo de OUU+SFN; sin embargo, se observó una pequeña tendencia en su incremento (Figura 6C,D). Dicha tendencia podría incrementar y ser significativa siguiendo la administración de SFN más allá de siete días posteriores a la obstrucción, lo cual podría permitir observar los cambios en ANT. Por otro lado, podemos atribuir el solo incremento de VDAC y no de ANT debido a que VDAC es un blanco de NRF1, lo cual ha sido previamente reportado por Patti y cols. (Patti et al., 2003). En este trabajo, los autores informaron que en la diabetes tipo 2, la reducción en los niveles de la proteína nuclear que codifica para la proteína mitocondrial VDAC estuvieron relacionados a la disminución de NRF1, indicando que esta proteína regula a VDAC a nivel transcripcional. En concordancia con estos datos, Guarino y cols. (Guarino et al., 2020) demostraron que NRF1 regula la expresión del gen de VDAC debido a que NRF1 contiene sitios de unión al promotor de VDAC. Por lo tanto, los datos obtenidos demuestran que la mejora en

la biogénesis mitocondrial a través de la inducción de PGC-1α y NRF1 conduce a un aumento en los niveles de VDAC, lo cual podría estar relacionado con el aumento en la masa mitocondrial.

Los datos obtenidos sobre los efectos mediados por el SFN sobre la ultraestructura mitocondrial demostraron que el SFN mejora la ultraestructura (Figura 15E,F). Además, en el grupo de OUU la estructura mitocondrial mostró la presencia de mitocondrias elongadas, así como la pérdida de las crestas mitocondriales (Figura 15C,D). Estas alteraciones fueron parcialmente reestauradas por el SFN en el grupo de OUU+SFN, lo que se hizo evidente por la presencia de mitocondrias con una apariencia más redondeada y una menor pérdida de crestas. La restauración de la morfología mitocondrial fue relacionada con la promoción de la biogénesis inducida por este antioxidante, debido a la generación de mitocondrias nuevas. Estos resultados son consistentes con los informes previos en un modelo de daño hepático inducido por una dieta alta en grasas, los cuales presentan una mejor estructura mitocondrial en el grupo administrado con SFN (Lei et al., 2019). Además, los estudios *in vitro* tambien revelaron que la pérdida del potencial de membrana y del ATP en un modelo de daño inducido por el peróxido de hidrógeno (H_2O_2) fueron prevenidos por la administración del SFN (de Oliveira et al., 2018). En conjunto, estos resultados resaltan el papel del SFN en la mejora de las alteraciones mitocondriales via PGC-1α, lo cual tiene como impacto a la fosforilación oxidativa.

De acuerdo con lo anterior, el PGC-1α es un factor de transcripción que regula la bioenergética a través de la regulación de la transcripción de proteínas del ciclo de Krebs y de la fosforilación oxidativa (Bhargava & Schnellmann, 2017; Fontecha-Barriuso et al., 2020). En el modelo de OUU, se ha informado sobre las alteraciones en el ciclo de Krebs debido a la acumulación de metabolitos tales como succinato y citrato, la última acompañada de la regulación a la baja de la citrato sintasa (H. Liu et al., 2017). Otros autores describieron que la deficiencia de la isocitrato deshidrogenasa 2 (IDH2), una enzima que metaboliza isocitrato a α-cetoglutarato, exacerba la producción de H_2O_2, la peroxidación lipídica y la inflamación en el riñón obstruído (Kim et al., 2021). Se describieron resultados similares en el modelo de

daño renal agudo inducido por cisplatino, en donde se informó que la deficiencia de IDH2 acelera la nefrotoxicidad, incrementando el daño tubular (Kong et al., 2018). Se ha demostrado en estudios previos la habilidad del SFN para potenciar la actividad del ciclo de Krebs. Por ejemplo, el SFN incrementa la actividad de la aconitasa y la α-cetoglutarato deshidrogenasa en un modelo *in vitro* en las células SHSY5Y derivadas de neuroblastoma expuestas a H_2O_2 y en los pulmones de ratones deficientes de Nrf2 (Cho et al., 2019; de Oliveira et al., 2018). El incremento en ambas enzimas fue relacionado con el efecto antioxidante del SFN en ambos modelos. De acuerdo con lo anterior, los resultados obtenidos en este trabajo demostraron que las actividades de la ACO2 junto con la de citrato sintasa aumentan con el SFN (Figura 9C,D), sugiriendo que el efecto del SFN sobre la mitocondria se refleja tambien por la mejora en el ciclo de Krebs. Hasta donde se sabe, no hay estudios previos que evidencien el efecto del SFN sobre la desregulación del ciclo de Krebs.

La inducción de la biogénesis mitocondrial tambien potencia la bioenergética mitocondrial (Ding et al., 2018; Gureev et al., 2019). Consistente con lo anterior, se demostró al evaluar las actividades de los complejos de la cadena de transporte de electrones que el SFN aumenta la actividad del CIII en el riñón obstruído (Figura 8C). En el riñón obstruído, también se observó que los niveles proteícos de la SDHB-CII y de UQCRC2-CIII (Figura 7B,C) estaban reducidos; sin embargo, el SFN solo fue capaz de aumentar los niveles de SDH-CII (Figura 8D). La restauración en los niveles de UQCRC2-CIII por el SFN podría ser parcialmente explicada por un mecanismo mediado por AMPK, tal como se ha documentado previamente (Lu et al., 2021). Se demostró que el AMPK induce la transcripción del gen de UQCRC2 y de acuerdo a estudios previos, el SFN es capaz de inducir los niveles de AMPK (Choi et al., 2014; Z. Li et al., 2020; Z. Zhang et al., 2014). Por lo tanto, el efecto del SFN sobre los niveles de UQCRC2 podráin deberse a este mecanismo; sin embargo, se requieren estudios futuros para clarificar estos datos en el modelo de obstrucción.

Aunque para el CIII los niveles proteícos de la subunidad evaluada coinciden con su actividad, este no fue el caso para el CII. Lo anterior podría ser explicado debido a que el anticuerpo cocktel empleado para la determinación de las proteínas de la fosforilación oxidativa detecta las subunidades más lábiles de los complejos. En este caso, la subunidad detectada para el CII, la SDHB, es una proteína que contiene un grupo Fe-S, lo cual posiblemente la hace más sensible a daño por estrés oxidante, que es una característica del modelo de obstrucción (Chung et al., 2012; Lo et al., 2022); por lo tanto su disminución posiblemente se asocie a este mecanismo que muy probablemente no impacta la actividad del complejo. De acuerdo con esto último, el CII contiene otras tres subunidades que potencían su actividad (SDHA, SDHC y SDHD) que no contienen el cluster Fe-S y que evitan la disminución de la actividad del CII (Saxena et al., 2016). Por lo tanto, los niveles proteícos podrían no afectar la actividad de todo el complejo. Adicionalmente, la actividad del CII depende de la regulación metabólica, ya que es tambien una enzima que participa en el ciclo de Krebs en la conversión de succinato a fumarato (B. Moosavi et al., 2020). Contrario a lo observado con las subunidades de los CII y CIII, para el caso de la ATP5A-CV fue evidente un aumento en sus niveles en el grupo de OUU y una disminución posterior a la administración con SFN (OUU+SFN) (Figura 7F). Los datos observados fueron relacionados con un mecanismo de rescate empleado por la mitocondria para producir más ATP y de este modo evitar su despolarización, por lo que el aumento en las subunidades de la ATP sintasa podría ayudar a mantener la estructura de la membrana mitocondrial interna. De acuerdo con lo anterior, se ha descrito que el aumento en los niveles de la subunidad ATP5B, otra subunidad de la ATP sintasa, en los túbulos proximales de pacientes con obstrucción estuvo relacionado con un aumento del gasto de ATP como mecanismo de adaptación a la presión urinaria en el riñón obstruído (Görmüş et al., 2020). Además, Zhao (Q. Zhao et al., 2016) encontraron que altos niveles de la ATP5B en ratas neonatas con la OUU. Por lo tanto, los resultados obtenidos sugieren que el SFN rescata las alteraciones en la bioenergética durante la OUU.

La disfunción mitocondrial causa anormalidades en el metabolismo de los lípidos y anormalidades en el metabolismo de los lípidos causa disfunción mitocondrial (Ge et al., 2020; Rong et al., 2022). El metabolismo de los lípidos depende de su homeostasis, el cual balancea la síntesis de los lípidos y su degradación vía β-oxidación (Houten & Wanders, 2010). El PGC-1α es un regulador maestro del metabolismo de los lípidos ya que interactúa con proteínas que sensan los niveles de energía como AMPK (Lee et al., 2012; Z. Zhang et al., 2014), por lo que la disminución en los niveles de PGC-1α se relaciona con la desregulación en la homeostasis de los lípidos. En este trabajo se demostró la acumulación de TGs en el tejido renal del riñón obstruído (Figura 10C), lo cual coincide con estudios previos en los cuales se informó sobre la acumulación de éstos 24 h posteriores a la obstrucción (Tannenbaum et al., 1983), sugiriendo que las alteraciones en el metabolismo de los ácidos grasos sucede desde tiempos tempranos. Debido a que las células tubulares epiteliales dependen principalmente de la β-oxidación, las alteraciones en este proceso comunmente causa la acumulación de lípidos en forma de gotas lipídicas (Afshinnia et al., 2018). Aunque la disfunción en β-oxidación es una característica del modelo de OUU, no se encontraron diferencias significativas en los niveles de CPT1A entre el grupo de los Sham y el de OUU (Figura 10A,B). Del manera similar, el SFN no indujo cambios en el grupo de OUU+SFN.

De acuerdo con otros autores, la acumulación de TGs observada en este trabajo fue atribuída a la alta regulación de CD36 (Figura 10A,B), lo cual incrementa la entrada de AG a las células renales (Okamura et al., 2009; Souza et al., 2016). El CD36 es un receptor de membrana que comúnmente es sobreexpresado en el modelo de OUU que no solo facilita el consumo de AG sino que también está relacionado con estrés oxidante, inflamación y fibrosis, todo esto contribuyendo al proceso fibrótico en el riñón obstruído (Pennathur et al., 2015; Souza et al., 2016). Los resultados obtenidos sugieren que los altos niveles de CD36 podría influenciar la inflamación y la fibrosis. En concordancia con lo anterior, en el modelo de daño renal agudo inducido por ácido fólico, la sobreexpresión de CD36 se correlacionó con los altos niveles de Col III (Jung et al., 2018), sugiriendo que CD36 está muy

relacionado con el aumento en la fibrosis. El tratamiento con SFN en el grupo de obstrucción reveló una disminución en los niveles de CD36 (Figura 10A,B). No existen estudios previos acerca del efecto del SFN sobre CD36 en el modelo de OUU.

Los datos presentados en este trabajo sugieren que el SFN disminuye parcialmente la acumulación de los lípidos en el grupo de OUU (Figura 11A,B) y de TGs (Figura 10C); sin embargo, en el grupo tratado solo con SFN se observó una leve acumulación de lípidos. Lo anterior podría ser parcialmente explicado debido a que la disminución o la falta de CD36 se relaciona con un aumento en la cantidad de lípidos en otros tipos de células renales tales como las células endoteliales (Son et al., 2018). Además, otros autores han demostrado que la deleción de CD36 en hepatocitos se asocia con la infiltración de macrófagos (Zhong et al., 2017). Por lo tanto, se requieren niveles canónicos de CD36 para mantener la homeostasis en las células.

Nuestros resultados sugieren que la restauración del ciclo de Krebs posiblemente previene la acumulación de acetil CoA, evitando la síntesis de AGs. En este mismo sentido, la disminución en la acumulación de TGs y otros lípidos por el SFN podría ser atribuído a la reducción en los niveles de las proteínas que llevan a cabo su síntesis, tal como fue observado en los niveles de SREBP1, FASN y DGAT1 (Figura 12A,B). En el grupo de OUU se determinó la alta regulación de la proteína DGAT1, lo cual coincide con el aumento en los TGs, pues esta proteína está involucrada en la conversión de diacilglicerol a acil glicerol-CoA y triacilglicerol. La alta regulación de esta proteína es encontrada en pacientes con síndrome metabólico y obesidad (Yen et al., 2008). De este modo, el aumento de los TGs concuerda con la alta regulación de DGAT1, y la reducción de los TGs por el SFN podría ser parcialmente explicada por la regulación a la baja de DGAT1 por este antioxidante. Ciertamente, la disminución en los niveles de las proteína SREBP1 y FASN podría ser atribuida a la regulación a la baja de CD36 debido a que este receptor participa en el procesamiento de SRBP1 a través del gen 2 inducido por insulina (INSIG2) (Zeng et al., 2022), promoviendo a la transcripción de de los genes lipogénicos tales como

FASN. Mecanisticamente, la insulina activa activa a CD36 lo que promueve la formación de un complejo entre CD36 y INSIG2. Dicho complejo interrumpe la unión entre la proteína activadora de escisión de SREBP (SCAP) e INSIG2 con SREBP1, induciendo la translocación de SREBP1 desde el retículo endoplásmico al aparato de Golgi. En el aparato de Golgi, SREBP1 se procesa proteolíticamente para activarse e inducir su translocación al núcleo para promover la transcripción de FASN (Adams et al., 2004). De este modo, la regulación a la baja de CD36 podría evitar el procesamiento de SREBP1. Otros autores han reportado la regulación de la lipogénesis por el SFN. Por ejemplo, el SFN disminuye la formación de lípidos *de novo* en enfermedades coronarias (Poletto Bonetto et al., 2022)y en la enfermedad hepática no alcohólica (Choi et al., 2012, 2014).

Las alteraciones en la ultraestructura mitochondrial son posiblemente atribuida a la fisión excesiva en el modelo de OUU evidenciada por la alta regulación de DRP1 (Figura 13 A,B). En contraste, los niveles de las proteínas de fusión OPA1 y MFN2 se encontraron disminuidos (Figura 13 A,C), indicando un cambio de fusión a fisión. Los altos niveles de DRP1 concuerdan con lo reportado por otros autores (Jiménez-Uribe et al., 2021; S. Li et al., 2020). Interesantemente, el SFN solamente fue capaz de reducir los niveles de DRP1, sin efecto alguno sobre las proteínas de la fusión mitocondrial (Figura 13 A,BC). En este sentido, un estudio realizado en células epiteliales de retina demostró que el SFN evita el reclutamiento de DRP1 a través de un mecanismo que fue independiente de Nrf2 (Tian et al., 2018), sugiriendo que la interacción del SFN con DRP1 podría ser directa por lo qe estudios futuros son requeridos para determinar el efecto del SFN sobre la fisión mitocondrial.

La fisión excesiva activa el proceso mitofágico, el cual implica la remoción de mitocondrias dañadas dentro de lisosomas (Bhatia & Choi, 2019). A nivel canónico, la mitofagia se activa mediante el reclutamiento de PINK1 a la membrana mitocondrial externa bajo condiciones de estrés oxidante, despolarización de la membrana o daño mitocondrial, lo cual recluta a Parkin (Kondapalli et al., 2012). Nuestros resultados revelaron que la mitofagia es disfuncional en el grupo de OUU, determinado por el incremento el incremento en los niveles de PINK1 pero no de

Parkin, lo que sugiere que el recambio mitocondrial podría estar comprometido (Figura 14A,B). Otra posible explicación es que el proceso de mitofagia sea independiente de la vía PINK1/Parkin, lo cual concuerda con lo sugerido por Jiménez-Uribe et al. (Jiménez-Uribe et al., 2021). En el grupo de OUU, se obervó un aumento en los niveles de beclina y una disminución de Bcl2, lo que indica que la inducción del proceso autofágico; sin embargo, los altos niveles de p62 y la disminución en la relación LC3II/LC3I son también observados (Figura 14C,D). En ambos procesos, la mitofagia y la autofagia, p62 funciona como una proteína que reconoce organelos o proteínas ubiquitinados (Lippai & Lőw, 2014) pero su acumulación indica un proceso mitofágico/autofágico deficiente, lo que sugiere una alteración en el proceso de degradación del autofagolisosoma. En acordancia con lo anterior, mediante MET pudimos observar la presencia de cuerpos autofágicos en el grupo de obstrucción (Figura 15C,I,L), lo cual concuerda con datos reportados anteriormente (Jiménez-Uribe et al., 2021). El tratamiento con SFN no tuvo ningún efecto significativo sobre los niveles de PINK1 y Parkin, (Figura 14A,B) pero disminuyó los niveles de beclina y aumentó los niveles de Bcl2 y la relación LC3II/LC3I (Figura 14C,D). Por su parte, la MET no reveló la presencia de cuerpos autofágicos en el grupo de OUU+SFN (Figura 15E,F), lo que indica la restauración del flujo autofágico.

Como resumen, el SFN disminuye el daño renal inducido por la nefropatía obstructiva en el modelo de OUU a través de la restauración de la función mitocondrial mediado por la inducción de la biogénesis mitocondrial. Además, el SFN restaura el metabolismo de los lípidos, evitando su síntesis y su acumulación en el riñón obstruído (Figura 16).
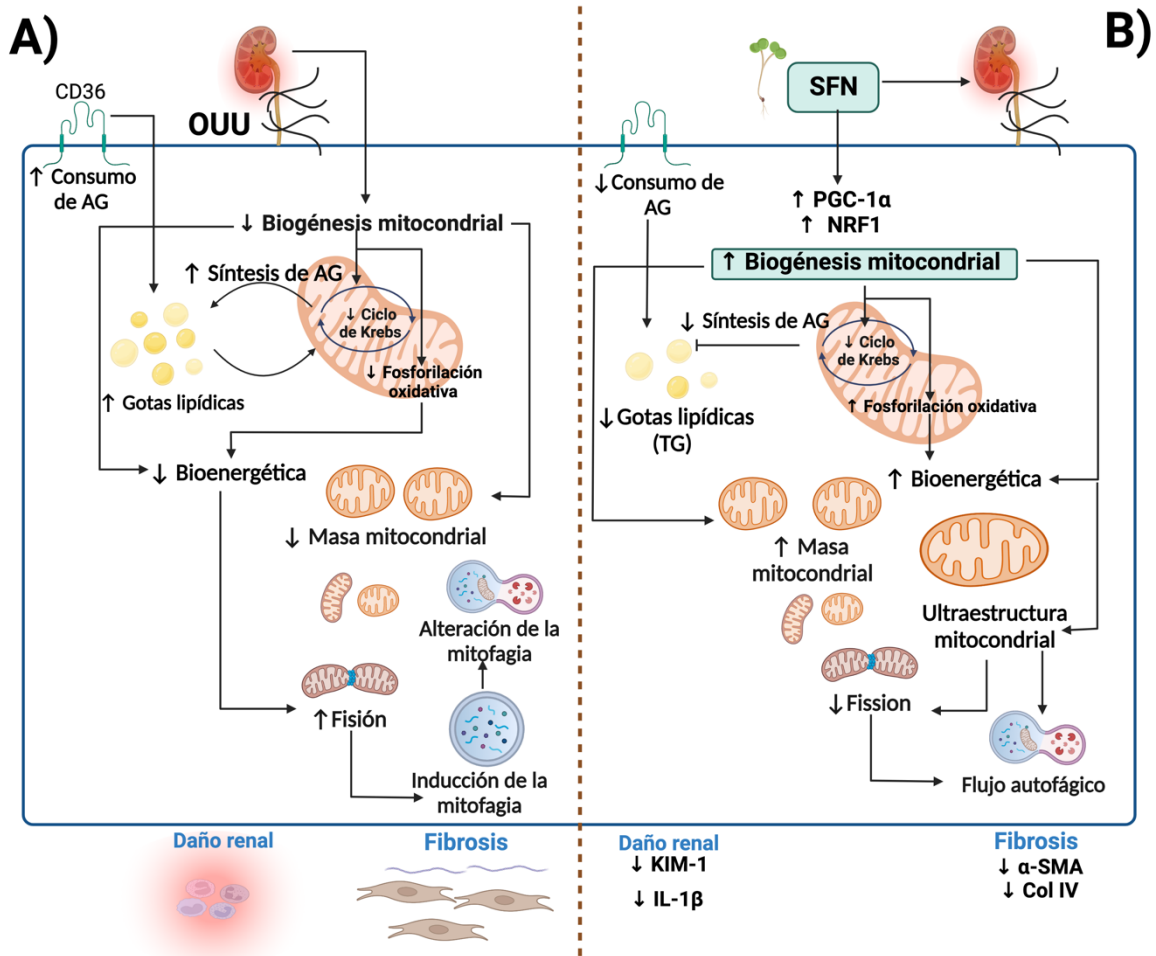
Figura 16. Figura integrativa. (A) En el modelo de obstrucción ureteral unilateral (OUU), la disfunción mitocondrial se debe principalmente a una biogénesis mitocondrial reducida, lo que lleva a una disminución de la masa mitocondrial. Además, la disminución de la biogénesis induce un deterioro bioenergético, observado por la disminución del ciclo de Krebs y la fosforilación oxidativa. La reducción del ciclo de Krebs promueve la síntesis de ácidos grasos (AG), lo que provoca la formación de gotas lipídicas, que también pueden dañar a las mitocondrias. El deterioro en la bioenergética promueve la captación de AG a través del receptor CD36, causando la acumulación de gotas lipídicas. La disminución en la bioenergética induce aún más la fisión excesiva, alterando la dinámica mitocondrial. La fisión excesiva activa la mitofagia para eliminar las mitocondrias dañadas; sin embargo, este proceso se ve afectado, lo que lleva a la acumulación de lisosomas. (B) El sulforafano (SFN) induce la biogénesis a través del coactivador 1α del receptor γ activado por el proliferador de peroxisomas (PGC-1α) y el factor respiratorio nuclear 1 (NRF1). La regulación positiva de la biogénesis restaura la estructura de las mitocondrias y las actividades del STE y el ciclo de Krebs. En consecuencia, se regula el metabolismo de los lípidos, caracterizado por la disminución de la acumulación de gotas de lípidos y la biogénesis de los lípidos. La restauración de la estructura y función de las mitocondrias reduce la fisión excesiva y regula el flujo mitofágico. KIM-1: molécula de daño renal-1; IL-1β: interleucina-1

beta; α-SMA: alfa-actina del músculo liso; Col IV: colágeno IV. ↑: aumento; ↓: disminuición.

12. CONCLUSIÓN

El SFN mejora la biogénesis mitocondrial previniendo la disfunción mitocondrial y la deposición de lípidos, lo que disminuye el daño renal y la fibrosis en el modelo de OUU. Los datos obtenidos en este trabajo podrían abrir nuevas avenidas en el uso de antioxidantes en enfermedades renales como la nefropatía obstructiva.

13. PERSPECTIVAS

1. Determinar si la administración prolongada de SFN, más allá de siete días revierte por completo la inflamación en el modelo de OUU.

2. Determinar el efecto del SFN sobre los demás componentes del ciclo de Krebs.

3. Evaluar si revertir la OUU en conjunto con la administración de SFN revierte por completo el daño renal.

14. REFERENCIAS BIBLIOGRÁFICAS

Adams, C. M., Reitz, J., Brabander, J. K. D., Feramisco, J. D., Li, L., Brown, M. S., & Goldstein, J. L. (2004). Cholesterol and 25-Hydroxycholesterol Inhibit Activation of SREBPs by Different Mechanisms, Both Involving SCAP and Insigs *. *Journal of Biological Chemistry*, *279*(50), 52772-52780. https://doi.org/10.1074/jbc.M410302200

Afshinnia, F., Rajendiran, T. M., Soni, T., Byun, J., Wernisch, S., Sas, K. M., Hawkins, J., Bellovich, K., Gipson, D., Michailidis, G., Pennathur, S., & Group, the M. K. T. C. C. I. (2018). Impaired β-Oxidation and Altered Complex Lipid Fatty Acid Partitioning with Advancing CKD. *Journal of the American Society of Nephrology*, *29*(1), 295-306. https://doi.org/10.1681/ASN.2017030350

Ai, J., Nie, J., He, J., Guo, Q., Li, M., Lei, Y., Liu, Y., Zhou, Z., Zhu, F., Liang, M., Cheng, Y., & Hou, F. F. (2015). GQ5 Hinders Renal Fibrosis in Obstructive Nephropathy by Selectively Inhibiting TGF- *β* –Induced Smad3 Phosphorylation. *Journal of the American Society of Nephrology*, *26*(8), 1827-1838. https://doi.org/10.1681/ASN.2014040363

Aparicio-Trejo, O. E., Avila-Rojas, S. H., Tapia, E., Rojas-Morales, P., León-Contreras, J. C., Martínez-Klimova, E., Hernández-Pando, R., Sánchez-Lozada, L. G., & Pedraza-Chaverri, J. (2020). Chronic impairment of mitochondrial bioenergetics and β-oxidation promotes experimental AKI-to-CKD transition induced by folic acid. *Free Radical Biology & Medicine*, *154*, 18-32. https://doi.org/10.1016/j.freeradbiomed.2020.04.016

Aparicio-Trejo, O. E., Reyes-Fermín, L. M., Briones-Herrera, A., Tapia, E., León-Contreras, J. C., Hernández-Pando, R., Sánchez-Lozada, L. G., & Pedraza-Chaverri, J. (2019a). Protective effects of N-acetyl-cysteine in mitochondria bioenergetics, oxidative stress, dynamics and S-glutathionylation alterations in acute kidney damage induced by folic acid. *Free Radical Biology and Medicine*, *130*, 379-396. https://doi.org/10.1016/j.freeradbiomed.2018.11.005

Aparicio-Trejo, O. E., Reyes-Fermín, L. M., Briones-Herrera, A., Tapia, E., León-Contreras, J. C., Hernández-Pando, R., Sánchez-Lozada, L. G., & Pedraza-Chaverri, J. (2019b). Protective effects of N-acetyl-cysteine in mitochondria bioenergetics, oxidative stress, dynamics and S-glutathionylation alterations in acute kidney damage induced by folic acid. *Free Radical Biology and Medicine*, *130*, 379-396. https://doi.org/10.1016/j.freeradbiomed.2018.11.005

Aparicio-Trejo, O. E., Rojas-Morales, P., Avila-Rojas, S. H., León-Contreras, J. C., Hernández-Pando, R., Jiménez-Uribe, A. P., Prieto-Carrasco, R., Sánchez-Lozada, L. G., Pedraza-Chaverri, J., & Tapia, E. (2020). Temporal Alterations in Mitochondrial β-Oxidation and Oxidative Stress Aggravate Chronic Kidney Disease Development in 5/6 Nephrectomy Induced Renal Damage. *International Journal of Molecular Sciences*, *21*(18), Article 18. https://doi.org/10.3390/ijms21186512

Aparicio-Trejo, O. E., Tapia, E., Molina-Jijón, E., Medina-Campos, O. N., Macías-Ruvalcaba, N. A., León-Contreras, J. C., Hernández-Pando, R., García-Arroyo, F. E., Cristóbal, M., Sánchez-Lozada, L. G., & Pedraza-Chaverri, J. (2017). Curcumin prevents mitochondrial dynamics disturbances in early 5/6 nephrectomy: Relation to oxidative stress and mitochondrial bioenergetics: Curcumin prevents mitochondrial dynamics disturbances. *BioFactors*, *43*(2), 293-310. https://doi.org/10.1002/biof.1338

Aranda-Rivera, A. K., Cruz-Gregorio, A., Aparicio-Trejo, O. E., & Pedraza-Chaverri, J. (2021). Mitochondrial Redox Signaling and Oxidative Stress in Kidney Diseases. *Biomolecules*, *11*(8), 1144. https://doi.org/10.3390/biom11081144

Avila-Rojas, S. H., Aparicio-Trejo, O. E., Briones-Herrera, A., Medina-Campos, O. N., Reyes-Fermín, L. M., Martínez-Klimova, E., León-Contreras, J. C., Hernández-Pando, R., Tapia, E., & Pedraza-Chaverri, J. (2020). Alterations in mitochondrial homeostasis in a potassium dichromate model of acute kidney injury and their mitigation by curcumin. *Food and Chemical Toxicology*, *145*, 111774. https://doi.org/10.1016/j.fct.2020.111774

Bhargava, P., & Schnellmann, R. G. (2017). Mitochondrial energetics in the kidney. *Nature Reviews Nephrology*, *13*(10), 629-646. https://doi.org/10.1038/nrneph.2017.107

Bhatia, D., & Choi, M. E. (2019). The Emerging Role of Mitophagy in Kidney Diseases. *Journal of life sciences (Westlake Village, Calif.)*, *1*(3), 13-22. https://doi.org/10.36069/jols/20191203

Braga, P. C., Alves, M. G., Rodrigues, A. S., & Oliveira, P. F. (2022). Mitochondrial Pathophysiology on Chronic Kidney Disease. *International Journal of Molecular Sciences*, *23*(3), 1776. https://doi.org/10.3390/ijms23031776

Briones-Herrera, A., Avila-Rojas, S. H., Aparicio-Trejo, O. E., Cristóbal, M., León-Contreras, J. C., Hernández-Pando, R., Pinzón, E., Pedraza-Chaverri, J., Sánchez-Lozada, L. G., & Tapia, E. (2018). Sulforaphane prevents maleic acid-induced nephropathy by modulating renal hemodynamics, mitochondrial bioenergetics and oxidative stress. *Food and Chemical Toxicology: An International Journal Published for the British Industrial Biological Research Association*, *115*, 185-197. https://doi.org/10.1016/j.fct.2018.03.016

Briones-Herrera, A., Ramírez-Camacho, I., Zazueta, C., Tapia, E., & Pedraza-Chaverri, J. (2020). Altered proximal tubule fatty acid utilization, mitophagy, fission and supercomplexes arrangement in experimental Fanconi syndrome are ameliorated by sulforaphane-induced mitochondrial biogenesis. *Free Radical Biology & Medicine*, *153*, 54-70. https://doi.org/10.1016/j.freeradbiomed.2020.04.010

Brooks, C., Wei, Q., Cho, S.-G., & Dong, Z. (2009). Regulation of mitochondrial dynamics in acute kidney injury in cell culture and rodent models. *The Journal of Clinical Investigation*, *119*(5), 1275-1285. https://doi.org/10.1172/JCI37829

Cantu, D., Schaack, J., & Patel, M. (2009). Oxidative Inactivation of Mitochondrial Aconitase Results in Iron and H2O2-Mediated Neurotoxicity in Rat Primary Mesencephalic Cultures. *PLOS ONE*, *4*(9), e7095. https://doi.org/10.1371/journal.pone.0007095

Carney, E. F. (2020). The impact of chronic kidney disease on global health. *Nature Reviews. Nephrology*, *16*(5), 251. https://doi.org/10.1038/s41581-020-0268-7

Chen, J.-F., Liu, H., Ni, H.-F., Lv, L.-L., Zhang, M.-H., Zhang, A.-H., Tang, R.-N., Chen, P.-S., & Liu, B.-C. (2013). Improved Mitochondrial Function Underlies the Protective Effect of Pirfenidone against Tubulointerstitial Fibrosis in 5/6 Nephrectomized Rats. *PLoS ONE*, *8*(12), e83593. https://doi.org/10.1371/journal.pone.0083593

Chen, T., Li, J., Liu, J., Li, N., Wang, S., Liu, H., Zeng, M., Zhang, Y., & Bu, P. (2015). Activation of SIRT3 by resveratrol ameliorates cardiac fibrosis and improves cardiac function via the TGF-β/Smad3 pathway. *American Journal of Physiology-Heart and Circulatory Physiology*, *308*(5), H424-H434. https://doi.org/10.1152/ajpheart.00454.2014

Cheng, X., Zheng, X., Song, Y., Qu, L., Tang, J., Meng, L., & Wang, Y. (2016). Apocynin attenuates renal fibrosis via inhibition of NOXs-ROS-ERK-myofibroblast accumulation in UUO rats. *Free Radical Research*, *50*(8), 840-852. https://doi.org/10.1080/10715762.2016.1181757

Chevalier, R. L. (2004). Perinatal Obstructive Nephropathy. *Seminars in Perinatology*, *28*(2), 124-131. https://doi.org/10.1053/j.semperi.2003.11.009

Chevalier, R. L. (2008). Chronic partial ureteral obstruction and the developing kidney.

Pediatric Radiology, *38*(S1), 35-40. https://doi.org/10.1007/s00247-007-0585-z

Chevalier, R. L., Forbes, M. S., & Thornhill, B. A. (2009). Ureteral obstruction as a model of renal interstitial fibrosis and obstructive nephropathy. *Kidney International*, *75*(11), 1145-1152. https://doi.org/10.1038/ki.2009.86

Cho, H.-Y., Miller-DeGraff, L., Blankenship-Paris, T., Wang, X., Bell, D. A., Lih, F., Deterding, L., Panduri, V., Morgan, D. L., Yamamoto, M., Reddy, A. J., Talalay, P., & Kleeberger, S. R. (2019). Sulforaphane enriched transcriptome of lung mitochondrial energy metabolism and provided pulmonary injury protection via Nrf2 in mice. *Toxicology and Applied Pharmacology*, *364*, 29-44. https://doi.org/10.1016/j.taap.2018.12.004

Choi, K.-M., Lee, Y.-S., Kim, W., Kim, S. J., Shin, K.-O., Yu, J.-Y., Lee, M. K., Lee, Y.-M., Hong, J. T., Yun, Y.-P., & Yoo, H.-S. (2014). Sulforaphane attenuates obesity by inhibiting adipogenesis and activating the AMPK pathway in obese mice. *The Journal of Nutritional Biochemistry*, *25*(2), 201-207. https://doi.org/10.1016/j.jnutbio.2013.10.007

Choi, K.-M., Lee, Y.-S., Sin, D.-M., Lee, S., Lee, M. K., Lee, Y.-M., Hong, J.-T., Yun, Y.-P., & Yoo, H.-S. (2012). Sulforaphane Inhibits Mitotic Clonal Expansion During Adipogenesis Through Cell Cycle Arrest. *Obesity*, *20*(7), 1365-1371. https://doi.org/10.1038/oby.2011.388

Chung, S. D., Lai, T. Y., Chien, C. T., & Yu, H. J. (2012). Activating Nrf-2 Signaling Depresses Unilateral Ureteral Obstruction-Evoked Mitochondrial Stress-Related Autophagy, Apoptosis and Pyroptosis in Kidney. *PLOS ONE*, *7*(10), e47299. https://doi.org/10.1371/journal.pone.0047299

de Oliveira, M. R., de Bittencourt Brasil, F., & Fürstenau, C. R. (2018). Sulforaphane Promotes Mitochondrial Protection in SH-SY5Y Cells Exposed to Hydrogen Peroxide by an Nrf2-Dependent Mechanism. *Molecular Neurobiology*, *55*(6), 4777-4787. https://doi.org/10.1007/s12035-017-0684-2

Diamond, J. R., Kees-Folts, D., Ricardo, S. D., Pruznak, A., & Eufemio, M. (1995). Early and persistent up-regulated expression of renal cortical osteopontin in experimental hydronephrosis. *The American Journal of Pathology*, *146*(6), 1455-1466.

Ding, H., Bai, F., Cao, H., Xu, J., Fang, L., Wu, J., Yuan, Q., Zhou, Y., Sun, Q., He, W., Dai, C., Zen, K., Jiang, L., & Yang, J. (2018). PDE/cAMP/Epac/C/EBP-β Signaling Cascade Regulates Mitochondria Biogenesis of Tubular Epithelial Cells in Renal Fibrosis. *Antioxidants & Redox Signaling*, *29*(7), 637-652. https://doi.org/10.1089/ars.2017.7041

Fedorova, L. V., Tamirisa, A., Kennedy, D. J., Haller, S. T., Budnyy, G., Shapiro, J. I., & Malhotra, D. (2013). Mitochondrial impairment in the five-sixth nephrectomy model of chronic renal failure: Proteomic approach. *BMC Nephrology*, *14*(1), 209. https://doi.org/10.1186/1471-2369-14-209

Feingold, K. R., Wang, Y., Moser, A., Shigenaga, J. K., & Grunfeld, C. (2008). LPS decreases fatty acid oxidation and nuclear hormone receptors in the kidney. *Journal of Lipid Research*, *49*(10), 2179-2187. https://doi.org/10.1194/jlr.M800233-JLR200

Fogo, A. B., Cohen, A. H., Colvin, R. B., Jennette, J. C., & Alpers, C. E. (2014). *Fundamentals of Renal Pathology*. Springer Berlin Heidelberg. https://doi.org/10.1007/978-3-642-39080-7

Folch, J., Lees, M., & Sloane Stanley, G. H. (1957). A simple method for the isolation and purification of total lipides from animal tissues. *The Journal of Biological Chemistry*, *226*(1), 497-509.

Fontecha-Barriuso, M., Martin-Sanchez, D., Martinez-Moreno, J. M., Monsalve, M., Ramos, A. M., Sanchez-Niño, M. D., Ruiz-Ortega, M., Ortiz, A., & Sanz, A. B. (2020).

The Role of PGC-1α and Mitochondrial Biogenesis in Kidney Diseases. *Biomolecules*, *10*(2), Article 2. https://doi.org/10.3390/biom10020347

Forbes, J. M. (2016). Mitochondria–Power Players in Kidney Function? *Trends in Endocrinology & Metabolism*, *27*(7), 441-442. https://doi.org/10.1016/j.tem.2016.05.002

Forbes, J. M., & Thorburn, D. R. (2018). Mitochondrial dysfunction in diabetic kidney disease. *Nature Reviews Nephrology*, *14*(5), 291-312. https://doi.org/10.1038/nrneph.2018.9

Foreman, K. J., Marquez, N., Dolgert, A., Fukutaki, K., Fullman, N., McGaughey, M., Pletcher, M. A., Smith, A. E., Tang, K., Yuan, C.-W., Brown, J. C., Friedman, J., He, J., Heuton, K. R., Holmberg, M., Patel, D. J., Reidy, P., Carter, A., Cercy, K., … Murray, C. J. L. (2018). Forecasting life expectancy, years of life lost, and all-cause and cause-specific mortality for 250 causes of death: Reference and alternative scenarios for 2016–40 for 195 countries and territories. *The Lancet*, *392*(10159), 2052-2090. https://doi.org/10.1016/S0140-6736(18)31694-5

Gai, Z., Wang, T., Visentin, M., Kullak-Ublick, G. A., Fu, X., & Wang, Z. (2019). Lipid Accumulation and Chronic Kidney Disease. *Nutrients*, *11*(4), 722. https://doi.org/10.3390/nu11040722

Galvan, D. L., Green, N. H., & Danesh, F. R. (2017). The hallmarks of mitochondrial dysfunction in chronic kidney disease. *Kidney International*, *92*(5), 1051-1057. https://doi.org/10.1016/j.kint.2017.05.034

Ge, M., Fontanesi, F., Merscher, S., & Fornoni, A. (2020). The Vicious Cycle of Renal Lipotoxicity and Mitochondrial Dysfunction. *Frontiers in Physiology*, *11*. https://www.frontiersin.org/articles/10.3389/fphys.2020.00732

Girardi, M., & Martin, N. (2015). Obstructive Uropathy. *Hospital Medicine Clinics*, *4*(3), 328-341. https://doi.org/10.1016/j.ehmc.2015.03.010

Görmüş, U., Kasap, M., Akpınar, G., Tuğtepe, H., Kanlı, A., & Özel, K. (2020). Comparative Proteome Analyses of Ureteropelvic Junction Obstruction and Surrounding Ureteral Tissue. *Cells Tissues Organs*, *209*(1), 2-12. https://doi.org/10.1159/000506736

Guarino, F., Zinghirino, F., Mela, L., Pappalardo, X. G., Ichas, F., De Pinto, V., & Messina, A. (2020). NRF-1 and HIF-1α contribute to modulation of human VDAC1 gene promoter during starvation and hypoxia in HeLa cells. *Biochimica et Biophysica Acta (BBA) - Bioenergetics*, *1861*(12), 148289. https://doi.org/10.1016/j.bbabio.2020.148289

Guebre-Egziabher, F., Alix, P. M., Koppe, L., Pelletier, C. C., Kalbacher, E., Fouque, D., & Soulage, C. O. (2013). Ectopic lipid accumulation: A potential cause for metabolic disturbances and a contributor to the alteration of kidney function. *Biochimie*, *95*(11), 1971-1979. https://doi.org/10.1016/j.biochi.2013.07.017

Guerrero-Beltrán, C. E., Calderón-Oliver, M., Martínez-Abundis, E., Tapia, E., Zarco-Márquez, G., Zazueta, C., & Pedraza-Chaverri, J. (2010). Protective effect of sulforaphane against cisplatin-induced mitochondrial alterations and impairment in the activity of NAD(P)H: Quinone oxidoreductase 1 and γ glutamyl cysteine ligase: Studies in mitochondria isolated from rat kidney and in LLC-PK1 cells. *Toxicology Letters*, *199*(1), 80-92. https://doi.org/10.1016/j.toxlet.2010.08.009

Guerrero-Beltrán, C. E., Calderón-Oliver, M., Pedraza-Chaverri, J., & Chirino, Y. I. (2012). Protective effect of sulforaphane against oxidative stress: Recent advances. *Experimental and Toxicologic Pathology*, *64*(5), 503-508. https://doi.org/10.1016/j.etp.2010.11.005

Guo, H., Bi, X., Zhou, P., Zhu, S., & Ding, W. (2017). NLRP3 Deficiency Attenuates Renal Fibrosis and Ameliorates Mitochondrial Dysfunction in a Mouse Unilateral Ureteral

Obstruction Model of Chronic Kidney Disease. *Mediators of Inflammation*, *2017*, 8316560. https://doi.org/10.1155/2017/8316560

Gureev, A. P., Shaforostova, E. A., & Popov, V. N. (2019). Regulation of Mitochondrial Biogenesis as a Way for Active Longevity: Interaction Between the Nrf2 and PGC-1α Signaling Pathways. *Frontiers in Genetics*, *10*. https://www.frontiersin.org/articles/10.3389/fgene.2019.00435

Hallan, S., & Sharma, K. (2016). The Role of Mitochondria in Diabetic Kidney Disease. *Current Diabetes Reports*, *16*(7), 61. https://doi.org/10.1007/s11892-016-0748-0

Herman-Edelstein, M., Scherzer, P., Tobar, A., Levi, M., & Gafter, U. (2014). Altered renal lipid metabolism and renal lipid accumulation in human diabetic nephropathy. *Journal of Lipid Research*, *55*(3), 561-572. https://doi.org/10.1194/jlr.P040501

Houten, S. M., & Wanders, R. J. A. (2010). A general introduction to the biochemistry of mitochondrial fatty acid β-oxidation. *Journal of Inherited Metabolic Disease*, *33*(5), 469-477. https://doi.org/10.1007/s10545-010-9061-2

Idrovo, J.-P., Yang, W.-L., Nicastro, J., Coppa, G. F., & Wang, P. (2012). Stimulation of carnitine palmitoyltransferase 1 improves renal function and attenuates tissue damage after ischemia/reperfusion. *The Journal of Surgical Research*, *177*(1), 157-164. https://doi.org/10.1016/j.jss.2012.05.053

Irazabal, M. V., Chade, A. R., & Eirin, A. (2022). Renal mitochondrial injury in the pathogenesis of CKD: mtDNA and mitomiRs. *Clinical Science (London, England: 1979)*, *136*(5), 345-360. https://doi.org/10.1042/CS20210512

Irrcher, I., Ljubicic, V., & Hood, D. A. (2009). Interactions between ROS and AMP kinase activity in the regulation of PGC-1alpha transcription in skeletal muscle cells. *American Journal of Physiology. Cell Physiology*, *296*(1), C116-123. https://doi.org/10.1152/ajpcell.00267.2007

Ishii, T., Itoh, K., Ruiz, E., Leake, D. S., Unoki, H., Yamamoto, M., & Mann, G. E. (2004). Role of Nrf2 in the regulation of CD36 and stress protein expression in murine macrophages: Activation by oxidatively modified LDL and 4-hydroxynonenal. *Circulation Research*, *94*(5), 609-616. https://doi.org/10.1161/01.RES.0000119171.44657.45

Jiang, H., Shao, X., Jia, S., Qu, L., Weng, C., Shen, X., Wang, Y., Huang, H., Wang, Y., Wang, C., Feng, S., Wang, M., Feng, H., Geekiyanage, S., Davidson, A. J., & Chen, J. (2019). The Mitochondria-Targeted Metabolic Tubular Injury in Diabetic Kidney Disease. *Cellular Physiology and Biochemistry: International Journal of Experimental Cellular Physiology, Biochemistry, and Pharmacology*, *52*(2), 156-171. https://doi.org/10.33594/000000011

Jiménez-Uribe, A. P., Bellido, B., Aparicio-Trejo, O. E., Tapia, E., Sánchez-Lozada, L. G., Hernández-Santos, J. A., Fernández-Valverde, F., Hernández-Cruz, E. Y., Orozco-Ibarra, M., & Pedraza-Chaverri, J. (2021). Temporal characterization of mitochondrial impairment in the unilateral ureteral obstruction model in rats. *Free Radical Biology and Medicine*, *172*, 358-371. https://doi.org/10.1016/j.freeradbiomed.2021.06.019

Jung, J. H., Choi, J. E., Song, J. H., & Ahn, S.-H. (2018). Human CD36 overexpression in renal tubules accelerates the progression of renal diseases in a mouse model of folic acid-induced acute kidney injury. *Kidney Research and Clinical Practice*, *37*(1), 30-40. https://doi.org/10.23876/j.krcp.2018.37.1.30

Kang, H. M., Ahn, S. H., Choi, P., Ko, Y.-A., Han, S. H., Chinga, F., Park, A. S. D., Tao, J., Sharma, K., Pullman, J., Bottinger, E. P., Goldberg, I. J., & Susztak, K. (2015). Defective fatty acid oxidation in renal tubular epithelial cells has a key role in kidney

fibrosis development. *Nature Medicine*, *21*(1), Article 1. https://doi.org/10.1038/nm.3762

Keum, Y.-S., Jeong, W.-S., & Kong, A. N. T. (2004). Chemoprevention by isothiocyanates and their underlying molecular signaling mechanisms. *Mutation Research*, *555*(1-2), 191-202. https://doi.org/10.1016/j.mrfmmm.2004.05.024

Kim, J. I., Noh, M. R., Yoon, G.-E., Jang, H.-S., Kong, M. J., & Park, and K. M. (2021). IDH2 gene deficiency accelerates unilateral ureteral obstruction-induced kidney inflammation through oxidative stress and activation of macrophages. *The Korean Journal of Physiology & Pharmacology*, *25*(2), 139-146. https://doi.org/10.4196/kjpp.2021.25.2.139

Kondapalli, C., Kazlauskaite, A., Zhang, N., Woodroof, H. I., Campbell, D. G., Gourlay, R., Burchell, L., Walden, H., Macartney, T. J., Deak, M., Knebel, A., Alessi, D. R., & Muqit, M. M. K. (2012). PINK1 is activated by mitochondrial membrane potential depolarization and stimulates Parkin E3 ligase activity by phosphorylating Serine 65. *Open Biology*, *2*(5), 120080. https://doi.org/10.1098/rsob.120080

Kong, M. J., Han, S. J., Kim, J. I., Park, J.-W., & Park, K. M. (2018). Mitochondrial NADP+-dependent isocitrate dehydrogenase deficiency increases cisplatin-induced oxidative damage in the kidney tubule cells. *Cell Death & Disease*, *9*(5), 488. https://doi.org/10.1038/s41419-018-0537-6

Kovesdy, C. P. (2022). Epidemiology of chronic kidney disease: An update 2022. *Kidney International Supplements*, *12*(1), 7-11. https://doi.org/10.1016/j.kisu.2021.11.003

Kume, S., Uzu, T., Araki, S., Sugimoto, T., Isshiki, K., Chin-Kanasaki, M., Sakaguchi, M., Kubota, N., Terauchi, Y., Kadowaki, T., Haneda, M., Kashiwagi, A., & Koya, D. (2007). Role of Altered Renal Lipid Metabolism in the Development of Renal Injury Induced by a High-Fat Diet. *Journal of the American Society of Nephrology*, *18*(10), 2715-2723. https://doi.org/10.1681/ASN.2007010089

LeBleu, V. S., Taduri, G., O'Connell, J., Teng, Y., Cooke, V. G., Woda, C., Sugimoto, H., & Kalluri, R. (2013). Origin and function of myofibroblasts in kidney fibrosis. *Nature Medicine*, *19*(8), Article 8. https://doi.org/10.1038/nm.3218

Lee, J.-H., Moon, M.-H., Jeong, J.-K., Park, Y.-G., Lee, Y.-J., Seol, J.-W., & Park, S.-Y. (2012). Sulforaphane induced adipolysis via hormone sensitive lipase activation, regulated by AMPK signaling pathway. *Biochemical and Biophysical Research Communications*, *426*(4), 492-497. https://doi.org/10.1016/j.bbrc.2012.08.107

Lei, P., Tian, S., Teng, C., Huang, L., Liu, X., Wang, J., Zhang, Y., Li, B., & Shan, Y. (2019). Sulforaphane Improves Lipid Metabolism by Enhancing Mitochondrial Function and Biogenesis In Vivo and In Vitro. *Molecular Nutrition & Food Research*, *63*(4), 1800795. https://doi.org/10.1002/mnfr.201800795

Levey, A. S., & Coresh, J. (2012). Chronic kidney disease. *The Lancet*, *379*(9811), 165-180. https://doi.org/10.1016/S0140-6736(11)60178-5

Lewy, P. R., Quintanilla, A., Levin, N. W., & Kessler, R. H. (1973). Renal Energy Metabolism and Sodium Reabsorption. *Annual Review of Medicine*, *24*(1), 365-384. https://doi.org/10.1146/annurev.me.24.020173.002053

Li, S., Lin, Q., Shao, X., Zhu, X., Wu, J., Wu, B., Zhang, M., Zhou, W., Zhou, Y., Jin, H., Zhang, Z., Qi, C., Shen, J., Mou, S., Gu, L., & Ni, Z. (2020). Drp1-regulated PARK2-dependent mitophagy protects against renal fibrosis in unilateral ureteral obstruction. *Free Radical Biology & Medicine*, *152*, 632-649. https://doi.org/10.1016/j.freeradbiomed.2019.12.005

Li, Y., Sha, Z., & Peng, H. (2021). Metabolic Reprogramming in Kidney Diseases:

Evidence and Therapeutic Opportunities. *International Journal of Nephrology*, *2021*, 5497346. https://doi.org/10.1155/2021/5497346

Li, Z. (2012). Development and verification of sulforaphane extraction method in cabbage (Brassica oleracea L. var. Capitata) and broccoli (Brassica oleracea L. var. Italica Planch.). *Journal of Medicinal Plants Research*, *6*(33). https://doi.org/10.5897/JMPR12.229

Li, Z., Guo, H., Li, J., Ma, T., Zhou, S., Zhang, Z., Miao, L., & Cai, L. (2020). Sulforaphane prevents type 2 diabetes-induced nephropathy via AMPK-mediated activation of lipid metabolic pathways and Nrf2 antioxidative function. *Clinical Science (London, England: 1979)*, *134*(18), 2469-2487. https://doi.org/10.1042/CS20191088

Liesa, M., & Shirihai, O. S. (2013). Mitochondrial dynamics in the regulation of nutrient utilization and energy expenditure. *Cell Metabolism*, *17*(4), 491-506. https://doi.org/10.1016/j.cmet.2013.03.002

Ling, L., Yang, M., Ding, W., & Gu, Y. (2019). Ghrelin attenuates UUO-induced renal fibrosis via attenuation of Nlrp3 inflammasome and endoplasmic reticulum stress. *American Journal of Translational Research*, *11*(1), 131-141.

Lippai, M., & Lőw, P. (2014). The Role of the Selective Adaptor p62 and Ubiquitin-Like Proteins in Autophagy. *BioMed Research International*, *2014*, e832704. https://doi.org/10.1155/2014/832704

Liu, H., Li, W., He, Q., Xue, J., Wang, J., Xiong, C., Pu, X., & Nie, Z. (2017). Mass Spectrometry Imaging of Kidney Tissue Sections of Rat Subjected to Unilateral Ureteral Obstruction. *Scientific Reports*, *7*, 41954. https://doi.org/10.1038/srep41954

Liu, Y. (2006). Renal fibrosis: New insights into the pathogenesis and therapeutics. *Kidney International*, *69*(2), 213-217. https://doi.org/10.1038/sj.ki.5000054

Lo, Y.-H., Yang, S.-F., Cheng, C.-C., Hsu, K.-C., Chen, Y.-S., Chen, Y.-Y., Wang, C.-W., Guan, S.-S., & Wu, C.-T. (2022). Nobiletin Alleviates Ferroptosis-Associated Renal Injury, Inflammation, and Fibrosis in a Unilateral Ureteral Obstruction Mouse Model. *Biomedicines*, *10*(3), Article 3. https://doi.org/10.3390/biomedicines10030595

Lu, X., Xuan, W., Li, J., Yao, H., Huang, C., & Li, J. (2021). AMPK protects against alcohol-induced liver injury through UQCRC2 to up-regulate mitophagy. *Autophagy*, *17*(11), 3622-3643. https://doi.org/10.1080/15548627.2021.1886829

Martínez-Klimova, E., Aparicio-Trejo, O. E., Gómez-Sierra, T., Jiménez-Uribe, A. P., Bellido, B., & Pedraza-Chaverri, J. (2020). Mitochondrial dysfunction and endoplasmic reticulum stress in the promotion of fibrosis in obstructive nephropathy induced by unilateral ureteral obstruction. *BioFactors*, *46*(5), 716-733. https://doi.org/10.1002/biof.1673

Martínez-Klimova, E., Aparicio-Trejo, O. E., Tapia, E., & Pedraza-Chaverri, J. (2019). Unilateral Ureteral Obstruction as a Model to Investigate Fibrosis-Attenuating Treatments. *Biomolecules*, *9*(4), 141. https://doi.org/10.3390/biom9040141

Matovinović, M. S. (2009). 1. Pathophysiology and Classification of Kidney Diseases. *EJIFCC*, *20*(1), 2-11.

Meguid El Nahas, A., & Bello, A. K. (2005). Chronic kidney disease: The global challenge. *Lancet (London, England)*, *365*(9456), 331-340. https://doi.org/10.1016/S0140-6736(05)17789-7

Miguel, V., Tituaña, J., Herrero, J. I., Herrero, L., Serra, D., Cuevas, P., Barbas, C., Puyol, D. R., Márquez-Expósito, L., Ruiz-Ortega, M., Castillo, C., Sheng, X., Susztak, K., Ruiz-Canela, M., Salas-Salvadó, J., González, M. A. M., Ortega, S., Ramos, R., & Lamas, S. (2021). Renal tubule Cpt1a overexpression protects from kidney fibrosis by restoring

mitochondrial homeostasis. *The Journal of Clinical Investigation*, *131*(5). https://doi.org/10.1172/JCI140695

Mohammad, R. S., Lokhandwala, M. F., & Banday, A. A. (2022). Age-Related Mitochondrial Impairment and Renal Injury Is Ameliorated by Sulforaphane via Activation of Transcription Factor NRF2. *Antioxidants*, *11*(1), Article 1. https://doi.org/10.3390/antiox11010156

Moosavi, B., Zhu, X.-L., Yang, W.-C., & Yang, G.-F. (2020). Genetic, epigenetic and biochemical regulation of succinate dehydrogenase function. *Biological Chemistry*, *401*(3), 319-330. https://doi.org/10.1515/hsz-2019-0264

Moosavi, S. M. S., Ashtiyani, S. C., Hosseinkhani, S., & Shirazi, M. (2010). Comparison of the effects of l-carnitine and α-tocopherol on acute ureteral obstruction-induced renal oxidative imbalance and altered energy metabolism in rats. *Urological Research*, *38*(3), 187-194. https://doi.org/10.1007/s00240-009-0238-9

Negrette-Guzmán, M., García-Niño, W. R., Tapia, E., Zazueta, C., Huerta-Yepez, S., León-Contreras, J. C., Hernández-Pando, R., Aparicio-Trejo, O. E., Madero, M., & Pedraza-Chaverri, J. (2015). Curcumin Attenuates Gentamicin-Induced Kidney Mitochondrial Alterations: Possible Role of a Mitochondrial Biogenesis Mechanism. *Evidence-Based Complementary and Alternative Medicine*, *2015*, 1-16. https://doi.org/10.1155/2015/917435

Nielsen, S., Kwon, T.-H., Fenton, R. A., & Prætorious, J. (2012). Anatomy of the Kidney. En *Brenner and Rector's The Kidney* (pp. 31-93). Elsevier. https://doi.org/10.1016/B978-1-4160-6193-9.10002-8

Nishikawa, T., Edelstein, D., Du, X. L., Yamagishi, S., Matsumura, T., Kaneda, Y., Yorek, M. A., Beebe, D., Oates, P. J., Hammes, H.-P., Giardino, I., & Brownlee, M. (2000). Normalizing mitochondrial superoxide production blocks three pathways of hyperglycaemic damage. *Nature*, *404*(6779), 787-790. https://doi.org/10.1038/35008121

Okamura, D. M., Pennathur, S., Pasichnyk, K., López-Guisa, J. M., Collins, S., Febbraio, M., Heinecke, J., & Eddy, A. A. (2009). CD36 regulates oxidative stress and inflammation in hypercholesterolemic CKD. *Journal of the American Society of Nephrology: JASN*, *20*(3), 495-505. https://doi.org/10.1681/ASN.2008010009

Opazo-Ríos, L., Mas, S., Marín-Royo, G., Mezzano, S., Gómez-Guerrero, C., Moreno, J. A., & Egido, J. (2020). Lipotoxicity and Diabetic Nephropathy: Novel Mechanistic Insights and Therapeutic Opportunities. *International Journal of Molecular Sciences*, *21*(7), Article 7. https://doi.org/10.3390/ijms21072632

Patti, M. E., Butte, A. J., Crunkhorn, S., Cusi, K., Berria, R., Kashyap, S., Miyazaki, Y., Kohane, I., Costello, M., Saccone, R., Landaker, E. J., Goldfine, A. B., Mun, E., DeFronzo, R., Finlayson, J., Kahn, C. R., & Mandarino, L. J. (2003). Coordinated reduction of genes of oxidative metabolism in humans with insulin resistance and diabetes: Potential role of PGC1 and NRF1. *Proceedings of the National Academy of Sciences*, *100*(14), 8466-8471. https://doi.org/10.1073/pnas.1032913100

Pennathur, S., Pasichnyk, K., Bahrami, N. M., Zeng, L., Febbraio, M., Yamaguchi, I., & Okamura, D. M. (2015). The Macrophage Phagocytic Receptor CD36 Promotes Fibrogenic Pathways on Removal of Apoptotic Cells during Chronic Kidney Injury. *The American Journal of Pathology*, *185*(8), 2232-2245. https://doi.org/10.1016/j.ajpath.2015.04.016

Poletto Bonetto, J. H., Luz de Castro, A., Fernandes, R. O., Corssac, G. B., Cordero, E. A., Schenkel, P. C., Sander da Rosa Araujo, A., & Belló-Klein, A. (2022). Sulforaphane Effects on Cardiac Function and Calcium-Handling–Related Proteins in 2 Experimental

Models of Heart Disease: Ischemia-Reperfusion and Infarction. *Journal of Cardiovascular Pharmacology*, *79*(3), 325. https://doi.org/10.1097/FJC.0000000000001191

Prieto-Carrasco, R., García-Arroyo, F. E., Aparicio-Trejo, O. E., Rojas-Morales, P., León-Contreras, J. C., Hernández-Pando, R., Sánchez-Lozada, L. G., Tapia, E., & Pedraza-Chaverri, J. (2021). Progressive Reduction in Mitochondrial Mass Is Triggered by Alterations in Mitochondrial Biogenesis and Dynamics in Chronic Kidney Disease Induced by 5/6 Nephrectomy. *Biology*, *10*(5), 349. https://doi.org/10.3390/biology10050349

Ren, Y., Chen, J., Chen, P., Hao, Q., Cheong, L.-K., Tang, M., Hong, L.-L., Hu, X.-Y., Celestial T Yap, Bay, B.-H., Ling, Z.-Q., & Shen, H.-M. (2021). Oxidative stress-mediated AMPK inactivation determines the high susceptibility of LKB1-mutant NSCLC cells to glucose starvation. *Free Radical Biology and Medicine*, *166*, 128-139. https://doi.org/10.1016/j.freeradbiomed.2021.02.018

Reyes-Fermín, L. M., Avila-Rojas, S. H., Aparicio-Trejo, O. E., Tapia, E., Rivero, I., & Pedraza-Chaverri, J. (2019). The Protective Effect of Alpha-Mangostin against Cisplatin-Induced Cell Death in LLC-PK1 Cells is Associated to Mitochondrial Function Preservation. *Antioxidants*, *8*(5), Article 5. https://doi.org/10.3390/antiox8050133

Romagnani, P., Remuzzi, G., Glassock, R., Levin, A., Jager, K. J., Tonelli, M., Massy, Z., Wanner, C., & Anders, H.-J. (2017). Chronic kidney disease. *Nature Reviews. Disease Primers*, *3*, 17088. https://doi.org/10.1038/nrdp.2017.88

Rong, Q., Han, B., Li, Y., Yin, H., Li, J., & Hou, Y. (2022). Berberine Reduces Lipid Accumulation by Promoting Fatty Acid Oxidation in Renal Tubular Epithelial Cells of the Diabetic Kidney. *Frontiers in Pharmacology*, *12*. https://www.frontiersin.org/articles/10.3389/fphar.2021.729384

Ruiz-Ortega, M., Rayego-Mateos, S., Lamas, S., Ortiz, A., & Rodrigues-Diez, R. R. (2020). Targeting the progression of chronic kidney disease. *Nature Reviews Nephrology*, *16*(5), 269-288. https://doi.org/10.1038/s41581-019-0248-y

Saxena, N., Maio, N., Crooks, D. R., Ricketts, C. J., Yang, Y., Wei, M.-H., Fan, T. W.-M., Lane, A. N., Sourbier, C., Singh, A., Killian, J. K., Meltzer, P. S., Vocke, C. D., Rouault, T. A., & Linehan, W. M. (2016). SDHB-Deficient Cancers: The Role of Mutations That Impair Iron Sulfur Cluster Delivery. *JNCI: Journal of the National Cancer Institute*, *108*(1), djv287. https://doi.org/10.1093/jnci/djv287

Schindelin, J., Arganda-Carreras, I., Frise, E., Kaynig, V., Longair, M., Pietzsch, T., Preibisch, S., Rueden, C., Saalfeld, S., Schmid, B., Tinevez, J.-Y., White, D. J., Hartenstein, V., Eliceiri, K., Tomancak, P., & Cardona, A. (2012). Fiji: An open-source platform for biological-image analysis. *Nature Methods*, *9*(7), 676-682. https://doi.org/10.1038/nmeth.2019

Schnaper, H. W. (2014). Remnant nephron physiology and the progression of chronic kidney disease. *Pediatric Nephrology*, *29*(2), 193-202. https://doi.org/10.1007/s00467-013-2494-8

Simon, N., & Hertig, A. (2015). Alteration of Fatty Acid Oxidation in Tubular Epithelial Cells: From Acute Kidney Injury to Renal Fibrogenesis. *Frontiers in Medicine*, *2*, 52. https://doi.org/10.3389/fmed.2015.00052

Son, N.-H., Basu, D., Samovski, D., Pietka, T. A., Peche, V. S., Willecke, F., Fang, X., Yu, S.-Q., Scerbo, D., Chang, H. R., Sun, F., Bagdasarov, S., Drosatos, K., Yeh, S. T., Mullick, A. E., Shoghi, K. I., Gumaste, N., Kim, K., Huggins, L.-A., … Goldberg, I. J. (2018). Endothelial cell CD36 optimizes tissue fatty acid uptake. *The Journal of Clinical Investigation*, *128*(10), 4329-4342. https://doi.org/10.1172/JCI99315

Souza, A. C. P., Bocharov, A. V., Baranova, I. N., Vishnyakova, T. G., Huang, Y. G., Wilkins, K. J., Hu, X., Street, J. M., Alvarez-Prats, A., Mullick, A. E., Patterson, A. P., Remaley, A. T., Eggerman, T. L., Yuen, P. S. T., & Star, R. A. (2016). Antagonism of scavenger receptor CD36 by 5A peptide prevents chronic kidney disease progression in mice independent of blood pressure regulation. *Kidney International*, *89*(4), 809-822. https://doi.org/10.1016/j.kint.2015.12.043

Srivastava, S. P., Li, J., Kitada, M., Fujita, H., Yamada, Y., Goodwin, J. E., Kanasaki, K., & Koya, D. (2018). SIRT3 deficiency leads to induction of abnormal glycolysis in diabetic kidney with fibrosis. *Cell Death & Disease*, *9*(10), 1-14. https://doi.org/10.1038/s41419-018-1057-0

Stadler, K., Goldberg, I. J., & Susztak, K. (2015). The evolving understanding of the contribution of lipid metabolism to diabetic kidney disease. *Current Diabetes Reports*, *15*(7), 40. https://doi.org/10.1007/s11892-015-0611-8

Stormark, T. A., Strømmen, K., Iversen, B. M., & Matre, K. (2007). Three-dimensional ultrasonography can detect the modulation of kidney volume in two-kidney, one-clip hypertensive rats. *Ultrasound in Medicine & Biology*, *33*(12), 1882-1888. https://doi.org/10.1016/j.ultrasmedbio.2007.06.010

Stuhr, N. L., Nhan, J. D., Hammerquist, A. M., Camp, B. V., Reoyo, D., & Curran, S. P. (2022). Rapid Lipid Quantification in Caenorhabditis elegans by Oil Red O and Nile Red Staining. *Bio-protocol*, *12*(5), e4340-e4340.

Tan, S. M., Ziemann, M., Thallas-Bonke, V., Snelson, M., Kumar, V., Laskowski, A., Nguyen, T.-V., Huynh, K., Clarke, M. V., Libianto, R., Baker, S. T., Skene, A., Power, D. A., MacIsaac, R. J., Henstridge, D. C., Wetsel, R. A., El-Osta, A., Meikle, P. J., Wilson, S. G., … Coughlan, M. T. (2020). Complement C5a Induces Renal Injury in Diabetic Kidney Disease by Disrupting Mitochondrial Metabolic Agility. *Diabetes*, *69*(1), 83-98. https://doi.org/10.2337/db19-0043

Tannenbaum, J., Purkerson, M. L., & Klahr, S. (1983). Effect of unilateral ureteral obstruction on metabolism of renal lipids in the rat. *American Journal of Physiology-Renal Physiology*, *245*(2), F254-F262. https://doi.org/10.1152/ajprenal.1983.245.2.F254

Thangapandiyan, S., Ramesh, M., Miltonprabu, S., Hema, T., Jothi, G. B., & Nandhini, V. (2019). Sulforaphane potentially attenuates arsenic-induced nephrotoxicity via the PI3K/Akt/Nrf2 pathway in albino Wistar rats. *Environmental Science and Pollution Research International*, *26*(12), 12247-12263. https://doi.org/10.1007/s11356-019-04502-w

Tian, S., Li, B., Lei, P., Yang, X., Zhang, X., Bao, Y., & Shan, Y. (2018). Sulforaphane Improves Abnormal Lipid Metabolism via Both ERS-Dependent XBP1/ACC &SCD1 and ERS-Independent SREBP/FAS Pathways. *Molecular Nutrition & Food Research*, *62*(6), 1700737. https://doi.org/10.1002/mnfr.201700737

Ucero, A. C., Benito-Martin, A., Izquierdo, M. C., Sanchez-Niño, M. D., Sanz, A. B., Ramos, A. M., Berzal, S., Ruiz-Ortega, M., Egido, J., & Ortiz, A. (2014). Unilateral ureteral obstruction: Beyond obstruction. *International Urology and Nephrology*, *46*(4), 765-776. https://doi.org/10.1007/s11255-013-0520-1

Ucero, A. C., Gonçalves, S., Benito-Martin, A., Santamaría, B., Ramos, A. M., Berzal, S., Ruiz-Ortega, M., Egido, J., & Ortiz, A. (2010). Obstructive renal injury: From fluid mechanics to molecular cell biology. *Research and Reports in Urology*, *2*, 41-55. https://doi.org/10.2147/RRU.S6597

Uittenbogaard, M., & Chiaramello, A. (s. f.). Mitochondrial Biogenesis: A Therapeutic Target for Neurodevelopmental Disorders and Neurodegenerative Diseases. *Current*

Pharmaceutical Design, *20*(35), 5574-5593.

Vela-Guajardo, J. E., Pérez-Treviño, P., Rivera-Álvarez, I., González-Mondellini, F. A., Altamirano, J., & García, N. (2017). The 8-oxo-deoxyguanosine glycosylase increases its migration to mitochondria in compensated cardiac hypertrophy. *Journal of the American Society of Hypertension*, *11*(10), 660-672. https://doi.org/10.1016/j.jash.2017.08.004

Wang, Y., Lu, M., Xiong, L., Fan, J., Zhou, Y., Li, H., Peng, X., Zhong, Z., Wang, Y., Huang, F., Chen, W., Yu, X., & Mao, H. (2020). Drp1-mediated mitochondrial fission promotes renal fibroblast activation and fibrogenesis. *Cell Death & Disease*, *11*(1), 1-14. https://doi.org/10.1038/s41419-019-2218-5

Waterborg, J. H., & Matthews, H. R. (1984). The lowry method for protein quantitation. *Methods in Molecular Biology (Clifton, N.J.)*, *1*, 1-3. https://doi.org/10.1385/0-89603-062-8:1

Webster, A. C., Nagler, E. V., Morton, R. L., & Masson, P. (2017). Chronic Kidney Disease. *Lancet (London, England)*, *389*(10075), 1238-1252. https://doi.org/10.1016/S0140-6736(16)32064-5

Xia, Z.-E., Xi, J.-L., & Shi, L. (2018). 3,3′-Diindolylmethane ameliorates renal fibrosis through the inhibition of renal fibroblast activation in vivo and in vitro. *Renal Failure*, *40*(1), 447-454. https://doi.org/10.1080/0886022X.2018.1490322

Yang, W., Luo, Y., Yang, S., Zeng, M., Zhang, S., Liu, J., Han, Y., Liu, Y., Zhu, X., Wu, H., Liu, F., Sun, L., & Xiao, L. (2018). Ectopic lipid accumulation: Potential role in tubular injury and inflammation in diabetic kidney disease. *Clinical Science*, *132*(22), 2407-2422. https://doi.org/10.1042/CS20180702

Yen, C.-L. E., Stone, S. J., Koliwad, S., Harris, C., & Farese, R. V. (2008). Thematic Review Series: Glycerolipids. DGAT enzymes and triacylglycerol biosynthesis. *Journal of Lipid Research*, *49*(11), 2283-2301. https://doi.org/10.1194/jlr.R800018-JLR200

Zeng, H., Qin, H., Liao, M., Zheng, E., Luo, X., Xiao, A., Li, Y., Chen, L., Wei, L., Zhao, L., Ruan, X. Z., Yang, P., & Chen, Y. (2022). CD36 promotes de novo lipogenesis in hepatocytes through INSIG2-dependent SREBP1 processing. *Molecular Metabolism*, *57*, 101428. https://doi.org/10.1016/j.molmet.2021.101428

Zhang, X., Agborbesong, E., & Li, X. (2021). The Role of Mitochondria in Acute Kidney Injury and Chronic Kidney Disease and Its Therapeutic Potential. *International Journal of Molecular Sciences*, *22*(20), 11253. https://doi.org/10.3390/ijms222011253

Zhang, Y., Wen, P., Luo, J., Ding, H., Cao, H., He, W., Zen, K., Zhou, Y., Yang, J., & Jiang, L. (2021). Sirtuin 3 regulates mitochondrial protein acetylation and metabolism in tubular epithelial cells during renal fibrosis. *Cell Death & Disease*, *12*(9), 1-13. https://doi.org/10.1038/s41419-021-04134-4

Zhang, Z., Wang, S., Zhou, S., Yan, X., Wang, Y., Chen, J., Mellen, N., Kong, M., Gu, J., Tan, Y., Zheng, Y., & Cai, L. (2014). Sulforaphane prevents the development of cardiomyopathy in type 2 diabetic mice probably by reversing oxidative stress-induced inhibition of LKB1/AMPK pathway. *Journal of Molecular and Cellular Cardiology*, *77*, 42-52. https://doi.org/10.1016/j.yjmcc.2014.09.022

Zhao, Q., Xue, Y., Yang, Y., Niu, Z., Wang, C., Hou, Y., & Chen, H. (2016). Screening and identification of the differentially expressed proteins in neonatal rat kidney after partial unilateral ureteral obstruction. *Molecular Medicine Reports*, *14*(1), 681-688. https://doi.org/10.3892/mmr.2016.5338

Zhao, Z., Liao, G., Zhou, Q., Lv, D., Holthfer, H., & Zou, H. (2016). Sulforaphane Attenuates Contrast-Induced Nephropathy in Rats via Nrf2/HO-1 Pathway. *Oxidative*

Medicine and Cellular Longevity, *2016*, 9825623. https://doi.org/10.1155/2016/9825623

Zhong, S., Zhao, L., Wang, Y., Zhang, C., Liu, J., Wang, P., Zhou, W., Yang, P., Varghese, Z., Moorhead, J. F., Chen, Y., & Ruan, X. Z. (2017). Cluster of Differentiation 36 Deficiency Aggravates Macrophage Infiltration and Hepatic Inflammation by Upregulating Monocyte Chemotactic Protein-1 Expression of Hepatocytes Through Histone Deacetylase 2-Dependent Pathway. *Antioxidants & Redox Signaling*, *27*(4), 201-214. https://doi.org/10.1089/ars.2016.6808

antioxidants

MDPI

Article

Sulforaphane Protects against Unilateral Ureteral Obstruction-Induced Renal Damage in Rats by Alleviating Mitochondrial and Lipid Metabolism Impairment

Ana Karina Aranda-Rivera [1,2], **Alfredo Cruz-Gregorio** [1], **Omar Emiliano Aparicio-Trejo** [3], **Edilia Tapia** [3], **Laura Gabriela Sánchez-Lozada** [3], **Fernando Enrique García-Arroyo** [3], **Isabel Amador-Martínez** [1,2], **Marisol Orozco-Ibarra** [4], **Francisca Fernández-Valverde** [5] and **José Pedraza-Chaverri** [1,*]

[1] Laboratorio F-315, Departamento de Biología, Facultad de Química, Universidad Nacional Autónoma de México, Mexico City 04510, Mexico

[2] Posgrado en Ciencias Biológicas, Universidad Nacional Autónoma de México, Ciudad Universitaria, Mexico City 04510, Mexico

[3] Departmento de Fisiopatología Cardio-Renal, Instituto Nacional de Cardiología "Ignacio Chávez", Mexico City 14080, Mexico

[4] Laboratorio de Neurobiología Molecular y Celular, Instituto Nacional de Neurología y Neurocirugía, Manuel Velasco Suárez, Av. Insurgentes Sur # 3877, La Fama, Alcaldía Tlalpan, Mexico City 14269, Mexico

[5] Laboratorio de Patología Experimental, Instituto Nacional de Neurología y Neurocirugía, Manuel Velasco Suárez, Av. Insurgentes Sur # 3877, La Fama, Alcaldía Tlalpan, Mexico City 14269, Mexico

* Correspondence: pedraza@unam.mx

Abstract: Unilateral ureteral obstruction (UUO) is an animal rodent model that allows the study of obstructive nephropathy in an accelerated manner. During UUO, tubular damage is induced, and alterations such as oxidative stress, inflammation, lipid metabolism, and mitochondrial impairment favor fibrosis development, leading to chronic kidney disease progression. Sulforaphane (SFN), an isothiocyanate derived from green cruciferous vegetables, might improve mitochondrial functions and lipid metabolism; however, its role in UUO has been poorly explored. Therefore, we aimed to determine the protective effect of SFN related to mitochondria and lipid metabolism in UUO. Our results showed that in UUO SFN decreased renal damage, attributed to increased mitochondrial biogenesis. We showed that SFN augmented peroxisome proliferator-activated receptor γ co-activator 1α (PGC-1α) and nuclear respiratory factor 1 (NRF1). The increase in biogenesis augmented the mitochondrial mass marker voltage-dependent anion channel (VDAC) and improved mitochondrial structure, as well as complex III (CIII), aconitase 2 (ACO2) and citrate synthase activities in UUO. In addition, lipid metabolism was improved, observed by the downregulation of cluster of differentiation 36 (CD36), sterol regulatory-element binding protein 1 (SREBP1), fatty acid synthase (FASN), and diacylglycerol O-acyltransferase 1 (DGAT1), which reduces triglyceride (TG) accumulation. Finally, restoring the mitochondrial structure reduced excessive fission by decreasing the fission protein dynamin-related protein-1 (DRP1). Autophagy flux was further restored by reducing beclin and sequestosome (p62) and increasing B-cell lymphoma 2 (Bcl2) and the ratio of microtubule-associated proteins 1A/1B light chain 3 II and I (LC3II/LC3I). These results reveal that SFN confers protection against UUO-induced kidney injury by targeting mitochondrial biogenesis, which also improves lipid metabolism.

Keywords: chronic kidney disease (CKD); kidney fibrosis; mitochondrial biogenesis; mitochondrial dysfunction; lipid metabolism; sulforaphane (SFN); unilateral ureteral obstruction (UUO)

1. Introduction

Obstructive nephropathy is one of the leading causes of chronic kidney disease (CKD) in newborns, children, and adults [1,2]. Obstructive nephropathy involves

hemodynamic alterations, oxidative stress, apoptosis, and inflammation, which trigger renal parenchyma loss, favor fibrosis development and induce CKD progression [3,4].

Unilateral ureteral obstruction (UUO) is an in vivo experimental animal model that mimics renal fibrosis associated with chronic obstructive nephropathy, which can be developed quickly [2]. Hemodynamic changes induce oxidative stress, inflammation, and cell death early after obstruction, principally in the S3 segment of tubular epithelial cells. Furthermore, our group and others have previously reported that mitochondria impairment, such as reduced mitochondrial biogenesis and mitophagy dysfunction, is related to CKD progression in UUO [5,6]. In addition, lipid metabolism is altered in this model, characterized by lipid deposition and β-oxidation dysfunction, which contributes to the fibrotic process [7,8].

Sulforaphane (SFN) is an isothiocyanate derived from green cruciferous vegetables, which has been shown to have anti-oxidative and anti-inflammatory properties [9]. In addition, SFN promotes mitochondrial biogenesis and improves mitochondrial dynamics, mitophagy, and autophagy, reducing kidney damage in cisplatin-induced acute kidney injury (AKI), maleate-induced AKI, and type 2 diabetes models [10–13]. Regarding the UUO model, Chung et al. [14] showed that SFN treatment alleviates inflammation and fibrosis by promoting the activation of nuclear factor erythroid 2-related factor 2 (Nrf2), which decreases mitochondrial oxidative stress, suggesting that SFN might have a significant role in the restoration of mitochondrial homeostasis. In CKD models such as diabetic nephropathy (DN), SFN improves lipid metabolism, preventing lipid accumulation [13]. Additionally, SFN regulates the levels of lipid biosynthesis proteins in nonalcoholic fatty liver disease [15]. Although a mitochondrial role for SFN in the UUO model has been suggested, it is unclear whether this antioxidant decreases kidney injury by modulating mitochondrial homeostasis through the induction of mitochondrial biogenesis and mitochondrial bioenergetics improvement. Even more, the role of SFN in lipid metabolism during UUO has not been explored. Therefore, we hypothesized that SFN might decrease renal damage by promoting mitochondrial biogenesis, enhancing the electron transport system (ETS), and even regulating mitophagy, autophagy, and lipid metabolism in the UUO model. In this study, we found that SFN reduced the levels of renal damage markers, kidney injury molecule 1 (KIM-1), alpha SMA (α-SMA), and interleukin-1 beta (IL-1β). These renal damage markers were reduced due to the restoration of mitochondrial biogenesis, observed through the upregulation of peroxisome proliferator-activated receptor γ co-activator 1α (PGC-1α) and nuclear respiratory factor 1 (NRF1) in the obstructed kidney. Consequently, the mitochondrial mass marker voltage-dependent anion channel (VDAC) was increased by SFN. The mitochondrial structure also was improved with SFN treatment. The enhancement of mitochondrial biogenesis further increased complex III (CIII), aconitase 2 (ACO2), and citrate synthase activities. In addition, SFN restored lipid metabolism through the downregulation of CD36, fatty acid synthase (FASN), diacylglycerol O-acyltransferase 1 (DGAT1), and sterol regulatory-element binding protein 1 (SREBP1), reducing the biosynthesis of triglycerides (TGs). The improvement in the mitochondrial structure by SFN decreased fission and the autophagy markers beclin and sequestosome (p62) and increased B-cell lymphoma (Bcl2) and microtubule-associated proteins 1A/1B light chain 3 II and I (LC3II/LC3I) ratio, restoring autophagy flux. Thus, our results reveal that SFN confers protection against UUO-induced renal injury by targeting mitochondrial biogenesis, which also restores lipid metabolism.

2. Methods

2.1. Experimental Design

The Institutional Animal Care Committee (Comité Institucional para el Cuidado y Uso de Animales de Laboratorio, CICUAL) approved the experimental protocol at the "Facultad de Química de la Universidad Nacional Autónoma de México" (FQ/CI-CUAL/441/21). The research was performed according to Mexican Official Norm Guides for producing, using, and caring of laboratory animals (NOM-062-ZOO-1999). In total, 46 male Wistar rats were used with an initial weight of 200–250 g, divided into four groups: (1) sham-operated rats, in which surgery was simulated without ligation of the ureter; (2) UUO; (3) UUO treated with SFN (UUO + SFN); and (4) control administered with SFN (SFN). UUO was conducted by double ligating the left ureter with 3–0 silk suture and 2 cm below the kidney. A racemic mix of D-/L-SFN was purchased from LKT Laboratories (St. Paul, MN, USA). SFN was administered intraperitoneally (i.p) at a 1 mg/kg dose. We selected the sulforaphane dose according to our previous studies reported in maleate and cisplatin-induced kidney damage experimental animal models [10,16,17]. SFN was administered for four days, beginning the second day after surgery and finishing one day before killing (Figure 1). In the same way, a group of rats, without undergoing surgical manipulation, were treated with SFN under the same scheme as the UUO + SFN group. The rats were maintained in a temperature-controlled environment with a 12–12 h light–dark cycle and with water and food provided ad libitum. The analysis was carried out seven days after UUO, killing the rats employing sodium pentobarbital (Sedalphorte®, purchased from Salud y Bienestar Animal S.A. de C.V. Mexico City, Mexico). The disposal of biological residues was conducted according to NOM-087-SEMARNAT-SSA1-2002. No animal died during or after surgery. Animal distribution was carried out as follows: for immunoblotting and ETS and TCA cycles activities were utilized with n = 3–5 per group. For immunoblotting of mitochondrial proteins and lipid metabolism, we used n = 3 rats per group. For histology and electronic microscopy, n = 3–4 per group. Some animals were excluded from the experiment for presenting atypical data. The exact number of animals utilized for each experiment is indicated in each figure legend in the results section.
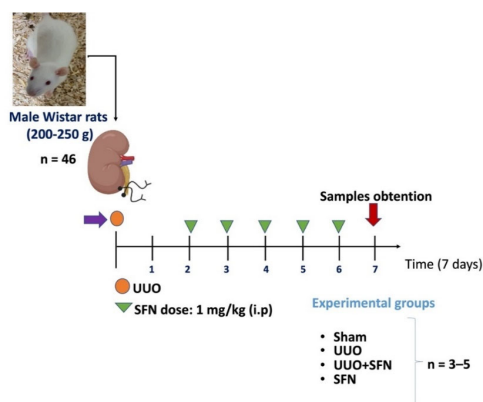
Figure 1. Experimental design. A total of 46 male Wistar rats were divided into four groups: (1) Sham group, in which surgery was simulated without ligation of the ureter, (2) unilateral ureteral obstruction (UUO) group, with double-ligating the left ureter for seven days; (3) UUO group treated with sulforaphane (SFN) at a dose of 1 mg/kg intraperitoneally (i.p) (UUO + SFN); and (4) SFN group, which did not have surgery manipulation but was treated with SFN. The number for each experiment was 3–5 per group (n = 3–5). The number of animals used for each experiment is specified in the figure legends for each experimental assay.

2.2. Kidney Histology

Seven days after UUO, the left kidney was obtained and transversally dissected. One-half of the kidney was fixed by immersion in near-freezing 2-methyl butane, covered with a cryoprotectant solution, and mounted on specimen holders. Next, the kidneys were cut into serial sections of 8 μm on a cryostat at −20 °C (CM-1520; Leica Microsystems, Nussloch, Germany) and later mounted on glass coverslips for staining. Kidney morphology was evaluated with hematoxylin and eosin (H&E) [5] and lipid accumulation with Nile red staining [18]. For Nile red staining, sections were washed with PBS pH = 7.4 and incubated for 10 min in darkness with 2.5 μg/mL Nile red dissolved in PBS with 1% acetone; Vectashield® was used as a mounting medium. The photomicrographs were taken using a Cytation 5 Cell Imaging Multi-Mode Reader (BioTek Instruments, Inc., Winooski, VT, USA). Nile red quantification was performed using Fiji [19] by ImageJ software (National Institutes of Health, Bethesda, MD, USA, https://imagej.nih.gov/ij/index.htm, accessed on 20 July 2022) according to a previously reported protocol [18].

2.3. Isolation of Renal Mitochondria

Renal mitochondria were isolated according to a previous report from our group [20]. Briefly, after being dissected, kidneys were transversally cut into small pieces and cooled by immersion in isolation buffer (225 mM D-mannitol, 75 mM sucrose, 1 mM EDTA, 5 mM HEPES 0.1% BSA, pH = 7.4) at 4 °C, and homogenized employing a Glass/Teflon Potter Elvehjem tissue grinder (Sigma-Aldrich, St. Louis, MO, USA). Then, renal mitochondria were obtained using differential centrifugation and the renal pellets were resuspended in 180 μL of isolation-free BSA buffer.

2.4. Protein Extraction and Western Blot

For total protein extraction, 100 mg of renal tissues were homogenized in 1 mL of radioimmunoprecipitation buffer (RIPA): 40 mM Tris-HCl, 150 mM NaCl, 2 mM EDTA, 1 mM EGTA, 5 mM NaF, 1 mM Na_3VO_4, 1 mM PMSF, 0.5% sodium deoxycholate, 0.1% sodium dodecyl sulfate (SDS, Sigma-Aldrich, St. Louis, MO, USA) pH 7.6, supplemented with protease inhibitor cocktail (Roche Applied Science, Mannheim, Germany). Tissue was homogenized with a Potter–Elvehjem tissue grinder and centrifuged at 15,000× *g* for 10 min at 4 °C, and the supernatants were recovered. The Lowry assay quantitated total renal proteins, according to the manufacturer's instructions [21]. Complete representative western blot membranes are found in Supplementary File S1.

2.5. Western Blot Assay

A total of 20–40 μg of proteins were denatured by dilution with 6X Laemmli sample buffer (60 mM Tris-Cl, pH = 6.8, 2% SDS, 10% glycerol, 5% β-mercaptoethanol, 0.01% bromophenol blue) and boiled for 5 min. Samples were loaded in SDS-polyacrylamide (acrylamide, Sigma-Aldrich, St. Louis, MO, USA) gels and submitted to electrophoresis. Proteins were transferred to polyvinylidene fluoride membranes (PVDF) and blocked with 5% non-fat dry milk in 0.1% Tween-Tris buffered solution (TBST) for 1 h at room temperature. Membranes were incubated with the recommended dilutions of antibodies overnight at 4 °C at constant stirring and the corresponding fluorescent secondary antibody (1:15,000) for 1 h 30 min at room temperature in darkness. The protein bands were detected using fluorescence in an Odyssey Sa scanner (LI-COR Biosciences, Lincoln, NE, USA). Protein band density was analyzed with ImageJ studio. Quantification of proteins was expressed as arbitrary units, representing the ratio of optical densities of protein of interest/loading control. In some cases, one membrane was used to detect more than one protein. For this, membranes were washed with stripping solution (100 mM glycine, 0.5% SDS pH 2.5) for 15 min at constant stirring and later washed three times with 0.1% TBST. Afterward, membranes were incubated with the recommended dilutions of antibodies (Table S1). Secondary antibodies were used with a 1:15000 dilution (680RD, 926-68074;

800RD, 926-32214; 680RD, 926-68073; 800RD, 926-32212; 800CW, 926-32213) and were purchased from LI-COR Inc. (Lincoln, NE, USA).

OXPHOS Protein Determination

The levels of OXPHOS proteins were evaluated for Western blot using an antibody cocktail (ab110413, Abcam, Cambridge, UK). This cocktail is composed of a mixture of five antibodies, one against each CI-CIV complex and ATP synthase. These proteins include NADH: ubiquinone oxidoreductase subunit B8 (NDUFB8) for CI, succinate dehydrogenase B (SDHB) for CII, ubiquinol-cytochrome c reductase core protein 2 (UQCRC2) for CIII, cytochrome c oxidase I for CIV, and ATP 5A for ATP synthase. These proteins are the most labile for each complex, and their decrease or increase is related to an alteration in OXPHOS [16,22,23]. According to the manufacturer's instructions, sample proteins were not heated to avoid signal decrease.

2.6. TCA Cycle Activities

The activities of ACO2 and citrate synthase were evaluated to determine the SFN effect over the tricarboxylic acid (TCA) cycle. ACO2 activity was measured in isolated mitochondria, obtained immediately after rats were sacrificed. ACO2 was assayed by determining the rate of formation of the intermediate product cis-aconitate at 240 nm, as previously described by Negrette-Guzmán [24]. The citrate synthase activity was also used as an indicator of mitochondrial mass [25]. Briefly, citrate synthase activity was determined by recording the increase in the absorbance at 412 nm of the 5-thio-2-nitrobenzoic acid (TNB, Sigma-Aldrich, St. Louis, MO, USA) adduct [25]. Both activities were expressed as nmol per minute per milligram of protein (nmol/min/mg of protein).

2.7. Mitochondrial Complex Activity

The activities of the mitochondrial complexes I (CI), II (CII), and III (CIII) were evaluated spectrophotometrically by using 20 μg of total protein or mitochondrial fraction at 37 °C using a Synergy HT microplate reader (Biotek Instruments, Winooski, VT, USA) as formerly reported [16]. Briefly, CI was measured by reducing decyl ubiquinone (DUB) to reduced decyl ubiquinone (DUBH$_2$) in a reaction coupled with the reduction of 2,6-dichlorophenolindophenol (DCPIP, Sigma-Aldrich, St. Louis, MO, USA); the activity of CI was proportional to the disappearance of oxidized DCPIP at 600 nm in the presence of 10 mM NADH, 2.5 μM antimycin A (Sigma-Aldrich, St. Louis, MO, USA), and 5 mM KCN. A non-specific reaction was subtracted by adding 2.5 μM rotenone to a parallel assay. The activity of CII was assessed similarly to CI, but the reaction was performed in the presence of 400 mM succinate, 2.5 μM rotenone, and 2.5 μM antimycin A. The non-specific reaction was obtained by adding 2.5 μM malonate. The activity of CIII was determined by following the generation of the reduced form of cytochrome c at 550 nm employing 0.312 mM DUBH$_2$ in the presence of 5 mM KCN, 2.5 μM rotenone, and 1 mM oxidized cytochrome c. The non-specific reduction of cytochrome c was obtained by adding 2.5 μM antimycin A. The activity of complex IV (CIV) was evaluated by following the oxidation of cytochrome c at 565 nm in the presence of 5 mM KCN, 1 mM antimycin A, and 1 mM reduced cytochrome c. The non-specific oxidation of cytochrome c was determined by adding 1M sodium azide. All activities were expressed as nmol per minute per milligram of protein (nmol/min/mg of protein).

2.8. Determination of Triglycerides in the Renal Cortex

Triglycerides (TGs) were assessed with a commercial kit (Triglycerides, Sekisui Diagnostics, Burlington, MA, USA). Intrarenal TG extraction was modified slightly from the Folch method [26]. Carefully, 20–40 mg of the renal cortex was homogenized in ice-cold phosphates buffer solution (PBS) 1X, and protein concentrations were determined. After that, 1.5 mL of a mix of 2:1 chloroform:methanol was added to the homogenates and were

centrifuged for 10 min at 2050× *g* at 4 °C. The organic phase was separated, dried, and dissolved with 200 μL of 5% Triton X-100. TGs were assessed according to the manufacturer's instructions using a glycerol standard curve and evaluated by colorimetry in a hybrid multimode reader (Sinergy H1, Biotek-Agilent, Santa Clara, CA, USA). Results were corrected per milligram of protein.

2.9. Transmission Electron Microscopy (TEM)

Kidney cubes of about 1 mm^3 were fixed in 2.5% glutaraldehyde for 1.5 h, washed with phosphate buffer at pH 7.2, and post-fixed with 0.5% osmium tetroxide for 1 h. Afterward, cubes were washed and dehydrated in ascending alcohol series, immersed in propylene oxide for 10 min, and pre-included in a 1:1 propylene oxide/Epon resin mix overnight. Finally, the tissue pieces were embedded in Epon resin at 60 °C for 24 h, and the resulting blocks were used to obtain semi-thin cuts 300 nm thick stained with toluidine blue to prove the region of interest's presence. Finally, serial ultra-thin sections of 60–90 nm-thick were obtained and contrasted with 4% uranyl acetate for 20 min and 1% lead citrate for 10 min. Samples were examined using a transmission electron microscope (JEM-1400 Plus, JEOL, Boston, MA, USA).

2.10. Statistical Analysis

Data are reported as mean ± standard error of the mean (SEM). The obtained results were analyzed with the R package Rapport [27] to eliminate outliers. The data presented a normal distribution and were tested using a one-way ANOVA with Tukey post-test to compare more than two groups. A *p*-value less than 0.05 was considered statistically significant. Data analysis was performed with Graph Pad Prism 7 (San Diego, CA, USA).

3. Results

3.1. Protective Effects of Sulforaphane against Kidney Damage in UUO

To assess renal damage induced by UUO and its improvement by SFN, we evaluated renal histology and markers. The functional renal damage was confirmed by measuring levels of the kidney damage markers KIM-1 and IL-1β, which were significantly augmented in the UUO group but not in the UUO group treated with SFN (Figure 2A,B). In agreement, the fibrosis markers' α-SMA and Col IV levels were lower in the UUO group treated with SFN than in the UUO group (Figure 2C,D).

Moreover, H&E renal histology showed that UUO triggers the loss of tubular structure, characterized by the loss of epithelial cells, tubular dilatation, leucocyte infiltration, and the presence of connective tissue between the tubules, which were decreased because of SFN treatment. Both UUO and UUO + SFN groups showed leukocyte infiltration (Figure 2E). Thus, our results suggest that SFN significantly decreases kidney damage in the UUO model.
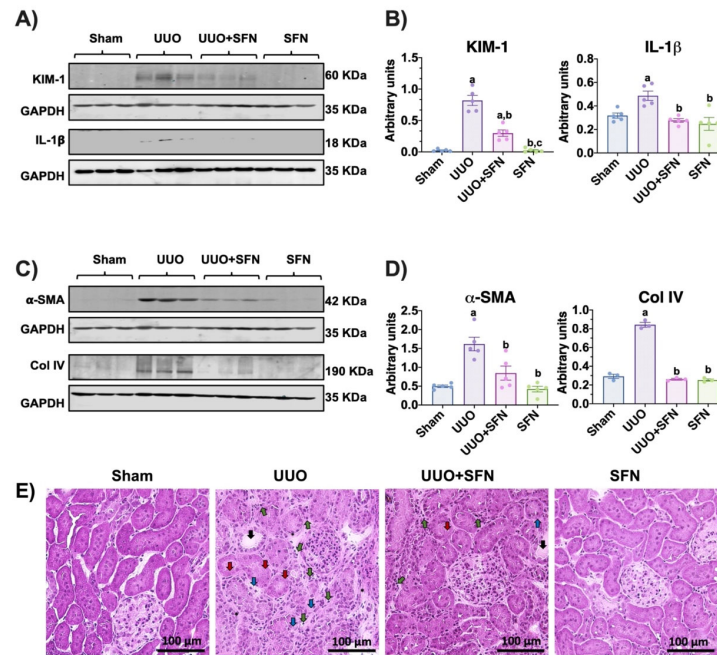
Figure 2. Sulforaphane (SFN) reduces kidney damage in the unilateral ureteral obstruction (UUO) model. (**A**) Representative immunoblotting and (**B**) densitometric analysis of kidney damage markers: kidney injury molecule-1 (KIM-1) and interleukin-1 beta (IL-1β). (**C**) Representative immunoblotting and (**D**) densitometric analysis of fibrotic markers' alpha-smooth muscle actin (α-SMA) and collagen IV (Col IV). Data are mean ± SEM, *n* = 5 per group (except for Col IV, *n* = 3), using a one-way ANOVA. Statistical differences were determined with multiple comparisons using Tukey's test. Glyceraldehyde 3-phosphate dehydrogenase (GAPDH) was used as a loading control. [a] $p < 0.05$ vs. Sham, [b] $p < 0.05$ vs. UUO, [c] $p < 0.05$ vs. UUO + SFN. (**E**) Representative hematoxylin and eosin (H&E) staining of the kidney cortex. The H&E staining revealed that UUO induced the loss of tubular structure, characterized by the loss of epithelial cells (red arrows), tubular dilatation (black arrows), and necrosis (blue arrows). UUO also induces polymorphonuclear and lymphocyte infiltration (green arrows) and the presence of connective tissue between the tubules (asterisks). The SFN treatment partially decreased kidney injury despite some necrotic areas, and leukocyte infiltration was observed. Scale bar = 100 μm. *n* = 3 for sham and SFN; *n* = 4 for UUO and UUO + SFN. Sham: simulated surgery without ligation of the ureter; UUO: unilateral ureteral obstruction with double ligating the left ureter for seven days; UUO + SFN: UUO treated with SFN (1 mg/kg, intraperitoneal) and SFN administered with SFN (1 mg/kg, intraperitoneal).

3.2. Mitochondrial Biogenesis Is Enhanced by Sulforaphane, Increasing Mitochondrial Mass in the UUO Model

Because we hypothesized that SFN ameliorates kidney damage via mitochondrial biogenesis in the UUO model, we determined the protein levels of PGC-1α and NRF1. We found that PGC-1α and NRF1 levels were decreased in the UUO group and SFN treatment increased them in UUO + SFN group (Figure 3A,B). To determine if the increase in mitochondrial biogenesis promoted by SFN was associated with higher mitochondrial mass, we evaluated the outer membrane protein VDAC and ANT protein levels as markers of mitochondrial mass of outer and inner membranes, respectively. The data showed that in

the UUO group, VDAC decreased, while in the group treated with SFN (UUO + SFN), VDAC levels significantly increased compared to the UUO group. Similarly, the levels of ANT significantly reduced in UUO, but SFN was unable to reestablish them in UUO + SFN group (Figure 3C,D).
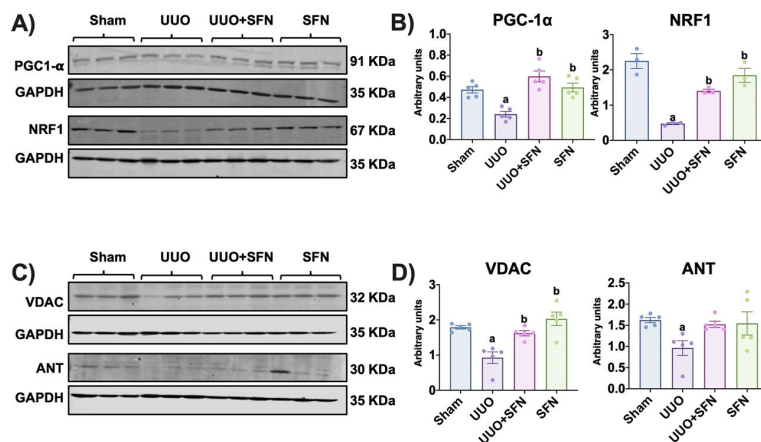
Figure 3. Sulforaphane (SFN) induces mitochondrial biogenesis and mitochondrial mass increase in the unilateral ureteral obstruction (UUO) model. (**A**) Representative immunoblotting and (**B**) densitometric analysis of mitochondrial biogenesis markers peroxisome proliferator-activated receptor-γ coactivator (PGC)-1α (PGC-1α) and nuclear respiratory factor 1 (NRF1). $n = 5$ per group for PGC-1α and $n = 3$ per group for NRF1. (**C**) Representative immunoblotting and (**D**) densitometric analysis of mitochondrial mass markers voltage-dependent anion channel (VDAC) and adenine nucleotide translocator (ANT), $n = 5$ per group. Data were analyzed using a one-way ANOVA, and statistical differences were determined with multiple comparisons using Tukey's test. Glyceraldehyde 3-phosphate dehydrogenase (GAPDH) was used as a loading control. [a] $p < 0.05$ vs. Sham, [b] $p < 0.05$ vs. UUO. Sham: simulated surgery without ligation of the ureter; UUO: unilateral ureteral obstruction with double ligation of the left ureter for seven days; UUO + SFN: UUO treated with SFN (1 mg/kg, intraperitoneal); and SFN: administered with SFN (1 mg/kg, intraperitoneal).

3.3. Sulforaphane Restores the Levels of Electron Transport System Complex Proteins

PGC-1α is a potent transcription factor regulating OXPHOS; thus, the reduction of biogenesis alters OXPHOS proteins [28]. On the other hand, the increase in PGC-1α might influence OXPHOS. In this way, we measured the protein levels of CI-CIV subunits and adenosine triphosphate (ATP) synthase. We found that the levels of the succinate dehydrogenase B (SDHB) of CII and ubiquinol-cytochrome c reductase core protein 2 (UQCRC2) of CIII decreased in UUO in comparison with the sham group (Figure 4A,C,D). On the other hand, SFN treatment augmented CIII-UQCRC2 protein levels in the UUO + SFN and SFN groups compared with the UUO group (Figure 4B). Likewise, CI- NADH: ubiquinone oxidoreductase subunit B8 (NDUFB8) and CII-SDHB protein levels increased in the SFN group compared with UUO (Figure 4B,C). We did not find changes for CIV-cytochrome c oxidase (MTCO1) for any of the groups (Figure 4A,E). Interestingly, we observed that the ATP synthase-α (ATP5A) subunit increased in UUO, compared with sham, while SFN decreased it (Figure 4A,F). These results suggest that SFN improves the OXPHOS function in the UUO model.
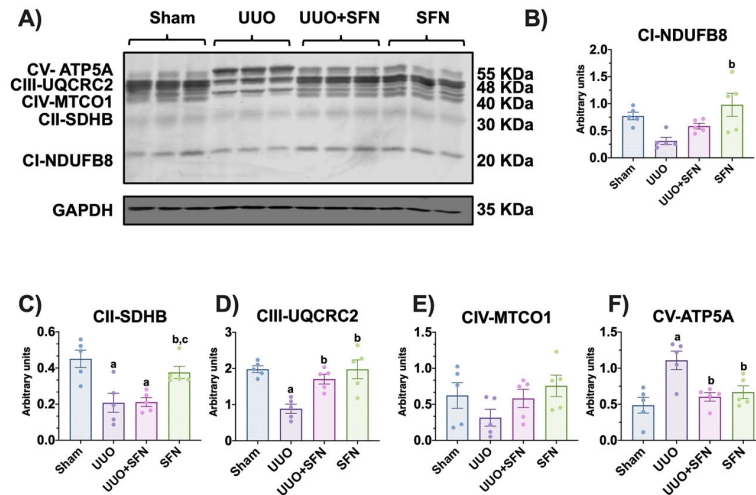
Figure 4. Effect of sulforaphane (SFN) on the levels of subunits of the electron transport system (ETS) complexes in the unilateral ureteral obstruction (UUO) model. (**A**) Representative immunoblotting and densitometric analysis of the levels of (**B**) the reduced form of nicotinamide adenine dinucleotide ubiquinone oxidoreductase subunit B8 (CI-NDUFB8), (**C**) succinate dehydrogenase complex iron-sulfur subunit B (CII-SDHB), (**D**) ubiquinol-cytochrome c reductase core protein 2 (CIII-UQCRC2), (**E**) cytochrome c oxidase subunit I (CIV-MTCO1), and (**F**) adenine triphosphate (ATP) synthase-α subunit (CV-ATP5A). Data are mean ± SEM, n = 5 per group, using a one-way ANOVA. Statistical differences were determined with multiple comparisons using Tukey's test. Glyceraldehyde phosphate dehydrogenase (GAPDH) was used as a loading control. [a] $p < 0.05$ vs. Sham, [b] $p < 0.05$ vs. UUO, [c] $p < 0.05$ vs. UUO + SFN. Sham: simulated surgery without ligation of the ureter; UUO: unilateral ureteral obstruction with double ligating the left ureter for seven days; UUO + SFN: UUO treated with SFN (1 mg/kg, intraperitoneal); and SFN: administered with SFN (1 mg/kg, intraperitoneal).

3.4. Sulforaphane Increases CIII Activity in the UUO Model

To determine if the increase in OXPHOS proteins improves ETS, we evaluated their activities. We found that the activity of CIII is significantly decreased in UUO compared with the sham group, and the treatment with SFN raised it in the UUO + SFN and SFN groups (Figure 5C). The observed results in this complex activity were similar to the findings for UQCRC2 of OXPHOS proteins. We did not show significant changes in the activities of CI, CII, and CIV (Figure 5A,B,D). Thus, the expression of complexes agrees with their activity, where SFN augmented CIII in the UUO + SFN group compared with UUO without treatment.
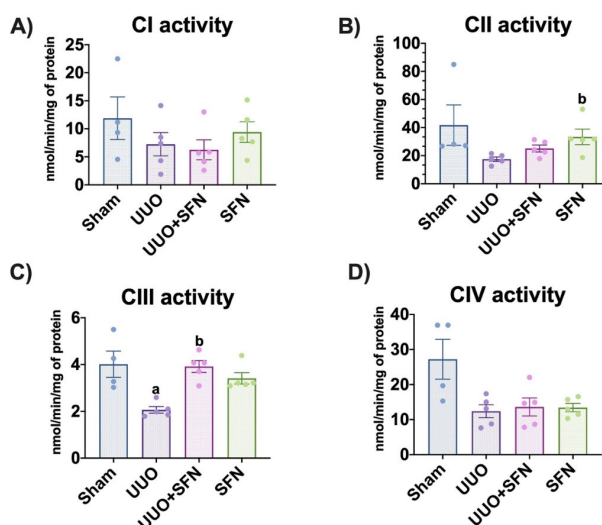
Figure 5. Effect of sulforaphane (SFN) on the enzymatic activities of the electron transport system (ETS) complexes in the unilateral ureteral obstruction (UUO) model. (**A**) Complex I (CI), (**B**) complex II (CII), (**C**) complex III (CIII), and (**D**) complex IV (CIV) were determined in the total renal cortex. Data are mean ± SEM, *n* = 4 for sham group and *n* = 5 for UUO, UUO + SFN, and SFN groups. Data were analyzed using a one-way ANOVA and statistical differences were determined with multiple comparisons using Tukey's test. [a] $p < 0.05$ vs. Sham, [b] $p < 0.05$ vs. UUO. Sham: simulated surgery without ligation of the ureter; UUO: unilateral ureteral obstruction with double ligation of the left ureter for seven days; UUO + SFN: UUO treated with SFN (1 mg/kg, intraperitoneal) and SFN administered with SFN (1 mg/kg, intraperitoneal).

3.5. Sulforaphane Increases TCA Cycle Activities

In the UUO model, alterations in the TCA cycle are previously reported as a mechanism involved in fibrosis [29]. We evaluated the protein levels of ACO2 and found that these decreased in the UUO compared with the sham group. The decrease in ACO2 indicates oxidative stress, as reported previously [20,30]. The treatment with SFN did not increase ACO2 levels in the UUO + SFN groups; however, we observed a significant increase in the SFN group compared with the UUO group (Figure 6A,B). We also determined ACO2 and citrate synthase activities and found a reduction in UUO compared to Sham, but SFN administration augmented them in the UUO group treated with SFN (Figure 6C,D). The reduction of both activities are attributed to TCA cycle dysfunction and their raised by SFN strongly suggest that SFN influences the TCA cycle improvement.
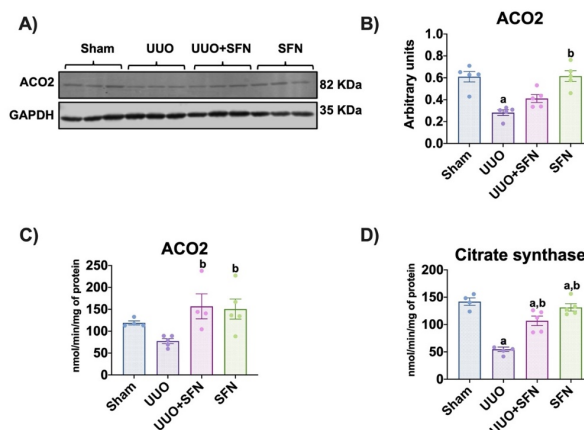
Figure 6. Sulforaphane (SFN) effect in the TCA cycle. (**A**) Representative immunoblotting and (**B**) densitometric analysis of the levels of aconitase 2 (ACO2). Data are mean ± SEM, *n* = 5 per group. Data were analyzed using a one-way ANOVA and statistical differences were determined by multiple comparisons using Tukey's test. Glyceraldehyde phosphate dehydrogenase (GAPDH) was used as a loading control. (**C**) ACO2 and (**D**) citrate synthase activities from the kidney cortex of the different experimental groups were evaluated in isolated mitochondria and total homogenates, respectively. Data are mean ± SEM, *n* = 5 per group (except for sham for ACO2 and citrate synthase, *n* = 4, and UUO + SFN for ACO2, *n* = 4). Data were analyzed using a one-way ANOVA, and statistical differences were determined with multiple comparisons using Tukey's test [a] $p < 0.05$ vs. Sham, [b] $p < 0.05$ vs. UUO. Sham: simulated surgery without ligation of the ureter; UUO: unilateral ureteral obstruction with double ligation of the left ureter for seven days; UUO + SFN: UUO treated with SFN (1 mg/kg, intraperitoneal) and SFN administered with SFN (1 mg/kg, intraperitoneal).

3.6. Sulforaphane Mediates Uptake of Fatty Acids in the UUO Model

Mitochondrial dysfunction in CKD models, including UUO, has been also associated with lipid metabolism impairment because of the upregulation of lipid biosynthesis and downregulation of its degradation via fatty acid (FA) oxidation (β-oxidation), inducing lipid accumulation in the renal cortex [31]. In addition, the impairment of bioenergetics leads to FA uptake because kidneys highly depend on β-oxidation [32]. Previous reports have demonstrated that SFN can modulate the metabolism of lipids by enhancing biogenesis [33]; thus, we investigated the SFN effect on the uptake and biosynthesis and utilization of FA in the obstructed kidney. We found that the levels of CD36, the protein responsible for capturing and internalizing FA, significantly increased in the UUO group, and SFN was able to decrease it in UUO + SFN group (Figure 7A,B). We also evaluated the levels of nuclear receptor PPAR-α, involved in FA metabolism. We observed that PPAR-α was upregulated in the UUO model while SFN decreased it (Figure 7A,B). We also evaluated the levels of CPT1A, which catalyzes the transport of long-chain FA into mitochondria for β-oxidation, and we did not find differences between the UUO and UUO + SFN groups; however, SFN augmented CPT1A and levels in the group treated with SFN (Figure 7A,B). Thus, our results suggest that SFN decreases FA uptake in UUO.
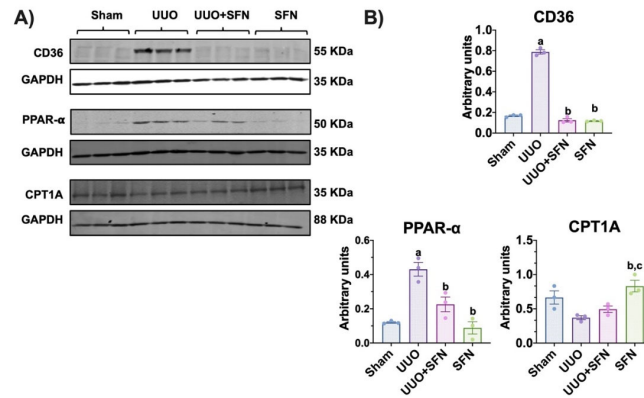
Figure 7. Effect of sulforaphane (SFN) on the uptake of fatty acids in the unilateral ureteral obstruction (UUO) model. (**A**) Representative immunoblotting and (**B**) densitometric analysis of cluster of differentiation 36 (CD36), peroxisome proliferator-activated receptor-alpha (PPAR-α), and carnitine palmitoyl transferase 1A (CPT1A). Data are mean ± SEM, n = 3 per group. Data were analyzed using one-way ANOVA and statistical differences were determined by multiple comparisons using Tukey's test. Glyceraldehyde 3-phosphate dehydrogenase (GAPDH) was used as a loading control. [a] $p < 0.05$ vs. Sham, [b] $p < 0.05$ vs. UUO, [c] $p < 0.05$ vs. UUO + SFN. Sham: simulated surgery without ligation of the ureter; UUO: unilateral ureteral obstruction with double ligation of the left ureter for seven days; UUO + SFN: UUO treated with SFN (1 mg/kg, intraperitoneal); and SFN: administered with SFN (1 mg/kg, intraperitoneal).

3.7. Sulforaphane Decreases Lipid Deposition in UUO

To determine if increased FA uptake in UUO triggers lipid deposition and the posterior decrease by SFN, we determined lipid accumulation in tissue sections through Nile red staining. We observed that lipids tended to accumulate in the UUO group, but they seemed partially prevented in the UUO + SFN group. Lipid accumulation was mainly found at the tubule epithelium. Interestingly, SFN alone also increased the total lipid content, but no accumulation in a particular structure was observed (Figure 8A,B).
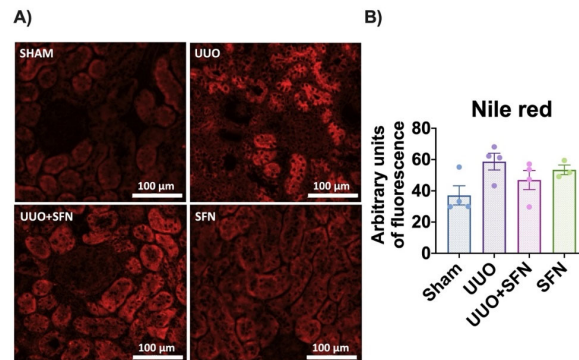
Figure 8. Effect of sulforaphane (SFN) on lipid deposition in the unilateral ureteral obstruction (UUO) model. (**A**) Representative micrographs of Nile red staining and (**B**) quantification of Nile

red stain. The Nile red staining showed a higher lipid deposition in the unilateral ureteral obstruction (UUO) group than in the sham group, while SFN decreased lipids in the UUO + SFN group. *n* = 4 for sham, UUO, and UUO + SFN and *n* = 3 for SFN. Data were analyzed using a one-way ANOVA, and statistical differences were determined with multiple comparisons using Tukey's test. Sham: simulated surgery without ligation of the ureter; UUO: unilateral ureteral obstruction with double ligation of the left ureter for seven days; UUO + SFN: UUO treated with SFN (1 mg/kg, intraperitoneal); and SFN: administered with SFN (1 mg/kg, intraperitoneal).

3.8. Sulforaphane Decreases Lipid Synthesis in UUO

Additionally, we determined the protein levels of enzymes involved in lipid metabolism in UUO and their possible improvement with SFN treatment. We found that in the obstructed kidney, FASN, DGAT1, and SREBP1 were increased compared to the sham group. In contrast, in the UUO + SFN group, the levels of these enzymes significantly decreased (Figure 9A,B). Finally, to elucidate if the decrease in the enzymes involved in lipogenesis decreased the levels of lipids with SFN treatment, we evaluated the quantity of intrarenal TGs. The result showed that TGs were augmented in the UUO group while SFN diminished them, suggesting that SFN avoids lipid accumulation in UUO (Figure 9C).
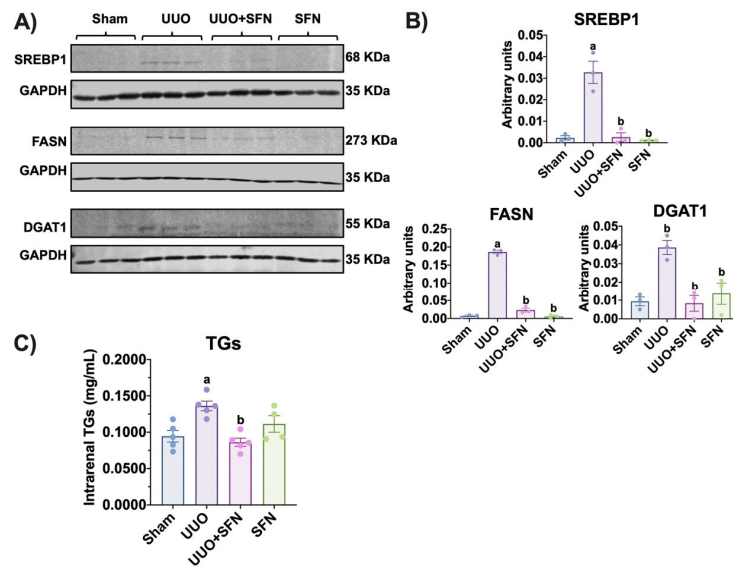
Figure 9. Effect of sulforaphane (SFN) on lipid synthesis in the unilateral ureteral obstruction (UUO) model. (**A**) Representative immunoblotting and (**B**) densitometric analysis of sterol regulatory-element binding proteins (SREBP1), fatty acid synthase (FASN), and diacylglycerol O-acyltransferase 1 (DGAT1) in the sham group, UUO, UUO treated with SFN (UUO + SFN), and a group treated with SFN (SFN). Data are mean ± SEM, *n* = 3 per group. Data were analyzed using a one-way ANOVA, and statistical differences were determined with multiple comparisons using Tukey's test. Glyceraldehyde phosphate dehydrogenase (GAPDH) was used as a loading control. (**C**) Intrarenal triglycerides (TGs) were determined in the renal cortex in all experimental groups. Data are mean ± SEM, *n* = 5 for sham, UUO, and UUO + SFN groups and n= 4 for the SFN group. Data were analyzed using a one-way ANOVA and statistical differences were determined with multiple comparisons using Tukey's test. [a] $p < 0.05$ vs. Sham, [b] $p < 0.05$ vs. UUO. Sham: simulated surgery without ligation of the ureter; UUO: unilateral ureteral obstruction with double ligation of the left ureter for seven days;

UUO + SFN: UUO treated with SFN (1 mg/kg, intraperitoneal); and SFN: administered with SFN (1 mg/kg, intraperitoneal).

3.9. Sulforaphane Decreases the Fission Process in the Obstructed Kidney

To elucidate if the restoration of the mitochondrial structure and bioenergetics by SFN modulates mitochondrial dynamics, a process involving fission and fusion, we determined in isolated mitochondria the levels of the proteins involved in this process. We observed that in the UUO group, the levels of the fission protein DRP1 increased compared with the sham group, and the SFN treatment decreased it (Figure 10A,B). Moreover, the fusion proteins OPA1 and MFN2 were downregulated in the mitochondrial fraction of UUO, which could not be restored by SFN treatment (Figure 10A,C). Taken together, our results show that SFN partially regulates mitochondrial dynamics by decreasing mitochondrial fission in obstructed kidney.
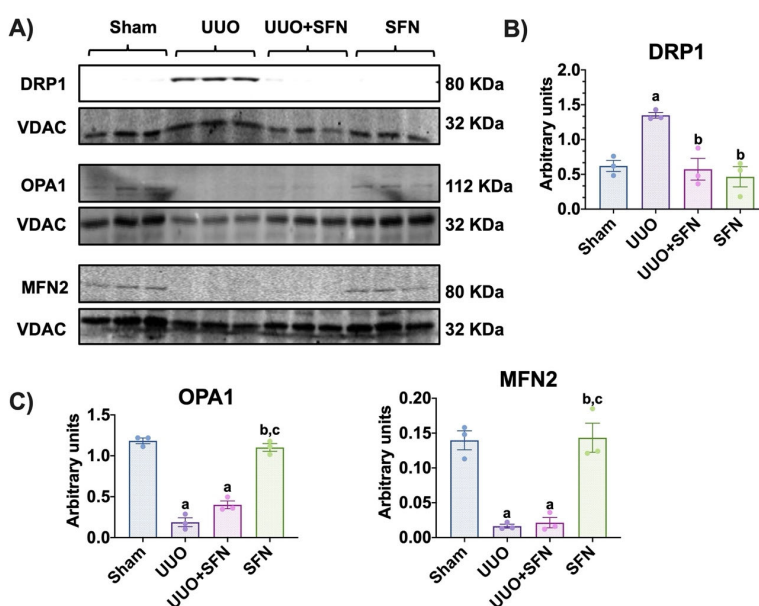
Figure 10. Sulforaphane (SFN) decreases the fission process in isolated mitochondria in the unilateral ureteral obstruction (UUO) model. (**A**) Representative immunoblotting and densitometric analysis of protein levels of the (**B**) fission protein dynamin-related protein-1 (DRP1) and (**C**) fusion proteins optic atrophy type 1 (OPA1) and mitofusin 2 (MFN2). Data are mean ± SEM, n = 3 per group. Data were analyzed using a one-way ANOVA, and statistical differences were determined by multiple comparisons using Tukey's test. A voltage-dependent anion channel (VDAC) was used as the loading control. [a] $p < 0.05$ vs. Sham, [b] $p < 0.05$ vs. UUO, [c] $p < 0.05$ vs. UUO + SFN. Sham: simulated surgery without ligation of the ureter; UUO: unilateral ureteral obstruction with double ligation of the left ureter for seven days; UUO + SFN: UUO treated with SFN (1 mg/kg, intraperitoneal); and SFN: administered with SFN (1 mg/kg, intraperitoneal).

3.10. Autophagy Flux Is Restored by Sulforaphane in the UUO Model

Disturbances in mitochondrial dynamics such as increased fission trigger mitophagy, a process that removes damaged mitochondria; however, in UUO, impaired mitophagy

is commonly reported [5,34,35]. We aimed to investigate if the improvement in mitochondria and bioenergetics and dynamics by SFN influenced mitophagy. We evaluated in isolated mitochondria the levels of PINK1 and Parkin and observed that in UUO, PINK1 increased significantly compared to the sham group but not the levels of Parkin. We also found that SFN did not affect mitophagy proteins PINK1 and Parkin (Figure 11A,B). Since PINK1/Parkin-mediated mitophagy is very related to macro autophagy, we wanted to study the SFN effect in the macroautophagic process. We found that the levels of the autophagy markers Beclin and p62 increased in UUO while Bcl2 levels decreased (Figure 11C,D). In UUO, SFN treatment reduced Beclin and p62 levels and augmented Bcl2, suggesting the restoration of autophagy flux. Additionally, we found that the LC3-II/LC3-I ratio decreased in the UUO group and SFN significantly increased it (Figure 11C,D), suggesting that autophagy flux is restored by SFN. Together, our results show that SFN restored autophagy flux in the obstructed kidney.
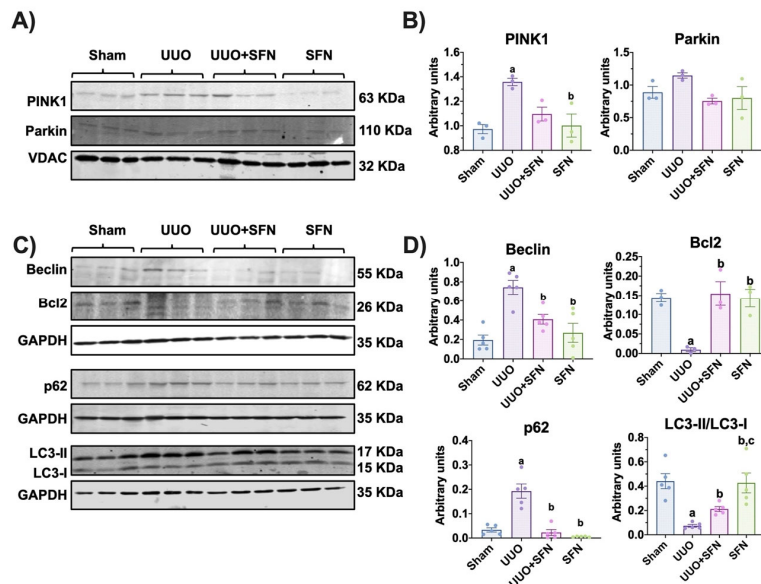
Figure 11. Sulforaphane (SFN) effect on the levels of mitophagy and autophagy proteins in the unilateral ureteral obstruction (UUO) model. (**A**) Representative immunoblotting and (**B**) densitometric analysis of levels of mitophagy markers phosphatase and tensin homolog deleted on chromosome 10 (PTEN)-induced kinase 1 (PINK1) and Parkin in isolated mitochondria. The voltage anion-dependent channel (VDAC) was used as the loading control. n = 3 per group. (**C**) Representative immunoblotting and (**D**) densitometric analysis of autophagy markers beclin, B-cell lymphoma 2 (Bcl2), sequestosome (p62), and microtubule-associated proteins 1A/1B light chain 3 (LC3I/LC3II) ratio. Data are mean ± SEM, n = 5 per group (except for Bcl2, n = 3 per group). Data were analyzed using a one-way ANOVA, and statistical differences were determined with multiple comparisons using Tukey's test. Glyceraldehyde phosphate dehydrogenase (GAPDH) was used as a loading control. [a] $p < 0.05$ vs. Sham, [b] $p < 0.05$ vs. UUO, [c] $p < 0.05$ vs. UUO + SFN. Sham: simulated surgery without ligation of the ureter; UUO: unilateral ureteral obstruction with double ligation of the left ureter for seven days; UUO + SFN: UUO treated with SFN (1 mg/kg, intraperitoneal); and SFN: administered with SFN (1 mg/kg, intraperitoneal).

3.11. SFN Ameliorates Ultrastructural Damage and Restores Autophagy Flux in the UUO Model

The renal cortex was analyzed by TEM to observe the changes in the mitochondrial distribution and morphology induced by seven-day obstruction and the SFN treatment. Mitochondrial cristae, membranes, and matrix integrity were reviewed. In agreement with previous findings [5], mitochondrial morphology changes and mitochondrial injury were observed in the UUO group, as mitochondria changed from a large and elongated morphology in the sham kidney (Figure 12A,B) to a smaller and rounder morphology in the obstructed kidney (Figure 12C,D). In addition, the obstructed kidney showed mitochondria that have lost the double-membrane continuity (Figure 12D, red arrow). The SFN group showed mitochondria with large and elongated morphology, similar to the control group (Figure 12G,H).

We also validated the restoration of autophagy by TEM to confirm if SFN effectively reestablished the autophagy flux. We found in UUO the presence of autophagic bodies suggestive of mitophagy (asterisks in Figure 12C,I–L). The UUO + SFN group did not show the presence of autophagic bodies despite some mitochondria exhibiting a rounder morphology and low electrodensity (Figure 12E,F). Thus, our results showed the recovery of the mitochondrial ultrastructure and mitophagy flux by SFN.
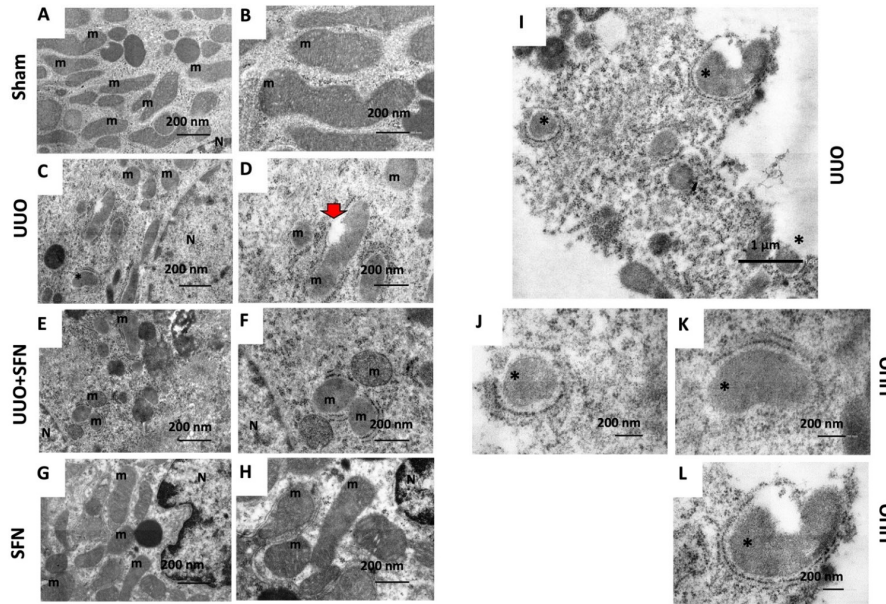
Figure 12. Mitochondrial morphology, autophagy, and mitophagy. The renal cortex was analyzed by TEM to observe mitochondrial distribution and morphology. (**A**,**B**) Sham. (**C**,**D**,**I**–**L**) UUO. (**E**,**F**) UUO + SFN. (**G**,**H**) SFN. m: mitochondria; N: nucleus; asterisks: autophagic bodies; red arrow: mitochondria that have lost the double-membrane continuity. Micrographs in the left column were taken at 10,000× (scale bar = 1 μm) and in the right column at 20,000× magnification (scale bar = 500 nm). *N* = 3 for sham and SFN groups and *n* = 4 for UUO and UUO + SFN. Sham: simulated surgery without ligation of the ureter; UUO: unilateral ureteral obstruction with double ligation of the left ureter for seven days; UUO + SFN: UUO treated with SFN (1 mg/kg, intraperitoneal); and SFN: administered with SFN (1 mg/kg, intraperitoneal).

4. Discussion

In UUO, mitochondrial dysfunction, such as biogenesis reduction, has been described as a mechanism leading to the progression of CKD [5,7,36–38]. Thus, mitochondrial protective schemes are required for the prevention and delaying of CKD. In this work, we used SFN, which has been shown to preserve mitochondrial function by promoting mitochondrial biogenesis, bioenergetics, and activating Nrf2 [16,17,39]. We conducted our study with male rats because, in the UUO model, male animals are preferred since female reproductive organs complicate the surgical procedure [2,40]. Both males and females tend to suffer from obstruction; however, this pathology is most common in males, attributed to prostatic hyperplasia [41]. Additionally, male rats are preferentially used as female sex hormones are a protective factor against several renal diseases, including obstructive nephropathy [42,43]. Therefore, the principal limitation of our study might be attributed to knowing if SFN-induced mitochondrial protective effects are influenced by sex hormones. We found that SFN confers protection by upregulating mitochondrial biogenesis. The protection was determined by evaluating the protein levels of KIM-1 and IL-1β (Figure 2A,B), as well as the fibrosis markers transforming growth factor-beta (TGF-β) pathway components such as α-SMA and Col IV (Figure 2C,D). Moreover, H&E staining showed decreased SFN-mediated damage, although leukocyte infiltration was still evident in the UUO group treated with SFN (Figure 2E). The presence of inflammatory cells in the UUO + SFN group might be partially explained since, in the UUO model, leukocyte infiltration begins 12 h after obstruction and continues throughout UUO [40,44]. In our work, we administered SFN on the second day after surgery (experimental design and Figure 1); thus, the presence of infiltrating leukocytes might be a consequence of the first hours of damage. Interestingly, we observed that the inflammatory marker IL-1β, released by inflammatory cells, decreased in UUO with SFN treatment, suggesting that inflammation is effectively attenuated with SFN (Figure 2A,B). Although SFN influences inflammatory markers, leukocyte infiltration is still present. It is possible that SFN after seven days can eliminate leukocyte infiltration, which deserves future studies. These findings are in agreement with previous studies showing that SFN decreases kidney damage through the reduction of IL-1β levels and TGF-β expression [14]. These authors showed that SFN's protection in UUO was related to decreasing mitochondrial stress through autophagic flux activation, suggesting a significant role of SFN in the recovery of mitochondria during UUO.

Reduced mitochondrial biogenesis has been previously linked to the fibrotic process in kidney diseases [45,46], and SFN has been shown to prevent it by activating PGC-1α, the main regulator of mitochondrial biogenesis in kidney damage models such as maleate-induced AKI and streptozotocin-induced DN [13,16,33]. PGC-1α induces biogenesis by activating NRF1 and NRF2, which in turn trigger the transcription of mitochondria proteins, including OXPHOS and TCA cycle proteins [47,48]. Our results effectively showed that the decrease in PGC-1α and NRF1 was restored by SFN (Figure 3A,B), which led to a significant increase in mitochondrial proteins like VDAC levels (Figure 3C,D). We did not observe significant changes in ANT, an inner mitochondrial-mass marker in the UUO group administered with SFN, compared with UUO (Figure 3C,D); however, we observed a trend in the increase in ANT in UUO with SFN. This tendency could increase and be significant in a temporal course of SFN administration (more than seven days after obstruction), allowing evidence of ANT changes. On the other hand, we might attribute the only significant increase in VDAC because VDAC is a target of NRF1, the companion of PGC-1α, as reported by Patti et al. [49]. The authors determined that in type 2 diabetes (T2D), the reduction in nuclear-encoded mitochondrial protein VDAC was related to the decrease in NRF1, suggesting that this protein regulates VDAC at transcriptional levels. Supporting the latter, Guarino et al. [50] showed that NRF1 regulates the expression of the VDAC gene by containing binding sites to the VDAC promoter. Therefore, SFN enhancement of mitochondrial biogenesis by PGC-1α augments NRF1, and the increase in NRF1 upregulates the transcription of VDAC, augmenting mitochondrial mass in UUO.

We showed an improvement in mitochondria ultrastructure by SFN treatment (Figure 12E,F). While in UUO, the mitochondrial structure also revealed the presence of elongated mitochondria and the loss of cristae (Figure 12C,D), in the UUO + SFN we appreciated that SFN partially restored mitochondrial morphology as cristae loss and round mitochondria seem less common than in the UUO group (Figure 12E,F). The restoration of mitochondria morphology by SFN is intimately related to mitochondria biogenesis enhancement due to the generation of new mitochondria. These results are consistent with previous reports showing a better mitochondria structure by SFN treatment in models as high diet-induced liver mitochondria dysfunction [33]. Moreover, in vitro studies showed that SFN prevents H_2O_2-induced loss of mitochondria membrane potential and ATP levels [51], the latter suggesting that SFN improves OXPHOS.

According to the latter, PGC-1α is a transcription factor regulating bioenergetics through the TCA cycle and OXPHOS proteins [45,47]. In UUO, metabolic analyses have previously demonstrated alterations in the TCA cycle, revealing the accumulation of metabolites such as succinate and citrate synthase, attributed to dysregulation of this process [29]. Furthermore, Kim et al. reported that the deficiency of isocitrate dehydrogenase 2 (IDH2), an enzyme that metabolizes isocitrate into alpha-ketoglutarate (αKG), exacerbates mitochondrial hydrogen peroxide (H_2O_2) production, lipid peroxidation, and inflammation in UUO [52]. Similar results were reported in cisplatin-induced AKI models, where the deletion of IDH2 accelerates nephrotoxicity, increasing tubular damage [53]. SFN has shown its ability to upregulate the TCA cycle activity in other studies. For instance, SFN increased aconitase and α-ketoglutarate dehydrogenase in human neuroblastoma SH-SY5Y cells exposed to H_2O_2 and the lungs of Nrf2-deficient mice, associated with oxidative stress reduction [51,54]. Our results showed that SFN increased citrate synthase and ACO2 activities in UUO (Figure 6C,D). Citrate synthase is regulated by PGC-1α at the mRNA level; thus, according to our results, the reduction in its activity is associated with biogenesis impairment. On the other hand, decreased ACO2 protein levels and activity are related to oxidative stress [55]. Both TCA cycle markers indicate TCA cycle dysfunction in UUO. As we know, there are no existing previous studies showing the SFN effect in the TCA cycle enzyme activity in UUO.

The upregulation of mitochondrial biogenesis is also related to the enhancement of mitochondrial bioenergetics [56,57]. Consistent with this, the evaluation of ETS activities showed that CIII activity is upregulated by SFN in UUO (Figure 5C). Additionally, the effect of SFN on bioenergetics was also observed in maleate-induced AKI, showing an improvement in complex activities and protein levels [16]. We showed that the protein levels of ETS subunits indicate that CII-SDHB and CIII-UQCRC2 subunits are decreased in UUO, but SFN only rescued CIII subunit levels (Figure 4C,D). The restoration of protein levels of UQCRC2-CIII by SFN in UUO might be indirectly attributed to Nrf2 through phosphorylated AMPK. A recent study demonstrated that phosphorylated AMPK could enhance UQCRC2 gene transcription by activating the NFE2L2/NRF2 gene [58]. According to previous studies, AMPK is also activated by SFN [13,59,60]. Future investigations may clarify if the SFN effect over UQCRC2 is direct or indirect in the UUO model.

Although for CIII, the protein levels matched with its activity, it was not the case for CII. According to our results, CII-SDHB decreased in UUO, but its activity was not affected (Figures 4C and 5B). Inconsistency in these results might be attributed to the fact that the antibody cocktail (OXPHOS) employed to identify CII protein levels detects the succinate dehydrogenase (SDH) B subunit, the most labile protein used for this antibody. This protein contains three iron-sulfur (Fe-S) clusters, making the SDH8 protein more sensitive to oxidative damage, which is found in UUO [14,61]. Moreover, the CII is composed of three additional subunits that enhance its activity: SDHA, SDHC, and SDHD, which do not have Fe-S clusters [62]. Thus, the protein levels could not reflect its activity. Additionally, the activity of CII depends on metabolic regulation because this complex is an enzyme of the TCA cycle, involved in the conversion of succinate to fumarate [63]. Therefore, activity might not be affected because other mechanisms of metabolic regulation are

present. Interestingly, we observed that the protein levels of the ATP5A subunit from ATP synthase are augmented in the UUO group and levels are reestablished with SFN treatment (Figure 4F). The increase in the levels of the ATP synthase subunit in UUO might be partially explained by a rescue mechanism employed by mitochondria to produce more ATP and to avoid mitochondria membrane depolarization. This increase is initially achieved through the increase in ATP protein levels, which help to maintain inner membrane structure. In agreement with this, it has been reported that the upregulation of ATP5B, another subunit of ATP synthase, in the proximal tubules of the obstructed kidney of patients was related to ATP expenditure increase as a mechanism of adaptation to urinary pressure in UUO [64]. Zhao et al. [65] also reported the upregulation of ATP5B in neonatal rats with UUO. These results suggest that bioenergetics alterations in UUO were partially rescued by SFN.

Mitochondrial dysfunction causes abnormalities in lipid metabolism, and lipid metabolism alterations strongly contribute to mitochondrial dysfunction [66,67]. Lipid metabolism depends on lipid homeostasis, which balances lipid synthesis and degradation via β-oxidation [68]. PGC-1α is a master regulator of lipid metabolism mediated by its interaction with proteins that sense energy levels, such as AMPK [60,69]. Therefore, the reduction of PGC-1α has been related to the loss of lipid homeostasis. Our data showed the accumulation of TGs in the obstructed kidney (Figure 9C). In this way, in UUO, the increase in TGs is reported 24 h after obstruction, suggesting that disturbances of FA metabolism occur from early on [70]. Because renal epithelial tubular cells highly rely on β-oxidation, it has been reported that disturbances in this process trigger lipid accumulation, observed by the formation of lipid droplets [71]. Although β-oxidation dysfunction is characteristic of the UUO model, we did not find changes in CPT1A, the rate-limiting enzyme for β-oxidation, between the sham group and UUO (Figure 7A,B). Likewise, SFN did not induce CPT1A levels in UUO but did induce them in the SFN group, suggesting that it might not act through β-oxidation in UUO (Figure 7A,B).

Together with other authors, we hypothesized that the accumulation of TGs was attributed to a significant FA uptake via CD36 (Figure 7A,B), which increases the entrance of FA into the cell [8,72]. CD36 is a membrane receptor commonly overexpressed in the obstructed kidney that not only facilities FA uptake but is related to oxidative stress, inflammation, and fibrosis, which contributes to CKD progression [72,73]. Our data suggest that the overexpression of CD36 might influence inflammation and fibrosis. In agreement, in folic-acid-induced AKI, the overexpression of CD36 in renal tubular cells of mice was correlated with collagen I (Col I) and collagen III (Col III) overexpression, suggesting that the upregulation of CD36 might be associated with fibrosis [74]. Interestingly, we observed an abrupt decrease in CD36 levels with SFN in UUO (Figure 7A,B). As we know, there are no previous studies about the SFN effect in CD36 in UUO. Nrf2, the principal SFN target, might regulate CD36 mRNA, but CD36 transcription depends on cellular type. For instance, in atherosclerosis, Nrf2 upregulation promotes CD36 transcription in macrophages, inducing free cholesterol accumulation, which later leads to the formation of foam cells, highly toxic to the cells [75]. Therefore, the involvement of SFN in CD36 requires future studies in the kidney diseases context.

We showed that SFN treatment partially reduced lipid accumulation in UUO (Figure 8A,B) and TGs (Figure 9C) in UUO. Surprisingly, we observed that lipid deposition slightly increased in the SFN group (Figure 8A,B). The latter might be partially explained because downregulation or lack of CD36 is related to lipid increase in other cell types such as endothelial cells [76]. Furthermore, other authors have reported that the CD36 deletion in hepatocytes [77] was associated with macrophage infiltration by increasing the levels of monocyte chemotactic protein-1 (MCP-1). These findings suggest that CD36 might have other roles related to protection; however, more studies are needed to determine the role of CD36 in CKD.

Our results showed the possible restoration of the TCA cycle, which could prevent the accumulation of acetyl-CoA to avoid FA synthesis. The decrease in the accumulation

of TGs and lipids by SFN might be attributed to the downregulation of the proteins that mediate their synthesis, which is supported by the downregulation of DGAT1, SREBP1 transcription factor, and FASN observed in our results (Figure 9A,B). Additionally, the decrease in lipid biogenesis might be related to restoration of bioenergetics. DGAT1 is a protein involved in converting diacylglycerol to fatty acyl CoA and triacylglycerol, and DGAT1 upregulation is found in obesity and metabolic diseases [78]. Thus, the augment of TGs agrees with DGAT1 upregulation, and the reduction of TGs by SFN might be partially related to the downregulation of DGAT1 by this antioxidant. Indeed, the decrease in SREBP1 and FASN proteins might be attributed to CD36 downregulation because CD36 participates in the processing of SREBP1 through insulin-induced gene-2 (INSIG2) [79], leading to the transcription of lipogenic genes such as FASN, which promotes lipogenesis. Mechanistically, insulin activates CD36, triggering the formation of a complex between CD36 and INSIG2. This complex disrupts the binding between SREBP cleavage activating protein (SCAP) and INSIG2 with SREBP1, inducing the translocation of SREBP1 from the endoplasmic reticulum to the Golgi apparatus. In the Golgi apparatus, SREBP1 undergoes proteolytic processing, which activates it and later induces its translocation to the nucleus to induce the transcription of lipogenic genes such as FASN [80]. Thus, SFN-mediated CD36 downregulation might avoid the processing of SREBP1, which also avoids FASN upregulation. Other authors have reported the regulation of lipogenesis via SFN. For instance, SFN decreases the formation of lipids de novo in coronary diseases [59,81] and non-alcoholic liver diseases [15,82,83]. Recently, it has been reported that the mechanism involved in SFN-induced downregulation of SREBP1 is via degradation of its precursor via proteasomes [84]. Therefore, SFN is capable of regulating lipid metabolism in UUO.

Alterations in mitochondrial ultrastructure are possibly attributed to excessive fission in UUO, observed by the upregulation of DRP1 (Figure 10A,B). In contrast, the OPA1 and MFN2 are downregulated, indicating a shift from fusion to fission (Figure 10A,B,C). The upregulation of DRP1 agrees with the findings reported by other authors [5,34]. Interestingly, we only observed that SFN decreased DRP1 levels but did not affect OPA1 and MFN2 (Figure 10A,B,C). In accordance with the latter, human retinal pigment epithelial treated with SFN avoids the recruitment of DRP1, a mechanism reported as Nrf2-independent [85]. Thus, SFN showed another mechanism beyond Nrf2 activation. The effect of SFN on mitochondrial fission has been reported before in AKI models, where the levels of fission proteins were decreased by SFN pretreatment [16]. Therefore, in UUO the data suggest that the improvement in the mitochondrial structure by SFN regulates dynamics, decreasing fission via DRP1.

Excessive fission leads to mitophagy induction, which implies the remotion of damaged mitochondria into lysosomes [86]. Furthermore, the reduced mitochondrial mass has also been attributed to mitophagy [37]. Canonically, mitophagy is triggered by the recruitment of PINK1 to the outer mitochondria membrane in conditions of membrane depolarization, oxidative stress, or mitochondrial damage, which in turn recruits Parkin [87]. We observed that mitophagy is dysfunctional in UUO, observed by the increase in PINK1 but not Parkin, suggesting that mitochondrial turnover might be compromised (Figure 11A,B). Another possible explanation is that the mitophagy mechanism is PINK1/Parkin-independent, which agrees with the proposal by Jimenez-Uribe [5]. In UUO, we observed the upregulation of beclin and the downregulation of Bcl2, suggesting that the first step of autophagy is triggered; however, the upregulation of p62 and the decrease of the LC3II/LC3I ratio are also observed (Figure 11C,D). In both mitophagy and autophagy, p62 functions as a cargo protein that recognizes ubiquitinated organelles and protein aggregate [88]. Although the authors support the idea that the increase in p62 indicates efficient autophagy, other authors have observed p62 accumulation without autolysosome formation using TEM imaging [89], suggesting an alteration in this step. Thus, the upregulation of p62 in UUO observed in our results might be characteristic of autophagic flux alteration where autophagolysosomes are not finally degraded and then accumulate. Supporting this, in UUO, TEM analysis showed the presence of several autophagic bodies in

the same field (Figure 12C,I–L), which agrees with data reported previously [5]. In UUO, SFN treatment had no effects on PINK1 and Parkin (Figure 11A,B) but decreased beclin, p62, and increased the Bcl2 and LC3I/LC3II ratio (Figure 11C,D). Through TEM analysis, no autophagic bodies were found in the UUO + SFN group (Figure 12E,F), suggesting the restoration of autophagy flux.

To summarize, SFN ameliorates obstructive nephropathy-induced kidney injury by targeting mitochondrial dysfunction through the induction of mitochondrial biogenesis, improving ETS, dynamics, and autophagy processes. Moreover, SFN improves lipid metabolism by downregulating lipid uptake and synthesis, avoiding lipid accumulation (Figure 13).

In this work, we used SFN in UUO as a potential molecule to alleviate mitochondrial dysfunction, such as mitochondrial biogenesis and lipid uptake and biogenesis in UUO. We found that by restoring mitochondrial biogenesis, mitochondrial processes such as bioenergetics, structure, and lipid metabolism are restored by SFN. Recovery of mitochondrial structure influences mitochondrial dynamics by reducing excessive fission and regulating autophagic flux. Thus, restoring the main factors that regulate biogenesis could be a key therapeutic target in diseases associated with kidney obstruction. These results could open new avenues of potential uses in patients with obstructive nephropathy, possibly giving clinical relevance in treating this disease and encouraging studies of clinical trials in phases 1 and 2 as a potential translation value.
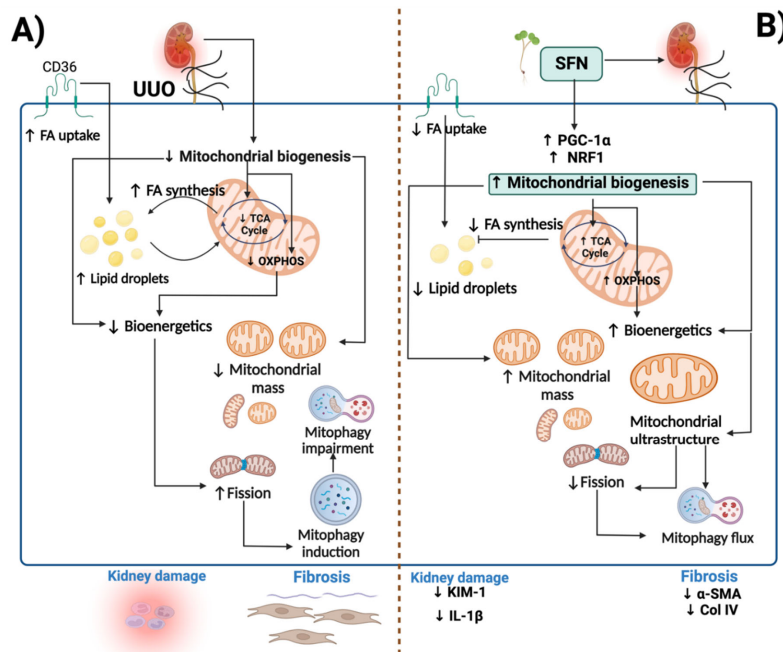
Figure 13. Integrative scheme. (**A**) In the unilateral ureteral obstruction (UUO) model, mitochondrial dysfunction is principally caused by reduced mitochondrial biogenesis, leading to a decrease in mitochondrial mass. Moreover, decreased biogenesis induces bioenergetics impairment, observed by the decline in the TCA cycle and oxidative phosphorylation (OXPHOS). The reduction of the TCA cycle leads to fatty acid (FA) synthesis, causing the formation of lipid droplets, which also

can damage the mitochondria. The impairment in bioenergetics induces FA uptake through the CD36 receptor, promoting lipid droplet accumulation. Decreased bioenergetics further induces excessive fission, altering mitochondrial dynamics. Excessive fission activates mitophagy to eliminate damaged mitochondria; however, this process is impaired, leading to the accumulation of lysosomes. (**B**) Sulforaphane (SFN) induces biogenesis through peroxisome proliferator-activated receptor γ co-activator 1α (PGC-1α) and nuclear respiratory factor 1 (NRF1). The upregulation of biogenesis restores mitochondria structure and ETS and TCA cycle activities. Consequently, lipid metabolism is regulated, characterized by the decrease in lipid droplet accumulation and lipid biogenesis. The restoration of mitochondria structure and function reduces excessive fission and regulates mitophagy flux. KIM-1: kidney injury molecule-1; IL-1β: interleukin-1 beta; α-SMA: alpha-smooth muscle actin; Col IV: collagen IV. ↑: increase; ↓: decrease. The figure was created using BioRender.

5. Conclusions

SFN improves mitochondrial biogenesis preventing mitochondrial dysfunction and lipid deposition, which decreases kidney damage and fibrosis in UUO.

References

1. Chevalier, R.L.; Forbes, M.S.; Thornhill, B.A. Ureteral Obstruction as a Model of Renal Interstitial Fibrosis and Obstructive Nephropathy. *Kidney Int.* **2009**, *75*, 1145–1152. https://doi.org/10.1038/ki.2009.86.
2. Martínez-Klimova, E.; Aparicio-Trejo, O.E.; Tapia, E.; Pedraza-Chaverri, J. Unilateral Ureteral Obstruction as a Model to Investigate Fibrosis-Attenuating Treatments. *Biomolecules* **2019**, *9*, 141. https://doi.org/10.3390/biom9040141.
3. Cheng, X.; Zheng, X.; Song, Y.; Qu, L.; Tang, J.; Meng, L.; Wang, Y. Apocynin Attenuates Renal Fibrosis via Inhibition of NOXs-ROS-ERK-Myofibroblast Accumulation in UUO Rats. *Free Radic. Res.* **2016**, *50*, 840–852. https://doi.org/10.1080/10715762.2016.1181757.
4. Nishida, H.; Kurahashi, T.; Saito, Y.; Otsuki, N.; Kwon, M.; Ohtake, H.; Yamakawa, M.; Yamada, K.-I.; Miyata, S.; Tomita, Y.; et al. Kidney Fibrosis Is Independent of the Amount of Ascorbic Acid in Mice with Unilateral Ureteral Obstruction. *Free Radic. Res.* **2014**, *48*, 1115–1124. https://doi.org/10.3109/10715762.2014.915031.
5. Jiménez-Uribe, A.P.; Bellido, B.; Aparicio-Trejo, O.E.; Tapia, E.; Sánchez-Lozada, L.G.; Hernández-Santos, J.A.; Fernández-Valverde, F.; Hernández-Cruz, E.Y.; Orozco-Ibarra, M.; Pedraza-Chaverri, J. Temporal Characterization of Mitochondrial Impairment in the Unilateral Ureteral Obstruction Model in Rats. *Free Radic. Biol. Med.* **2021**, *172*, 358–371. https://doi.org/10.1016/j.freeradbiomed.2021.06.019.

6. Yan, Q.; Song, Y.; Zhang, L.; Chen, Z.; Yang, C.; Liu, S.; Yuan, X.; Gao, H.; Ding, G.; Wang, H. Autophagy Activation Contributes to Lipid Accumulation in Tubular Epithelial Cells during Kidney Fibrosis. *Cell Death Discov.* **2018**, *4*, 39. https://doi.org/10.1038/s41420-018-0065-2.

7. Kang, H.M.; Ahn, S.H.; Choi, P.; Ko, Y.-A.; Han, S.H.; Chinga, F.; Park, A.S.D.; Tao, J.; Sharma, K.; Pullman, J.; et al. Defective Fatty Acid Oxidation in Renal Tubular Epithelial Cells Has a Key Role in Kidney Fibrosis Development. *Nat. Med.* **2015**, *21*, 37–46. https://doi.org/10.1038/nm.3762.

8. Okamura, D.M.; Pennathur, S.; Pasichnyk, K.; López-Guisa, J.M.; Collins, S.; Febbraio, M.; Heinecke, J.; Eddy, A.A. CD36 Regulates Oxidative Stress and Inflammation in Hypercholesterolemic CKD. *J. Am. Soc. Nephrol.* **2009**, *20*, 495–505. https://doi.org/10.1681/ASN.2008010009.

9. Liebman, S.E.; Le, T.H. Eat Your Broccoli: Oxidative Stress, NRF2, and Sulforaphane in Chronic Kidney Disease. *Nutrients* **2021**, *13*, 266. https://doi.org/10.3390/nu13010266.

10. Briones-Herrera, A.; Avila-Rojas, S.H.; Aparicio-Trejo, O.E.; Cristóbal, M.; León-Contreras, J.C.; Hernández-Pando, R.; Pinzón, E.; Pedraza-Chaverri, J.; Sánchez-Lozada, L.G.; Tapia, E. Sulforaphane Prevents Maleic Acid-Induced Nephropathy by Modulating Renal Hemodynamics, Mitochondrial Bioenergetics and Oxidative Stress. *Food Chem. Toxicol.* **2018**, *115*, 185–197. https://doi.org/10.1016/j.fct.2018.03.016.

11. Guerrero-Beltrán, C.E.; Mukhopadhyay, P.; Horváth, B.; Rajesh, M.; Tapia, E.; García-Torres, I.; Pedraza-Chaverri, J.; Pacher, P. Sulforaphane, a Natural Constituent of Broccoli, Prevents Cell Death and Inflammation in Nephropathy. *J. Nutr. Biochem.* **2012**, *23*, 494–500. https://doi.org/10.1016/j.jnutbio.2011.02.004.

12. Kim, T.; Kim, Y.-J.; Han, I.-H.; Lee, D.; Ham, J.; Kang, K.S.; Lee, J.W. The Synthesis of Sulforaphane Analogues and Their Protection Effect against Cisplatin Induced Cytotoxicity in Kidney Cells. *Bioorg. Med. Chem. Lett.* **2015**, *25*, 62–66. https://doi.org/10.1016/j.bmcl.2014.11.014.

13. Li, Z.; Guo, H.; Li, J.; Ma, T.; Zhou, S.; Zhang, Z.; Miao, L.; Cai, L. Sulforaphane Prevents Type 2 Diabetes-Induced Nephropathy via AMPK-Mediated Activation of Lipid Metabolic Pathways and Nrf2 Antioxidative Function. *Clin. Sci.* **2020**, *134*, 2469–2487. https://doi.org/10.1042/CS20191088.

14. Chung, S.D.; Lai, T.Y.; Chien, C.T.; Yu, H.J. Activating Nrf-2 Signaling Depresses Unilateral Ureteral Obstruction-Evoked Mitochondrial Stress-Related Autophagy, Apoptosis and Pyroptosis in Kidney. *PLoS ONE* **2012**, *7*, e47299. https://doi.org/10.1371/journal.pone.0047299.

15. Li, J.; Xie, S.; Teng, W. Sulforaphane Attenuates Nonalcoholic Fatty Liver Disease by Inhibiting Hepatic Steatosis and Apoptosis. *Nutrients* **2021**, *14*, 76. https://doi.org/10.3390/nu14010076.

16. Briones-Herrera, A.; Ramírez-Camacho, I.; Zazueta, C.; Tapia, E.; Pedraza-Chaverri, J. Altered Proximal Tubule Fatty Acid Utilization, Mitophagy, Fission and Supercomplexes Arrangement in Experimental Fanconi Syndrome Are Ameliorated by Sulforaphane-Induced Mitochondrial Biogenesis. *Free Radic. Biol. Med.* **2020**, *153*, 54–70. https://doi.org/10.1016/j.freeradbiomed.2020.04.010.

17. Guerrero-Beltrán, C.E.; Calderón-Oliver, M.; Martínez-Abundis, E.; Tapia, E.; Zarco-Márquez, G.; Zazueta, C.; Pedraza-Chaverri, J. Protective Effect of Sulforaphane against Cisplatin-Induced Mitochondrial Alterations and Impairment in the Activity of NAD(P)H: Quinone Oxidoreductase 1 and γ Glutamyl Cysteine Ligase: Studies in Mitochondria Isolated from Rat Kidney and in LLC-PK1 Cells. *Toxicol. Lett.* **2010**, *199*, 80–92. https://doi.org/10.1016/j.toxlet.2010.08.009.

18. Stuhr, N.; Nhan, J.; Hammerquist, A.; Van Camp, B.; Reoyo, D.; Curran, S. Rapid Lipid Quantification in Caenorhabditis Elegans by Oil Red O and Nile Red Staining. *BIO-PROTOCOL* **2022**, *12*, e4340. https://doi.org/10.21769/BioProtoc.4340.

19. Schindelin, J.; Arganda-Carreras, I.; Frise, E.; Kaynig, V.; Longair, M.; Pietzsch, T.; Preibisch, S.; Rueden, C.; Saalfeld, S.; Schmid, B.; et al. Fiji: An Open-Source Platform for Biological-Image Analysis. *Nat. Methods* **2012**, *9*, 676–682, doi:10.1038/nmeth.2019.

20. Aparicio-Trejo, O.E.; Reyes-Fermín, L.M.; Briones-Herrera, A.; Tapia, E.; León-Contreras, J.C.; Hernández-Pando, R.; Sánchez-Lozada, L.G.; Pedraza-Chaverri, J. Protective Effects of N-Acetyl-Cysteine in Mitochondria Bioenergetics, Oxidative Stress, Dynamics and S-Glutathionylation Alterations in Acute Kidney Damage Induced by Folic Acid. *Free. Radic. Biol. Med.* **2019**, *130*, 379–396. https://doi.org/10.1016/j.freeradbiomed.2018.11.005.

21. Waterborg, J.H.; Matthews, H.R. The Lowry Method for Protein Quantitation. In *Methods in Molecular Biology*; Humana Press: Totowa, NJ, USA, 1984; Volume 1, pp. 1–3. https://doi.org/10.1385/0-89603-062-8:1.

22. Bosoi, C.R.; Vandal, M.; Tournissac, M.; Leclerc, M.; Fanet, H.; Mitchell, P.L.; Verreault, M.; Trottier, J.; Virgili, J.; Tremblay, C.; et al. High-Fat Diet Modulates Hepatic Amyloid β and Cerebrosterol Metabolism in the Triple Transgenic Mouse Model of Alzheimer's Disease. *Hepatol. Commun.* **2021**, *5*, 446–460. https://doi.org/10.1002/hep4.1609.

23. Boran, T.; Akyildiz, A.G.; Jannuzzi, A.T.; Alpertunga, B. Extended Regorafenib Treatment Can Be Linked with Mitochondrial Damage Leading to Cardiotoxicity. *Toxicol. Lett.* **2021**, *336*, 39–49. https://doi.org/10.1016/j.toxlet.2020.11.003.

24. Negrette-Guzmán, M.; García-Niño, W.R.; Tapia, E.; Zazueta, C.; Huerta-Yepez, S.; León-Contreras, J.C.; Hernández-Pando, R.; Aparicio-Trejo, O.E.; Madero, M.; Pedraza-Chaverri, J. Curcumin Attenuates Gentamicin-Induced Kidney Mitochondrial Alterations: Possible Role of a Mitochondrial Biogenesis Mechanism. *Evid.-Based Complementary Altern. Med.* **2015**, *2015*, e917435. https://doi.org/10.1155/2015/917435.

25. Vela-Guajardo, J.E.; Pérez-Treviño, P.; Rivera-Álvarez, I.; González-Mondellini, F.A.; Altamirano, J.; García, N. The 8-Oxo-Deoxyguanosine Glycosylase Increases Its Migration to Mitochondria in Compensated Cardiac Hypertrophy. *J. Am. Soc. Hypertens.* **2017**, *11*, 660–672. https://doi.org/10.1016/j.jash.2017.08.004.

26. Folch, J.; Lees, M.; Sloane Stanley, G.H. A Simple Method for the Isolation and Purification of Total Lipides from Animal Tissues. *J. Biol. Chem.* **1957**, *226*, 497–509.

27. Daróczi, A.B.; Rapport, G. A Report Templating System 2012. R package version 1.1, https://cran.r-project.org/package=rapport. (Accessed on 7 September 2022).

28. Svensson, K.; Schnyder, S.; Cardel, B.; Handschin, C. Loss of Renal Tubular PGC-1α Exacerbates Diet-Induced Renal Steatosis and Age-Related Urinary Sodium Excretion in Mice. *PLoS ONE* **2016**, *11*, e0158716. https://doi.org/10.1371/journal.pone.0158716.

29. Liu, H.; Li, W.; He, Q.; Xue, J.; Wang, J.; Xiong, C.; Pu, X.; Nie, Z. Mass Spectrometry Imaging of Kidney Tissue Sections of Rat Subjected to Unilateral Ureteral Obstruction. *Sci. Rep.* **2017**, *7*, 41954. https://doi.org/10.1038/srep41954.

30. Cantu, D.; Schaack, J.; Patel, M. Oxidative Inactivation of Mitochondrial Aconitase Results in Iron and H2O2-Mediated Neurotoxicity in Rat Primary Mesencephalic Cultures. *PLoS ONE* **2009**, *4*, e7095. https://doi.org/10.1371/journal.pone.0007095.

31. Stadler, K.; Goldberg, I.J.; Susztak, K. The Evolving Understanding of the Contribution of Lipid Metabolism to Diabetic Kidney Disease. *Curr. Diabetes Rep.* **2015**, *15*, 40. https://doi.org/10.1007/s11892-015-0611-8.

32. Lewy, P.R.; Quintanilla, A.; Levin, N.W.; Kessler, R.H. Renal Energy Metabolism and Sodium Reabsorption. *Annu. Rev. Med.* **1973**, *24*, 365–384. https://doi.org/10.1146/annurev.me.24.020173.002053.

33. Lei, P.; Tian, S.; Teng, C.; Huang, L.; Liu, X.; Wang, J.; Zhang, Y.; Li, B.; Shan, Y. Sulforaphane Improves Lipid Metabolism by Enhancing Mitochondrial Function and Biogenesis In Vivo and In Vitro. *Mol. Nutr. Food Res.* **2019**, *63*, 1800795. https://doi.org/10.1002/mnfr.201800795.

34. Li, S.; Lin, Q.; Shao, X.; Zhu, X.; Wu, J.; Wu, B.; Zhang, M.; Zhou, W.; Zhou, Y.; Jin, H.; et al. Drp1-Regulated PARK2-Dependent Mitophagy Protects against Renal Fibrosis in Unilateral Ureteral Obstruction. *Free Radic. Biol. Med.* **2020**, *152*, 632–649. https://doi.org/10.1016/j.freeradbiomed.2019.12.005.

35. Bhatia, D.; Chung, K.-P.; Nakahira, K.; Patino, E.; Rice, M.C.; Torres, L.K.; Muthukumar, T.; Choi, A.M.; Akchurin, O.M.; Choi, M.E. Mitophagy-Dependent Macrophage Reprogramming Protects against Kidney Fibrosis. *JCI Insight* **2019**, *4*, 132826. https://doi.org/10.1172/jci.insight.132826.

36. Aranda-Rivera, A.K.; Cruz-Gregorio, A.; Aparicio-Trejo, O.E.; Ortega-Lozano, A.J.; Pedraza-Chaverri, J. Redox Signaling Pathways in Unilateral Ureteral Obstruction (UUO)-Induced Renal Fibrosis. *Free. Radic. Biol. Med.* **2021**, *172*, 65–81. https://doi.org/10.1016/j.freeradbiomed.2021.05.034.

37. Martínez-Klimova, E.; Aparicio-Trejo, O.E.; Gómez-Sierra, T.; Jiménez-Uribe, A.P.; Bellido, B.; Pedraza-Chaverri, J. Mitochondrial Dysfunction and Endoplasmic Reticulum Stress in the Promotion of Fibrosis in Obstructive Nephropathy Induced by Unilateral Ureteral Obstruction. *BioFactors* **2020**, *46*, 716–733. https://doi.org/10.1002/biof.1673.

38. Miguel, V.; Tituaña, J.; Herrero, J.I.; Herrero, L.; Serra, D.; Cuevas, P.; Barbas, C.; Puyol, D.R.; Márquez-Expósito, L.; Ruiz-Ortega, M.; et al. Renal Tubule Cpt1a Overexpression Protects from Kidney Fibrosis by Restoring Mitochondrial Homeostasis. *J. Clin. Investig.* **2021**, *131*, 140695. https://doi.org/10.1172/JCI140695.

39. Mohammad, R.S.; Lokhandwala, M.F.; Banday, A.A. Age-Related Mitochondrial Impairment and Renal Injury Is Ameliorated by Sulforaphane via Activation of Transcription Factor NRF2. *Antioxidants* **2022**, *11*, 156. https://doi.org/10.3390/antiox11010156.

40. Ucero, A.C.; Benito-Martin, A.; Izquierdo, M.C.; Sanchez-Niño, M.D.; Sanz, A.B.; Ramos, A.M.; Berzal, S.; Ruiz-Ortega, M.; Egido, J.; Ortiz, A. Unilateral Ureteral Obstruction: Beyond Obstruction. *Int. Urol. Nephrol.* **2014**, *46*, 765–776. https://doi.org/10.1007/s11255-013-0520-1.

41. Yenli, E.M.T.; Aboah, K.; Gyasi-Sarpong, C.K.; Azorliade, R.; Arhin, A.A. Acute and Chronic Urine Retention among Adults at the Urology Section of the Accident and Emergency Unit of Komfo Anokye Teaching Hospital, Kumasi, Ghana. *Afr. J. Urol.* **2015**, *21*, 129–136. https://doi.org/10.1016/j.afju.2014.08.009.

42. Mehta, R.L.; Pascual, M.T.; Soroko, S.; Chertow, G.M.; for the PICARD Study Group Diuretics, Mortality, and Nonrecovery of Renal Function in Acute Renal Failure. *JAMA* **2002**, *288*, 2547–2553. https://doi.org/10.1001/jama.288.20.2547.

43. Müller, V.; Losonczy, G.; Heemann, U.; Vannay, Á.; Fekete, A.; Reusz, G.; Tulassay, T.; Szabó, A.J. Sexual Dimorphism in Renal Ischemia-Reperfusion Injury in Rats: Possible Role of Endothelin. *Kidney Int.* **2002**, *62*, 1364–1371. https://doi.org/10.1111/j.1523-1755.2002.kid590.x.

44. Diamond, J.R.; Kees-Folts, D.; Ricardo, S.D.; Pruznak, A.; Eufemio, M. Early and Persistent Up-Regulated Expression of Renal Cortical Osteopontin in Experimental Hydronephrosis. *Am. J. Pathol.* **1995**, *146*, 1455–1466.

45. Bhargava, P.; Schnellmann, R.G. Mitochondrial Energetics in the Kidney. *Nat. Rev. Nephrol.* **2017**, *13*, 629–646. https://doi.org/10.1038/nrneph.2017.107.

46. Prieto-Carrasco, R.; García-Arroyo, F.E.; Aparicio-Trejo, O.E.; Rojas-Morales, P.; León-Contreras, J.C.; Hernández-Pando, R.; Sánchez-Lozada, L.G.; Tapia, E.; Pedraza-Chaverri, J. Progressive Reduction in Mitochondrial Mass Is Triggered by Alterations in Mitochondrial Biogenesis and Dynamics in Chronic Kidney Disease Induced by 5/6 Nephrectomy. *Biology* **2021**, *10*, 349. https://doi.org/10.3390/biology10050349.

47. Fontecha-Barriuso, M.; Martin-Sanchez, D.; Martinez-Moreno, J.; Monsalve, M.; Ramos, A.; Sanchez-Niño, M.; Ruiz-Ortega, M.; Ortiz, A.; Sanz, A. The Role of PGC-1α and Mitochondrial Biogenesis in Kidney Diseases. *Biomolecules* **2020**, *10*, 347. https://doi.org/10.3390/biom10020347.

48. Uittenbogaard, M.; Chiaramello, A. Mitochondrial Biogenesis: A Therapeutic Target for Neurodevelopmental Disorders and Neurodegenerative Diseases. *Curr. Pharm. Des.* **2014**, *20*, 5574–5593. https://doi.org/10.2174/1381612820666140305224906.

49. Patti, M.E.; Butte, A.J.; Crunkhorn, S.; Cusi, K.; Berria, R.; Kashyap, S.; Miyazaki, Y.; Kohane, I.; Costello, M.; Saccone, R.; et al. Coordinated Reduction of Genes of Oxidative Metabolism in Humans with Insulin Resistance and Diabetes: Potential Role of PGC1 and NRF1. *Proc. Natl. Acad. Sci. USA* **2003**, *100*, 8466–8471. https://doi.org/10.1073/pnas.1032913100.

50. Guarino, F.; Zinghirino, F.; Mela, L.; Pappalardo, X.G.; Ichas, F.; De Pinto, V.; Messina, A. NRF-1 and HIF-1α Contribute to Modulation of Human VDAC1 Gene Promoter during Starvation and Hypoxia in HeLa Cells. *Biochim. Biophys. Acta Bioenerg.* **2020**, *1861*, 148289. https://doi.org/10.1016/j.bbabio.2020.148289.

51. de Oliveira, M.R.; de Bittencourt Brasil, F.; Fürstenau, C.R. Sulforaphane Promotes Mitochondrial Protection in SH-SY5Y Cells Exposed to Hydrogen Peroxide by an Nrf2-Dependent Mechanism. *Mol. Neurobiol.* **2018**, *55*, 4777–4787. https://doi.org/10.1007/s12035-017-0684-2.

52. Kim, J.I.; Noh, M.R.; Yoon, G.-E.; Jang, H.-S.; Kong, M.J.; Park, K.M. IDH2 Gene Deficiency Accelerates Unilateral Ureteral Obstruction-Induced Kidney Inflammation through Oxidative Stress and Activation of Macrophages. *Korean J. Physiol. Pharmacol.* **2021**, *25*, 139–146. https://doi.org/10.4196/kjpp.2021.25.2.139.

53. Kong, M.J.; Han, S.J.; Kim, J.I.; Park, J.-W.; Park, K.M. Mitochondrial NADP+-Dependent Isocitrate Dehydrogenase Deficiency Increases Cisplatin-Induced Oxidative Damage in the Kidney Tubule Cells. *Cell Death Dis.* **2018**, *9*, 488. https://doi.org/10.1038/s41419-018-0537-6.

54. Cho, H.-Y.; Miller-DeGraff, L.; Blankenship-Paris, T.; Wang, X.; Bell, D.A.; Lih, F.; Deterding, L.; Panduri, V.; Morgan, D.L.; Yamamoto, M.; et al. Sulforaphane Enriched Transcriptome of Lung Mitochondrial Energy Metabolism and Provided Pulmonary Injury Protection via Nrf2 in Mice. *Toxicol. Appl. Pharmacol.* **2019**, *364*, 29–44. https://doi.org/10.1016/j.taap.2018.12.004.

55. Larsen, S.; Nielsen, J.; Hansen, C.N.; Nielsen, L.B.; Wibrand, F.; Stride, N.; Schroder, H.D.; Boushel, R.; Helge, J.W.; Dela, F.; et al. Biomarkers of Mitochondrial Content in Skeletal Muscle of Healthy Young Human Subjects. *J. Physiol.* **2012**, *590*, 3349–3360. https://doi.org/10.1113/jphysiol.2012.230185.

56. Ding, H.; Bai, F.; Cao, H.; Xu, J.; Fang, L.; Wu, J.; Yuan, Q.; Zhou, Y.; Sun, Q.; He, W.; et al. PDE/CAMP/Epac/C/EBP-β Signaling Cascade Regulates Mitochondria Biogenesis of Tubular Epithelial Cells in Renal Fibrosis. *Antioxid. Redox Signal.* **2018**, *29*, 637–652. https://doi.org/10.1089/ars.2017.7041.

57. Gureev, A.P.; Shaforostova, E.A.; Popov, V.N. Regulation of Mitochondrial Biogenesis as a Way for Active Longevity: Interaction Between the Nrf2 and PGC-1α Signaling Pathways. *Front. Genet.* **2019**, *10*, 435. https://doi.org/10.3389/fgene.2019.00435.

58. Lu, X.; Xuan, W.; Li, J.; Yao, H.; Huang, C.; Li, J. AMPK Protects against Alcohol-Induced Liver Injury through UQCRC2 to up-Regulate Mitophagy. *Autophagy* **2021**, *17*, 3622–3643. https://doi.org/10.1080/15548627.2021.1886829.

59. Choi, K.-M.; Lee, Y.-S.; Kim, W.; Kim, S.J.; Shin, K.-O.; Yu, J.-Y.; Lee, M.K.; Lee, Y.-M.; Hong, J.T.; Yun, Y.-P.; et al. Sulforaphane Attenuates Obesity by Inhibiting Adipogenesis and Activating the AMPK Pathway in Obese Mice. *J. Nutr. Biochem.* **2014**, *25*, 201–207. https://doi.org/10.1016/j.jnutbio.2013.10.007.

60. Zhang, Z.; Wang, S.; Zhou, S.; Yan, X.; Wang, Y.; Chen, J.; Mellen, N.; Kong, M.; Gu, J.; Tan, Y.; et al. Sulforaphane Prevents the Development of Cardiomyopathy in Type 2 Diabetic Mice Probably by Reversing Oxidative Stress-Induced Inhibition of LKB1/AMPK Pathway. *J. Mol. Cell. Cardiol.* **2014**, *77*, 42–52. https://doi.org/10.1016/j.yjmcc.2014.09.022.

61. Lo, Y.-H.; Yang, S.-F.; Cheng, C.-C.; Hsu, K.-C.; Chen, Y.-S.; Chen, Y.-Y.; Wang, C.-W.; Guan, S.-S.; Wu, C.-T. Nobiletin Alleviates Ferroptosis-Associated Renal Injury, Inflammation, and Fibrosis in a Unilateral Ureteral Obstruction Mouse Model. *Biomedicines* **2022**, *10*, 595. https://doi.org/10.3390/biomedicines10030595.

62. Saxena, N.; Maio, N.; Crooks, D.R.; Ricketts, C.J.; Yang, Y.; Wei, M.-H.; Fan, T.W.-M.; Lane, A.N.; Sourbier, C.; Singh, A.; et al. SDHB-Deficient Cancers: The Role of Mutations That Impair Iron Sulfur Cluster Delivery. *J. Natl. Cancer Inst.* **2016**, *108*, djv287. https://doi.org/10.1093/jnci/djv287.

63. Moosavi, B.; Zhu, X.; Yang, W.-C.; Yang, G.-F. Genetic, Epigenetic and Biochemical Regulation of Succinate Dehydrogenase Function. *Biol. Chem.* **2020**, *401*, 319–330. https://doi.org/10.1515/hsz-2019-0264.

64. Görmüş, U.; Kasap, M.; Akpınar, G.; Tuğtepe, H.; Kanlı, A.; Özel, K. Comparative Proteome Analyses of Ureteropelvic Junction Obstruction and Surrounding Ureteral Tissue. *Cells Tissues Organs* **2020**, *209*, 2–12. https://doi.org/10.1159/000506736.

65. Zhao, Q.; Xue, Y.; Yang, Y.; Niu, Z.; Wang, C.; Hou, Y.; Chen, H. Screening and Identification of the Differentially Expressed Proteins in Neonatal Rat Kidney after Partial Unilateral Ureteral Obstruction. *Mol. Med. Rep.* **2016**, *14*, 681–688. https://doi.org/10.3892/mmr.2016.5338.

66. Ge, M.; Fontanesi, F.; Merscher, S.; Fornoni, A. The Vicious Cycle of Renal Lipotoxicity and Mitochondrial Dysfunction. *Front. Physiol.* **2020**, *11*, 732.

67. Rong, Q.; Han, B.; Li, Y.; Yin, H.; Li, J.; Hou, Y. Berberine Reduces Lipid Accumulation by Promoting Fatty Acid Oxidation in Renal Tubular Epithelial Cells of the Diabetic Kidney. *Front. Pharmacol.* **2022**, *12*, 729384.

68. Houten, S.M.; Wanders, R.J.A. A General Introduction to the Biochemistry of Mitochondrial Fatty Acid β-Oxidation. *J. Inherit. Metab. Dis.* **2010**, *33*, 469–477. https://doi.org/10.1007/s10545-010-9061-2.

69. Lee, J.-H.; Moon, M.-H.; Jeong, J.-K.; Park, Y.-G.; Lee, Y.-J.; Seol, J.-W.; Park, S.-Y. Sulforaphane Induced Adipolysis via Hormone Sensitive Lipase Activation, Regulated by AMPK Signaling Pathway. *Biochem. Biophys. Res. Commun.* **2012**, *426*, 492–497. https://doi.org/10.1016/j.bbrc.2012.08.107.

70. Tannenbaum, J.; Purkerson, M.L.; Klahr, S. Effect of Unilateral Ureteral Obstruction on Metabolism of Renal Lipids in the Rat. *Am. J. Physiol.* **1983**, *245*, F254–F262. https://doi.org/10.1152/ajprenal.1983.245.2.F254.

71. Afshinnia, F.; Rajendiran, T.M.; Soni, T.; Byun, J.; Wernisch, S.; Sas, K.M.; Hawkins, J.; Bellovich, K.; Gipson, D.; Michailidis, G.; et al. Impaired β-Oxidation and Altered Complex Lipid Fatty Acid Partitioning with Advancing CKD. *J. Am. Soc. Nephrol.* **2018**, *29*, 295–306. https://doi.org/10.1681/ASN.2017030350.

72. Souza, A.C.P.; Bocharov, A.V.; Baranova, I.N.; Vishnyakova, T.G.; Huang, Y.G.; Wilkins, K.J.; Hu, X.; Street, J.M.; Alvarez-Prats, A.; Mullick, A.E.; et al. Antagonism of Scavenger Receptor CD36 by 5A Peptide Prevents Chronic Kidney Disease Progression in Mice Independent of Blood Pressure Regulation. *Kidney Int.* **2016**, *89*, 809–822. https://doi.org/10.1016/j.kint.2015.12.043.

73. Pennathur, S.; Pasichnyk, K.; Bahrami, N.M.; Zeng, L.; Febbraio, M.; Yamaguchi, I.; Okamura, D.M. The Macrophage Phagocytic Receptor CD36 Promotes Fibrogenic Pathways on Removal of Apoptotic Cells during Chronic Kidney Injury. *Am. J. Pathol.* **2015**, *185*, 2232–2245. https://doi.org/10.1016/j.ajpath.2015.04.016.

74. Jung, J.H.; Choi, J.E.; Song, J.H.; Ahn, S.-H. Human CD36 Overexpression in Renal Tubules Accelerates the Progression of Renal Diseases in a Mouse Model of Folic Acid-Induced Acute Kidney Injury. *Kidney Res. Clin. Pract.* **2018**, *37*, 30–40. https://doi.org/10.23876/j.krcp.2018.37.1.30.

75. Hayes, J.D.; Dinkova-Kostova, A.T. The Nrf2 Regulatory Network Provides an Interface between Redox and Intermediary Metabolism. *Trends Biochem. Sci.* **2014**, *39*, 199–218. https://doi.org/10.1016/j.tibs.2014.02.002.

76. Son, N.-H.; Basu, D.; Samovski, D.; Pietka, T.A.; Peche, V.S.; Willecke, F.; Fang, X.; Yu, S.-Q.; Scerbo, D.; Chang, H.R.; et al. Endothelial Cell CD36 Optimizes Tissue Fatty Acid Uptake. *J. Clin. Investig.* **2018**, *128*, 4329–4342. https://doi.org/10.1172/JCI99315.

77. Zhong, S.; Zhao, L.; Wang, Y.; Zhang, C.; Liu, J.; Wang, P.; Zhou, W.; Yang, P.; Varghese, Z.; Moorhead, J.F.; et al. Cluster of Differentiation 36 Deficiency Aggravates Macrophage Infiltration and Hepatic Inflammation by Upregulating Monocyte Chemotactic Protein-1 Expression of Hepatocytes Through Histone Deacetylase 2-Dependent Pathway. *Antioxid. Redox Signal.* **2017**, *27*, 201–214. https://doi.org/10.1089/ars.2016.6808.

78. Yen, C.-L.E.; Stone, S.J.; Koliwad, S.; Harris, C.; Farese, R.V. Thematic Review Series: Glycerolipids. DGAT Enzymes and Triacylglycerol Biosynthesis. *J. Lipid Res.* **2008**, *49*, 2283–2301. https://doi.org/10.1194/jlr.R800018-JLR200.

79. Zeng, H.; Qin, H.; Liao, M.; Zheng, E.; Luo, X.; Xiao, A.; Li, Y.; Chen, L.; Wei, L.; Zhao, L.; et al. CD36 Promotes de Novo Lipogenesis in Hepatocytes through INSIG2-Dependent SREBP1 Processing. *Mol. Metab.* **2022**, *57*, 101428. https://doi.org/10.1016/j.molmet.2021.101428.

80. Adams, C.M.; Reitz, J.; De Brabander, J.K.; Feramisco, J.D.; Li, L.; Brown, M.S.; Goldstein, J.L. Cholesterol and 25-Hydroxycholesterol Inhibit Activation of SREBPs by Different Mechanisms, Both Involving SCAP and Insigs*. *J. Biol. Chem.* **2004**, *279*, 52772–52780. https://doi.org/10.1074/jbc.M410302200.

81. Choi, K.-M.; Lee, Y.-S.; Sin, D.-M.; Lee, S.; Lee, M.K.; Lee, Y.-M.; Hong, J.-T.; Yun, Y.-P.; Yoo, H.-S. Sulforaphane Inhibits Mitotic Clonal Expansion During Adipogenesis Through Cell Cycle Arrest. *Obesity* **2012**, *20*, 1365–1371. https://doi.org/10.1038/oby.2011.388.

82. Teng, W.; Li, Y.; Du, M.; Lei, X.; Xie, S.; Ren, F. Sulforaphane Prevents Hepatic Insulin Resistance by Blocking Serine Palmitoyltransferase 3-Mediated Ceramide Biosynthesis. *Nutrients* **2019**, *11*, 1185. https://doi.org/10.3390/nu11051185.

83. Tian, S.; Li, B.; Lei, P.; Yang, X.; Zhang, X.; Bao, Y.; Shan, Y. Sulforaphane Improves Abnormal Lipid Metabolism via Both ERS-Dependent XBP1/ACC &SCD1 and ERS-Independent SREBP/FAS Pathways. *Molecular Nutrition & Food Research* **2018**, *62*, 1700737. https://doi.org/10.1002/mnfr.201700737.

84. Miyata, S.; Kodaka, M.; Kikuchi, A.; Matsunaga, Y.; Shoji, K.; Kuan, Y.-C.; Iwase, M.; Takeda, K.; Katsuta, R.; Ishigami, K.; et al. Sulforaphane Suppresses the Activity of Sterol Regulatory Element-Binding Proteins (SREBPs) by Promoting SREBP Precursor Degradation. *Sci. Rep.* **2022**, *12*, 8715. https://doi.org/10.1038/s41598-022-12347-6.

85. O'Mealey, G.B.; Berry, W.L.; Plafker, S.M. Sulforaphane Is a Nrf2-Independent Inhibitor of Mitochondrial Fission. *Redox Biol.* **2017**, *11*, 103–110. https://doi.org/10.1016/j.redox.2016.11.007.

86. Bhatia, D.; Choi, M.E. The Emerging Role of Mitophagy in Kidney Diseases. *J. Life Sci.* **2019**, *1*, 13–22. https://doi.org/10.36069/jols/20191203.

87. Kondapalli, C.; Kazlauskaite, A.; Zhang, N.; Woodroof, H.I.; Campbell, D.G.; Gourlay, R.; Burchell, L.; Walden, H.; Macartney, T.J.; Deak, M.; et al. PINK1 Is Activated by Mitochondrial Membrane Potential Depolarization and Stimulates Parkin E3 Ligase Activity by Phosphorylating Serine 65. *Open Biol.* **2012**, *2*, 120080. https://doi.org/10.1098/rsob.120080.

88. Lippai, M.; Lőw, P. The Role of the Selective Adaptor P62 and Ubiquitin-Like Proteins in Autophagy. *BioMed Res. Int.* **2014**, *2014*, 832704. https://doi.org/10.1155/2014/832704.

89. Liu, T.; Yang, Q.; Zhang, X.; Qin, R.; Shan, W.; Zhang, H.; Chen, X. Quercetin Alleviates Kidney Fibrosis by Reducing Renal Tubular Epithelial Cell Senescence through the SIRT1/PINK1/Mitophagy Axis. *Life Sci.* **2020**, *257*, 118116. https://doi.org/10.1016/j.lfs.2020.118116.

15.2 Artículos publicados durante el doctorado

REVIEW

WILEY

Regulation of autophagy by high- and low-risk human papillomaviruses

Ana Karina Aranda-Rivera[1,2] | Alfredo Cruz-Gregorio[3] | Alfredo Briones-Herrera[1,4] | José Pedraza-Chaverri[1]

[1]Laboratorio 315, Departamento de Biología, Facultad de Química, Universidad Nacional Autónoma de México, Mexico City, México

[2]Posgrado en Ciencias Biológicas, Universidad Nacional Autónoma de México, Ciudad Universitaria, Mexico City, México

[3]Laboratorio 225, Departamento de Biología, Facultad de Química, Universidad Nacional Autónoma de México, Mexico City, México

[4]Programa de Maestría y Doctorado en Ciencias Bioquímicas, Universidad Nacional Autónoma de México, Ciudad Universitaria, Mexico City, México

Correspondence

Alfredo Cruz-Gregorio, Laboratorio 225, Departamento de Biología, Facultad de Química, Universidad Nacional Autónoma de México, 04510, Mexico City, México.
Email: cruzgalfredo@gmail.com

José Pedraza-Chaverri, Laboratorio 315, Departamento de Biología, Facultad de Química, Universidad Nacional Autónoma de México, 04510, Mexico City, México.
Email: pedraza@unam.mx

Funding information

Programa de Apoyo a la Investigación y al Posgrado, Grant/Award Number: PAIP, 5000-9105; Programa de Apoyo a Proyectos de Investigación e Innovación Tecnológica, Dirección General de Asuntos del Personal Académico, Universidad Nacional Autónoma de México (UNAM), Grant/Award Number: PAPIIT, IN201316

Summary

While high-risk human papillomavirus (HR-HPV) infection is related to the development of cervical, vulvar, anal, penile and oropharyngeal cancer, low-risk human papillomavirus (LR-HPV) infection is implicated in about 90% of genital warts, which rarely progress to cancer. The carcinogenic role of HR-HPV is due to the over-expression of HPV E5, E6 and E7 oncoproteins which target and modify cellular proteins implicated in cell proliferation, apoptosis and immortalization. LR-HPV proteins also target and modify some of these processes; however, their oncogenic potential is lower than that of HR-HPV. HR-HPVs have substantial differences with LR-HPVs such as viral integration into the cell genome, induction of p53 and retinoblastoma protein degradation, alternative splicing in HR-HPV E6-E7 open reading frames, among others. In addition, LR-HPV can activate the autophagy process in infected cells while HR-HPV infection deactivates it. However, in cancer HR-HPV might reactivate autophagy in advance stages. Autophagy is a catabolic process that maintains cell homoeostasis by lysosomal degradation and recycling of damaged macromolecules and organelles; nevertheless, depending upon cellular context autophagy may also induce cell death. Therefore, autophagy can contribute either as a promotor or as a suppressor of tumours. In this review, we focus on the role of HR-HPV and LR-HPV in autophagy during viral infection and cancer development. Additionally, we review key regulatory molecules such as microRNAs in HPV present during autophagy, and we emphasize the potential use of cancer treatments associated with autophagy in HPV-related cancers.

KEYWORDS

autophagy, high-risk HPV (HR-HPV), HPV proteins, low-risk HPV (LR-HPV), microRNAs, treatments

Review

Human Papillomavirus-related Cancers and Mitochondria

Alfredo Cruz-Gregorio[a,*], Ana Karina Aranda-Rivera[b,c], José Pedraza-Chaverri[b]

[a] Faculty of Chemistry, Biology Department, Laboratories F-225, National Autonomous University of Mexico, CDMX, 04510, Mexico
[b] Faculty of Chemistry, Biology Department, Laboratories F-315, National Autonomous University of Mexico, CDMX, 04510, Mexico
[c] Posgrado en Ciencias Biológicas, Universidad Nacional Autónoma de México, Ciudad Universitaria, Ciudad de México, 04510, Mexico

A B S T R A C T

Although it has been established that persistent infection with high risk human papillomavirus (HR-HPV) is the main cause in the development of cervical cancer, the HR-HPV infection is also related with the cause of a significant fraction of other human malignancies from the mucosal squamous epithelial such as anus, vagina, vulva, penis and oropharynx. HR-HPV infection induces cell proliferation, cell death evasion and genomic instability resulting in cell transformation, due to HPV proteins, which target and modify the function of differents cell molecules and organelles, such as mitochondria. Mitochondria are essential in the production of the cellular energy by oxidative phosphorylation (OXPHOS), in the metabolism of nucleotides, aminoacids (aa), and fatty acids, even in the regulation of cell death processes such as apoptosis or mitophagy. Thus, mitochondria have a significant role in the HPV-related cancer development. This review focuses on the role of HPV and mitochondria in HPV-related cancer development, and treatments associated to mitochondrial apoptosis.

1. Introduction

Epidemiological and molecular studies have established persistent infection with high risk human papillomavirus (HR-HPV) as a risk factor for the development of cervical cancer (Walboomers et al., 1999). Moreover, HR-HPV infection is also related with the cause of a significant fraction of other human malignancies from the mucosal squamous epithelial of penis, vulva, vagina and oropharynx (Bray et al., 2018). More than 200 types of HPV have been identified, of which types HR-HPV16 and 18 are the most persistent (Burd, 2003). HPV is a small virus of approximately 55 nm, not enveloped which belongs to the family *Papillomaviridae* (de Villiers, 2013). Viruses of this family are widely distributed in nature, and infect specifically the squamous epithelium of more than 20 different species of mammals, as well as birds and reptiles (Egawa et al., 2015; Marschang, 2011). Regarding HPV, its capsid is made up of 72 capsomeres (60 hexamers and 12 pentamers), consisting of the structural proteins L1 and L2 that house the viral genome (Humans, 2007). Viral genome consists of double stranded circular deoxyribonucleic acid (DNA) from 7,200 to 8,000 base pairs (bp), with more than 10 open reading frames (ORFs) and usually a thread is transcriptionally active (Doorbar et al., 2012). Viral genome has been divided into three regions: early region (E: Early) which codes for genes involved in replication and maintenance of the viral genome (E1-E8); late region (L: Late), which encodes the structural proteins of

the L1 capsid and L2, and finally, the long control region (LCR: Long Control Region), which contains the regulatory sites for viral transcription and replication (Zheng and Baker, 2006).

It has been shown that the overexpression of E6 and E7 oncoproteins, which have as molecular targets a wide range of cell molecules, induce cancer development (Tomaić, 2016). HR-HPV E1^E4 and E2 proteins, as well as E6 and E7 oncoproteins bind to diverse proteins in the infected cell, either in the cytosol or in organelles such as mitochondria, that modify their function and influence the HR-HPV life cycle and cell transformation. This review focuses on the role of HR-HPV over mitochondria in the development of HPV-related cancer and treatments associated with mitochondrial apoptosis.

2. Mitochondria and cancer

2.1. Mitochondria, oxidative stress (OS) and cancer development

Mitochondria are responsible for an extensive range of critical functions for metabolism, cell growth, cell survival and apoptosis, having a major role in the development of cancer. By regulating the metabolism, mitochondria coordinate bioenergetic processes such as tricarboxylic acid cycle (TCA), electron transport system (ETS) and fatty acid oxidation (FAO); as well as biosynthetic processes such as synthesis of aminoacids (aa), lipids and nucleotides (Vyas et al., 2016). Glucose is

REVIEW

WILEY

Redox-sensitive signalling pathways regulated by human papillomavirus in HPV-related cancers

Alfredo Cruz-Gregorio[1] ⬤ | **Ana Karina Aranda-Rivera**[2,3] ⬤

[1]Laboratorio F-225, Departamento de Biología, Facultad de Química, Universidad Nacional Autónoma de México, México City, México

[2]Laboratorio F-315, Departamento de Biología, Facultad de Química, Universidad Nacional Autónoma de México, México City, México

[3]Posgrado en Ciencias Biológicas, Universidad Nacional Autónoma de México, Ciudad Universitaria, México City, México

Correspondence
Alfredo Cruz-Gregorio, Laboratorio F-225, Departamento de Biología, Facultad de Química, Universidad Nacional Autónoma de México, México City 04360, Mexico.
Email: cruzgalfredo@gmail.com

Summary

High-risk human papillomavirus (HR-HPV) chronic infection is associated with the induction of different HPV-related cancers, such as cervical, anus, vaginal, vulva, penis and oropharynx. HPV-related cancers have been related to oxidative stress (OS), where OS has a significant role in cancer development and maintenance. Surgical resection is the treatment of choice for localised HPV-related cancers; however, these malignancies commonly progress to metastasis. In advanced stages, systemic therapies are the best option against HPV-related cancers. These therapies include cytokine therapy or a combination of tyrosine kinase inhibitors with immunotherapies. Nevertheless, these strategies are still insufficient. Cell redox-sensitive signalling pathways have been poorly studied, although they have been associated with the development and maintenance of HPV-related cancers. In this review, we analyse the known alterations of the following redox-sensitive molecules and signalling pathways by HR-HPV in HPV-related cancers: MAPKs, Akt/TSC2/mTORC1, Wnt/β-Cat, NFkB/IkB/NOX2, HIF/VHL/VEGF and mitochondrial signalling pathways as potential targets for redox therapy.

KEYWORDS
high-risk human papillomavirus (HR-HPV), HPV-related cancer, oxidative stress, redox-sensitive signalling pathways, redox state, redox therapy

wileyonlinelibrary.com/journal/rmv

© 2021 John Wiley & Sons Ltd. | **1 of 12**

Redox signaling pathways in unilateral ureteral obstruction (UUO)-induced renal fibrosis

Ana Karina Aranda-Rivera [a,b], Alfredo Cruz-Gregorio [c], Omar Emiliano Aparicio-Trejo [a], Ariadna Jazmín Ortega-Lozano [a], José Pedraza-Chaverri [a,*]

[a] Laboratorio F-315, Departamento de Biología, Facultad de Química, Universidad Nacional Autónoma de México, 04510, Ciudad de México, Mexico
[b] Posgrado en Ciencias Biológicas, Universidad Nacional Autónoma de México, Ciudad Universitaria, Laboratorio F-225, Ciudad de México, 04510, Mexico
[c] Laboratorio F-225, Departamento de Biología, Facultad de Química, Universidad Nacional Autónoma de México, 04510, Ciudad de México, Mexico

A B S T R A C T

Unilateral ureteral obstruction (UUO) is an experimental rodent model that mimics renal fibrosis associated with obstructive nephropathy in an accelerated manner. After UUO, the activation of the renin-angiotensin system (RAS), nicotinamide adenine dinucleotide phosphate (NADPH) oxidases (NOXs) and mitochondrial dysfunction lead to reactive oxygen species (ROS) overproduction in the kidney. ROS are secondary messengers able to induce post-translational modifications (PTMs) in redox-sensitive proteins, which activate or deactivate signaling pathways. Therefore, in UUO, it has been proposed that ROS overproduction causes changes in said pathways promoting inflammation, oxidative stress, and apoptosis that contribute to fibrosis development. Furthermore, mitochondrial metabolism impairment has been associated with UUO, contributing to renal damage in this model. Although ROS production and oxidative stress have been studied in UUO, the development of renal fibrosis associated with redox signaling pathways has not been addressed. This review focuses on the current information about the activation and deactivation of signaling pathways sensitive to a redox state and their effect on mitochondrial metabolism in the fibrosis development in the UUO model.

1. Introduction

Obstructive nephropathy is a significant health problem in the world that predominantly affects neonates and children. It is characterized by a blockage in the flow of urine that causes hydronephrosis and, ultimately, renal failure [1,2]. Moreover, given the silent nature of the disease, obstructive nephropathy favors the development of chronic kidney disease (CKD) [3].

Unilateral ureteral obstruction (UUO) is an in vivo model that mimics renal fibrosis associated with chronic obstructive nephropathy, which can be developed in a short period of time [4]. The UUO consists of the ligation of the left ureter with a silk thread. In this model, the ligated ureter kidney is named obstructed kidney, while the non-ligated (contralateral) is the non-obstructed kidney [4,5]. After UUO, the rise in the hydrostatic pressure caused by urine stagnation triggers the activation of the renin-angiotensin system (RAS) through the production of angiotensin II (Ang II). Ang II, in turn, activates nicotinamide adenine dinucleotide phosphate (NADPH) oxidases (NOXs), producing reactive oxygen species (ROS). ROS production leads to oxidative stress and inflammation, ultimately producing cell death by apoptosis or necrosis [6]. These mechanisms also induce myofibroblast activation from resident fibroblasts in the kidney, replacing the lost epithelial cells with extracellular matrix (ECM), promoting progressive fibrosis [6,7].

Mitochondria are the primary energy source needed for tubular reabsorption through oxidative phosphorylation (OXPHOS) in the kidney [8]. In UUO, mitochondria dysfunction is associated with the genesis and progression of renal disease, principally by the overproduction of ROS that generates oxidative stress [9]. In addition to mitochondria, NOXs and endoplasmic reticulum (ER) are important ROS sources that can induce the activation of several signaling pathways, promoting inflammation and fibrosis [10,11].

Since ROS act as second messengers necessary to maintain cellular homeostasis, their concentration, as well as their production and elimination, are under tight control by the antioxidant system. Thus, ROS can regulate signaling pathways implicated in growth, differentiation, inflammation, apoptosis, and epithelial-mesenchymal transition (EMT), among others [12].

* Corresponding author.
E-mail addresses: anaaranda025@gmail.com (A.K. Aranda-Rivera), cruzgalfredo@gmail.com (A. Cruz-Gregorio), emilianoaparicio91@gmail.com (O.E. Aparicio-Trejo), arijol.sk@gmail.com (A.J. Ortega-Lozano), pedraza@unam.mx (J. Pedraza-Chaverri).

Review

Mitochondrial Redox Signaling and Oxidative Stress in Kidney Diseases

Ana Karina Aranda-Rivera [1,2] , **Alfredo Cruz-Gregorio** [3] , **Omar Emiliano Aparicio-Trejo** [4] and **José Pedraza-Chaverri** [1,*]

1   Laboratorio F-315, Departamento de Biología, Facultad de Química, Universidad Nacional Autónoma de México, Mexico City 04510, Mexico; anaaranda025@gmail.com
2   Posgrado en Ciencias Biológicas, Universidad Nacional Autónoma de México, Ciudad Universitaria, Mexico City 04510, Mexico
3   Laboratorio F-225, Departamento de Biología, Facultad de Química, Universidad Nacional Autónoma de México, Mexico City 04510, Mexico; cruzgalfredo@gmail.com
4   Departmento de Fisiopatología Cardio-Renal, Instituto Nacional de Cardiología "Ignacio Chávez", Mexico City 14080, Mexico; emilianoaparicio91@gmail.com
*   Correspondence: pedraza@unam.mx; Tel.: +52-555622-3878

Abstract: Mitochondria are essential organelles in physiology and kidney diseases, because they produce cellular energy required to perform their function. During mitochondrial metabolism, reactive oxygen species (ROS) are produced. ROS function as secondary messengers, inducing redox-sensitive post-translational modifications (PTM) in proteins and activating or deactivating different cell signaling pathways. However, in kidney diseases, ROS overproduction causes oxidative stress (OS), inducing mitochondrial dysfunction and altering its metabolism and dynamics. The latter processes are closely related to changes in the cell redox-sensitive signaling pathways, causing inflammation and apoptosis cell death. Although mitochondrial metabolism, ROS production, and OS have been studied in kidney diseases, the role of redox signaling pathways in mitochondria has not been addressed. This review focuses on altering the metabolism and dynamics of mitochondria through the dysregulation of redox-sensitive signaling pathways in kidney diseases.

1. Introduction

Kidney diseases are a severe health problem that causes high economic costs worldwide in medical attention, emergency, therapies, among others [1,2]. These are divided into acute kidney injury (AKI) and chronic kidney diseases (CKD). AKI encompasses a set of pathologies characterized by the rapid loss of renal function in a short period [3]. AKI is often caused by the use of chemotherapeutics agents such as cisplatin, episodes of renal ischemia/reperfusion (I/R), and exposure to contaminants [4]. AKI is associated with high morbidity and mortality, contributing to CKD development and affecting approximately between 7% and 12% of the world [5]. CKD cause renal fibrosis development [6–8]. The latter comprises an unsatisfactory repair process and is the consequence of severe and persistent damage that does not restore organ function [9]. Renal fibrosis, in turn, is one of the principal mechanisms involved in AKI to CKD transition [5].

Mitochondria are responsible for several cell functions such as cell growth, cell survival, and apoptosis induction, playing a significant role in kidney physiology and the development of kidney diseases. Mitochondria also coordinate the biosynthesis of lipids, amino acids, and nucleotides and bioenergetics processes such as tricarboxylic acid (TCA) cycles, electron transport systems (ETSs), and fatty acids (FA) β-oxidation [10]. During

Review Article

Lipid metabolism and oxidative stress in HPV-related cancers

Alfredo Cruz-Gregorio [a,*], Ana Karina Aranda-Rivera [b,c], Ariadna Jazmin Ortega-Lozano [b], José Pedraza-Chaverri [b], Francisco Mendoza-Hoffmann [d,e]

[a] *Laboratorio F-225, Departamento de Biología, Facultad de Química, Universidad Nacional Autónoma de México, 04510, Ciudad de México, Mexico*
[b] *Laboratorio F-315, Departamento de Biología, Facultad de Química, Universidad Nacional Autónoma de México, 04510, Ciudad de México, Mexico*
[c] *Posgrado en Ciencias Biológicas, Universidad Nacional Autónoma de México, Ciudad Universitaria, Ciudad de México 04510, Mexico*
[d] *IHuman Institute, ShanghaiTech University, China*
[e] *Laboratorio F-206, Departamento de Biología, Facultad de Química, Universidad Nacional Autónoma de México, 04510, Ciudad de México, Mexico*

A B S T R A C T

High-risk human papillomavirus (HR-HPVs) are associated with the development of cervical, anus, vagina, vulva, penis, and oropharynx cancer. HR-HPVs target and modify the function of different cell biomolecules such as glucose, amino acids, lipids, among others. The latter induce cell proliferation, cell death evasion, and genomic instability resulting in cell transformation. Moreover, lipids are essential biomolecules in HR-HPVs infection and cell vesicular trafficking. They are also critical in producing cellular energy, the epithelial-mesenchymal transition (EMT) process, and therapy resistance of HPV-related cancers. HPV proteins induce oxidative stress (OS), which in turn promotes lipid peroxidation and cell damage, resulting in cell death such as apoptosis, autophagy, and ferroptosis. HR-HPV-related cancer cells cope with OS and lipid peroxidation, preventing cell death; however, these cells are sensitized by OS, which could be used as a target for redox therapies to induce their elimination. This review focuses on the role of lipids in HR-HPV infection and HPV-related cancer development, maintenance, resistance to therapy, and the possible treatments associated with lipids. Furthermore, we emphasize the significant role of OS in lipid peroxidation to induce cell death through apoptosis, autophagy, and ferroptosis to eliminate HPV-related cancers.

1. Introduction

It has been established that persistent infection with high-risk human papillomavirus (HR-HPV) induces the development of cervical cancer [1]. Furthermore, HR-HPV infection is also related to developing of penis, vulva, vagina, and oropharynx cancers [2]. The induction of cancer by HR-HPV is associated with the overexpression of its E5, E6, and E7 oncoproteins. These oncoproteins regulate different molecules such as the members of the epidermal growth factor receptor (EGFRs) family, p53, and retinoblastoma protein (pRb) respectively [3], and organelles such as mitochondria [4,5]. Moreover, these oncoproteins regulate different cell signaling pathways [6,7] and different cellular processes such as autophagy [8], and apoptosis [9], among others.

Lipid metabolism (digestion, absorption, catabolism, biosynthesis, and peroxidation) is crucial in HR-HPV infection and cancer development related to HR-HPV. For instance, lipid composition in the cell membrane allows HR-HPV infection efficacy [10]. Immune system

evasion is another characteristic that is associated with lipid metabolism [11]. Additionally, in HR-HPV-induced carcinogenesis, lipids such as phosphatidylinositol (3,4,5)-trisphosphate (PIP3) produced by the activation of phosphatidylinositol 3-kinase catalytic alpha (PI3KCA) are essential to activate cell signaling pathways associated with protein kinase B (Akt) [12]. Lipids are also critical energy biomolecules in cellular energy reprogramming induced in HR-HPV-related cancers. Furthermore, the shifting of cell membrane composition grants the epithelial-mesenchymal transition (EMT) associated with metastasis in HPV-related cancers. Thus, lipids are essential in HR-HPV infection and HPV-related cancer development and may also be an important target for new approaches associated with treatments during HR-HPV infection or cancer development.

HPV proteins induce oxidative stress (OS), promoting lipid peroxidation and cell damage. This could result in cell death, i.e., apoptosis, autophagy, and ferroptosis; however, HPV-related cancers can cope with OS, avoiding lipid peroxidation and cell death. Interestingly, this cell condition can also become a target of redox therapies for eliminating

---

REVIEW ARTICLE

Biofactors WILEY

Redox-sensitive signaling pathways in renal cell carcinoma

Alfredo Cruz-Gregorio[1] | Ana Karina Aranda-Rivera[2] | José Pedraza-Chaverri[2] | José D. Solano[1] | María Elena Ibarra-Rubio[1]

[1]Laboratorio F-225, Departamento de Biología, Facultad de Química, Universidad Nacional Autónoma de México, Ciudad de México, Mexico

[2]Laboratorio F-315, Departamento de Biología, Facultad de Química, Universidad Nacional Autónoma de México, Ciudad de México, Mexico

Correspondence
Alfredo Cruz-Gregorio and María Elena Ibarra-Rubio, Laboratorio F-225, Departamento de Biología, Facultad de Química, Universidad Nacional Autónoma de México, 04510, Ciudad de México, Mexico.
Email: cruzgalfredo@gmail.com and meir@unam.mx

Abstract

Renal cell carcinoma (RCC) is one of the most lethal urological cancers, highly resistant to chemo and radiotherapy. Obesity and smoking are the best-known risk factors of RCC, both related to oxidative stress presence, suggesting a significant role in RCC development and maintenance. Surgical resection is the treatment of choice for localized RCC; however, this neoplasia is hardly diagnosable at its initial stages, occurring commonly in late phases and even when metastasis is already present. Systemic therapies are the option against RCC in these more advanced stages, such as cytokine therapy or a combination of tyrosine kinase inhibitors with immunotherapies; nevertheless, these strategies are still insufficient. A field poorly analyzed in this neoplasia is the status of cell

Abbreviations: ˙SNO, S-nitrosothiol; 4E-BP, eukaryotic translation initiation factor 4E (eIF4E)-binding protein; β-cat, β-catenin; AKT, protein kinase B; AP-1, activator protein 1; APC, adenoma polyposis coli; ASK, apoptosis signal-regulating kinase; ATF2, activating transcription factor 2; CAT, catalase; CBP, CREB-binding protein; CK1, casein kinase 1; CREB, cAMP response element-binding; Cys, cysteine; DUOXs, dual oxidase; DUSP3, dual-specific phosphatase 3; EGF, epidermal growth factor; EGFR, EGF receptor; Elk, ETS like-1; EPAS1, endothelial PAS domain-containing protein 1; ER, endoplasmic reticulum; ERK, extracellular regulated kinase; ETC, electron transport chain; FASL, Fas ligand; FBXW1A, F-box/WD repeat-containing protein 1A; FeNTA, ferric nitrilotriacetate; FIH, factor inhibiting hypoxia-inducible factor; G6PD, glucose-6-phosphate dehydrogenase; GCK, germinal center kinase; GDP, guanine diphosphate; GFR, growth factor receptor; GPx, glutathione peroxidase; GR, glutathione reductase; GRB2, growth factor receptor-bound protein 2; GSH, glutathione; GSK3, glycogen synthase kinase 3; H_2O_2, hydrogen peroxide; H_2S, hydrogen sulfide; HIF, hypoxia-inducible factor; IkB, inhibitor of κB; IKK, IκB kinase complex; IKKβ, IκB kinase β; IL, interleukin; JNKs, C-Jun N-terminal; LRP, low-density lipoprotein receptor-related protein; MAP2K, MAP kinase kinase; MAP3K, MAP kinase kinase kinase; MAPK, mitogen-activated protein kinase; MEK 1/2, mitogen-activated protein kinase kinase 1, 2; Met, methionine; MetO, methionine sulfoxide; MetO2, methionine sulfone; MKP, MAPK phosphatase; MLK, mixed lineage kinase; MMP2, matrix metalloproteinase 2; mRCC, metastatic RCC; Msr, methionine sulfoxide reductase; mTOR, mammalian target of rapamycin; mTORC1, mammalian target of rapamycin C1; NADPH, nicotinamide adenine dinucleotide phosphate; NFAT, nuclear factor of activated T cell; NF-κB, nuclear factor κB; NO, nitric oxide; NOS, nitric oxide synthase; NOX, NADPH oxidase; NSAID, nonsteroidal anti-inflammatory drug; $O_2^{•−}$, superoxide anion radical; OH, hydroxyl radical; $ONOO^−$, peroxynitrite; ox-PTM, oxidative post-translational modification; PDGF, platelet-derived growth factor; PDGFR, PDGF receptor; PDK1, phosphoinositide-dependent kinase-1; p-ERK1, phosphorylation of ERK1; PHD, prolyl hydroxylase; PI3K, phosphatidylinositol 3-kinase; PIP2, phosphatidylinositol 4,5; PIP3, phosphatidylinositol 3,4,5 triphosphate; p-JNK1, phosphorylation of JNK1; PKCζ, protein kinase Cζ; p-p38α/β, phosphorylation of p38α/β; PPP, pentose phosphate pathway; PRDX, peroxiredoxin; PTEN, phosphatase and tensin homolog; PTK, protein tyrosine kinase; PTP, protein tyrosine phosphatase; RAF, rapidly accelerated fibrosarcoma; RCC, renal cell carcinoma; Rheb, RAS homolog enriched in brain; ROS, reactive oxygen species; R-S(O)-S-R, thiosulfinate; R-SN-R', sulfenamide; R-SO2H, sulfinic acid; R-SO3H, sulfonic acid; R-SOH, sulfenic acid; RSSH, persulfide; RTK, receptor tyrosine kinase; S-, thiolate anion; S6K, S6 kinase; Sap-1a, SRF accessory protein-1a; SAPK, stress-activated protein kinase; Ser, serine; Ser/Thr, serine/threonine; —SH, sulfhydryl; SH2, homology domain Sarc 2; S_N2, nucleophilic substitution; SOD, superoxide dismutase; SOS, son of sevenless; Sp5, specificity protein transcription factor 5; S—S, disulfide bonds; SSG, glutathionylation; STAT3, signal transducer and activator of transcription 3; TAK1, transforming growth factor beta-activated kinase 1; TF, transcription factor; Thr, threonine; TKI, tyrosine kinase inhibitor; TNF, tumor necrosis factor; Tpl2, tumor progression locus 2; TRAF, TNF receptor associated factor; TSC2, tuberous sclerosis complex 2; TXN, thioredoxin; Tyr, tyrosine; UV, ultraviolet; VEGF, vascular endothelial growth factor; VHL, Von Hippel Lindau; XO, xanthine oxidase.

REVIEW

WILEY

Antioxidant/anti-inflammatory effect of Mg^{2+} in coronavirus disease 2019 (COVID-19)

Yalith Lyzet Arancibia-Hernández ⓘ | Ana Karina Aranda-Rivera ⓘ | Alfredo Cruz-Gregorio ⓘ | José Pedraza-Chaverri ⓘ

Facultad de Química, Departamento de Biología, Laboratorio F-315, Universidad Nacional Autónoma de México, Mexico City, Mexico

Correspondence
José Pedraza-Chaverri and Alfredo Cruz-Gregorio, Facultad de Química, Departamento de Biología, Laboratorio F-315, Universidad Nacional Autónoma de México, 04510 Mexico City, Mexico.
Email: pedraza@unam.mx and cruzgalfredo@comunidad.unam.mx

Abstract

Severe acute respiratory syndrome coronavirus type 2 (SARS-CoV-2) causes coronavirus disease 2019 (COVID-19), characterised by high levels of inflammation and oxidative stress (OS). Oxidative stress induces oxidative damage to lipids, proteins, and DNA, causing tissue damage. Both inflammation and OS contribute to multi-organ failure in severe cases. Magnesium (Mg^{2+}) regulates many processes, including antioxidant and anti-inflammatory responses, as well as the proper functioning of other micronutrients such as vitamin D. In addition, Mg^{2+} participates as a second signalling messenger in the activation of T cells. Therefore, Mg^{2+} deficiency can cause immunodeficiency, exaggerated acute inflammatory response, decreased antioxidant response, and OS. Supplementation with Mg^{2+} has an anti-inflammatory response by reducing the levels of nuclear factor kappa B (NF-κB), interleukin (IL) - 6, and tumor necrosis factor alpha. Furthermore, Mg^{2+} supplementation improves mitochondrial function and increases the antioxidant glutathione (GSH) content, reducing OS. Therefore, Mg^{2+} supplementation is a potential way to reduce inflammation and OS, strengthening the immune system to manage COVID-19. This narrative review will address Mg^{2+} deficiency associated with a worse disease prognosis, Mg^{2+} supplementation as a potent antioxidant and anti-inflammatory therapy during and after COVID-19 disease, and suggest that randomised controlled trials are indicated.

KEYWORDS
COVID-19, inflammation, magnesium deficiency, oxidative stress, post-COVID-19 manifestations, SARS-CoV-2

Abbreviations: 4-HNE, 4-hydroxynonenal; ACE2, angiotensin-converting enzyme 2; Ang II, angiotensin II; ATP, adenosine triphosphate; CAT, catalase; COPD, chronic obstructive pulmonary disease; COVID-19, coronavirus disease 2019; CRP, C-reactive protein; E protein, envelope protein; eNOS, endothelial nitric oxide synthase; ETC, electron transport chain; GCL, γ-glutamyl-cysteine ligase; GCSF, granulocyte-colony stimulating factor; GGT, γ-glutamyl-transpeptidase; GPx, glutathione peroxidase; GR, glutathione reductase; GS, glutathione synthetase; GSH, glutathione; GST, glutathione S-transferase; H$_2$O$_2$, hydrogen peroxide; ICU, intensive care unit; IFN-γ, interferon-gamma; IL, interleukin; IP-10, interferon-γ-inducible protein 10; M protein, membrane protein; MagT1, magnesium transporter 1; MCP-1, monocyte chemoattractant protein 1; MDA, malondialdehyde; Mg^{2+}, magnesium; MgSO$_4$, magnesium sulphate; MIP-1A, macrophage inflammatory proteins; N protein, nucleocapsid protein; NF-κB, nuclear factor kappa B; NK, natural killer; NKG2D, NK activator receptor; non-ICU, non-intensive care unit; NOXs, NADPH oxidases; Nrf2, nuclear factor erythroid 2-related factor 2; nsps, non-structural proteins; O$_2$, oxygen; O$_2^{·-}$, superoxide radical; OH, hydroxyl radical; ORF, open reading frame; OS, oxidative stress; PAF, platelet-activating factor; pp, polyprotein; RBD, receptor-binding domain; ROS, reactive oxygen species; RTC, replication and transcription complex; S protein, spike glycoprotein; SARS, severe acute respiratory syndrome; SARS-CoV-2, severe acute respiratory syndrome coronavirus type 2; SOD, superoxide dismutase; TCR, T cell receptor; TF, tissue factor; TMPRSS2, transmembrane protease serine 2; TNF-α, tumour necrosis factor-alpha; VDBP, vitamin D binding protein; VDR, vitamin D receptor; XMEN, X-linked immunodeficiency with Mg^{2+} deficiency, Epstein-Barr virus infection, and neoplasia; XO, xanthine oxidase.

wileyonlinelibrary.com/journal/rmv

| **1 of 16**

Magnesium and type 2 diabetes mellitus: Clinical and molecular mechanisms

Luis Soriano-Pérez [a], Ana Karina Aranda-Rivera [a,b], Alfredo Cruz-Gregorio [a,*], José Pedraza-Chaverri [a,*]

[a] Laboratorio F-315, Departamento de Biología, Facultad de Química, Universidad Nacional Autónoma de México, Ciudad de México 04510, Mexico
[b] Posgrado en Ciencias Biologicas, Universidad Nacional Autónoma de México, Ciudad Universitaria, Saludos cordiales, Mexico

ABSTRACT

Type 2 diabetes mellitus (T2DM) is one of the most common chronic diseases, affecting hundreds of millions of people worldwide. Environmental factors influence the progressive development of diabetes, the main ones being obesity, hypertension, dyslipidemia, and genetic factors. In addition to the above factors, magnesium (Mg^{2+}) deficiency has been linked to an increased risk of developing T2DM in the general population. The homeostasis of this ion is highly regulated by absorption in the intestine, storage in bone, and renal excretion. However, Mg^{2+} content in the diet, the primary source for the body, and the content of Mg^{2+} in fruits and vegetables have progressively decreased, so Western-style diets currently contain between 30 and 50% of the minimum recommended magnesium. Since Mg^{2+} deficiency has been associated with higher fasting glucose concentrations, glycosylated hemoglobin, or higher insulin resistance rates in patients with T2DM, Mg^{2+} supplementation may be a potential therapy to treat T2DM. Although Mg^{2+} deficiency has been widely studied in T2DM, the molecular clinical and molecular mechanisms are poorly reviewed. This review examines the recent literature linking T2DM to altered Mg^{2+} homeostasis, from experimental observations and clinical trials to the molecular mechanisms by which Mg^{2+} influences glucose homeostasis in T2DM.

1. Introduction

Type 2 diabetes mellitus (T2DM), previously called non-insulin-dependent diabetes mellitus, is the most common type of diabetes, accounting for approximately 90% of these cases worldwide [1]. It is characterized by insulin resistance of tissues such as the liver, skeletal and adipose tissues, and impaired insulin secretion, translating into hyperglycemia. Hyperglycemia initially induces an increase in circulating insulin levels, but during the disease progression, β-cell function declines progressively and can ultimately result in an insulin-dependent state [1,2]. Both insulin resistance and altered secretion progressively produce a dysregulation of carbohydrate, lipid, and protein metabolisms [3].

Magnesium (Mg^{2+}) is one of the most abundant ions in the human body and is essential for many physiological processes. For example, Mg^{2+} is a cofactor of hundreds of enzymes involved in cellular bioenergetics, protein metabolism, and cell signaling pathways. Thus, Mg^{2+} deficiency in the development and persistence of T2DM. Although Mg^{2+} deficiency has been widely studied in T2DM [4–9], the molecular clinical and molecular mechanisms are poorly reviewed. This review ex-

amines the recent literature linking type 2 diabetes to altered Mg^{2+} homeostasis, from experimental observations and clinical trials to the molecular mechanisms by which Mg^{2+} influences glucose homeostasis in type 2 diabetes.

2. Glucose metabolism and insulin release

Glucose homeostasis is primarily regulated by the pancreas, the liver, and muscle and adipose tissue [1]. In the β-cells of the pancreatic islets, glucose enters the cells via the transmembrane protein glucose transporter 2 (GLUT2). Once inside, glucose is phosphorylated by glucokinase (GCK), producing glucose-6 phosphate (glucose-6P), the rate-limiting step of insulin secretion [3]. Subsequently, glucose-6P is transformed to adenosine triphosphate (ATP) through glycolysis and the Krebs cycle, increasing the ATP/adenosine diphosphate (ADP) ratio in the cell [3]. The increase in this ratio closes the K_{ATP} channel, where Mg^{2+} functions as a cofactor of this process [2,10]. The closure of K_{ATP} channels promotes membrane depolarization, which allows the opening of L-type calcium (Ca^{2+}) ion channels, permitting Ca^{2+} entry. The latter encourages the fusion of the insulin-secreting vesicles to the membrane, releasing their insulin content (Fig. 1) [11].

* Corresponding authors. Laboratory F-315, Department of Biology, Faculty of Chemistry, National Autonomous University of Mexico, Mexico City 04510, Mexico. Phone: +52 55 56223878.
E-mail addresses: cruzgalfredo@gmail.com (A. Cruz-Gregorio), pedraza@unam.mx (J. Pedraza-Chaverri).

Review

Involvement of Inflammasome Components in Kidney Disease

Ana Karina Aranda-Rivera [1,†] , Anjali Srivastava [2,†] , Alfredo Cruz-Gregorio [1] , José Pedraza-Chaverri [1] , Shrikant R. Mulay [2] and Alexandra Scholze [3,*]

1   Laboratory F-315, Department of Biology, Faculty of Chemistry, National Autonomous University of Mexico, Mexico City 04510, Mexico; anaaranda025@gmail.com (A.K.A.-R.); cruzgalfredo@gmail.com (A.C.-G.); pedraza@unam.mx (J.P.-C.)
2   Division of Pharmacology, CSIR-Central Drug Research Institute, Lucknow 226031, India; srivastavaanjali2324@gmail.com (A.S.); shrikantrmulay@gmail.com (S.R.M.)
3   Department of Nephrology, Odense University Hospital, Odense, Denmark, and Institute of Clinical Research, University of Southern Denmark, 5000 Odense C, Denmark
*   Correspondence: ascholze@health.sdu.dk
†   These authors contributed equally to this work.

Abstract: Inflammasomes are multiprotein complexes with an important role in the innate immune response. Canonical activation of inflammasomes results in caspase-1 activation and maturation of cytokines interleukin-1β and -18. These cytokines can elicit their effects through receptor activation, both locally within a certain tissue and systemically. Animal models of kidney diseases have shown inflammasome involvement in inflammation, pyroptosis and fibrosis. In particular, the inflammasome component nucleotide-binding domain-like receptor family pyrin domain containing 3 (NLRP3) and related canonical mechanisms have been investigated. However, it has become increasingly clear that other inflammasome components are also of importance in kidney disease. Moreover, it is becoming obvious that the range of molecular interaction partners of inflammasome components in kidney diseases is wide. This review provides insights into these current areas of research, with special emphasis on the interaction of inflammasome components and redox signalling, endoplasmic reticulum stress, and mitochondrial function. We present our findings separately for acute kidney injury and chronic kidney disease. As we strictly divided the results into preclinical and clinical data, this review enables comparison of results from those complementary research specialities. However, it also reveals that knowledge gaps exist, especially in clinical acute kidney injury inflammasome research. Furthermore, patient comorbidities and treatments seem important drivers of inflammasome component alterations in human kidney disease.

Keywords: acute kidney injury; chronic kidney disease; kidney transplantation; inflammasome; redox signalling; endoplasmic reticulum stress; interleukin-18; interleukin-1β; NLRP3; AIM2; caspase-8

1. Introduction to Kidney Disease and Inflammation in Kidney Disease

The 2020 analysis of the Global Burden of Disease Study 1990–2017 estimated the global prevalence of chronic kidney disease (CKD) to be 9.1%, corresponding to 697.5 million cases [1,2]. The all-age global prevalence of CKD increased by 29.3% during this period due to aging of the population globally. The number of deaths at all ages attributable to CKD increased by 41.5%. While age-standardized CKD mortality did not change between 1990 and 2017, it declined by 41.3% for chronic obstructive pulmonary disease, 30.4% for cardiovascular disease, and 14.9% for cancer [1,2]. Therefore, new strategies for early detection and prevention of CKD and the development of more effective therapies are needed.

CKD can result from kidney injuries of any cause if the process of injury was of sufficient duration and/or intensity. It is defined by the presence of decreased kidney function or kidney damage for more than three months, while acute kidney injury (AKI)

MDPI

Review

Extracellular Vesicles in Redox Signaling and Metabolic Regulation in Chronic Kidney Disease

Omar Emiliano Aparicio-Trejo [1], Ana Karina Aranda-Rivera [2], Horacio Osorio-Alonso [1], Elena Martínez-Klimova [2,†], Laura Gabriela Sánchez-Lozada [1], José Pedraza-Chaverri [2] and Edilia Tapia [1,*]

[1] Departamento de Fisiopatología Cardio-Renal, Instituto Nacional de Cardiología "Ignacio Chávez", Mexico City 14080, Mexico; omar.aparicio@cardiologia.org.mx (O.E.A.-T.); horacio.osorio@cardiologia.org.mx (H.O.-A.); laura.sanchez@cardiologia.org.mx (L.G.S.-L.)
[2] Laboratorio F-315, Departamento de Biología, Facultad de Química, Universidad Nacional Autónoma de México, Mexico City 04510, Mexico; anitaaranda023@comunidad.unam.mx (A.K.A.-R.); Elena.Martinezklimova@abo.fi (E.M.-K.); pedraza@unam.mx (J.P.-C.)
* Correspondence: edilia.tapia@cardiologia.org.mx
† Current address: Cell Fate Lab, Åbo Akademi University, Cell Biology, Tykistökatu 6, 20520 Turku, Finland.

Abstract: Chronic kidney disease (CKD) is a world health problem increasing dramatically. The onset of CKD is driven by several mechanisms; among them, metabolic reprogramming and changes in redox signaling play critical roles in the advancement of inflammation and the subsequent fibrosis, common pathologies observed in all forms of CKD. Extracellular vesicles (EVs) are cell-derived membrane packages strongly associated with cell-cell communication since they transfer several biomolecules that serve as mediators in redox signaling and metabolic reprogramming in the recipient cells. Recent studies suggest that EVs, especially exosomes, the smallest subtype of EVs, play a fundamental role in spreading renal injury in CKD. Therefore, this review summarizes the current information about EVs and their cargos' participation in metabolic reprogramming and mitochondrial impairment in CKD and their role in redox signaling changes. Finally, we analyze the effects of these EV-induced changes in the amplification of inflammatory and fibrotic processes in the progression of CKD. Furthermore, the data suggest that the identification of the signaling pathways involved in the release of EVs and their cargo under pathological renal conditions can allow the identification of new possible targets of injury spread, with the goal of preventing CKD progression.

Keywords: extracellular vesicles; exosomes; chronic kidney disease; metabolic reprogramming; redox signaling; microvesicles; mitochondrial impairment; lipotoxicity; oxidative stress; inflammation; fibrosis

1. Introduction

Chronic kidney disease (CKD) is a term used to include several disorders characterized by progressive loss in the glomerular filtration rate (GFR) and nephron number for a time period of at least 3 months, usually accompanied by the increase in clinical renal damage markers and fibrotic processes [1,2]. CKD is a global pandemic that is increasing dramatically [3–5], and in several cases, the current treatments do not significantly prevent illness [6]. This is partially attributable to the lack of understanding of the several pathological mechanisms that trigger CKD and its progression [6,7].

Extracellular vesicles (EVs) are cell-derived membrane packages released in extracellular medium with a short half-life, from minutes up to 5.5 h after their release. EVs have an essential role in cell-to-cell communication and the maintenance of cellular homeostasis. EVs are currently divided into three groups depending on their origins (biogenesis) and size: exosomes, microvesicles (MVs), and apoptotic bodies [8,9]. The smallest EVs are the exosomes, with a length of 30–150 nm and a density of 1.10–1.18 g/mL [8,10] that are formed by the fusion of intracellular multivesicular bodies, known as endosomes, with the

MDPI

Review

Nrf2 Activation in Chronic Kidney Disease: Promises and Pitfalls

Ana Karina Aranda-Rivera [1], Alfredo Cruz-Gregorio [1], José Pedraza-Chaverri [1] and Alexandra Scholze [2,3,*]

[1] Laboratory F-315, Department of Biology, Faculty of Chemistry, National Autonomous University of Mexico, Mexico City 04510, Mexico; anaaranda025@gmail.com (A.K.A.-R.); cruzgalfredo@gmail.com (A.C.-G.); pedraza@unam.mx (J.P.-C.)
[2] Department of Nephrology, Odense University Hospital, 5000 Odense C, Denmark
[3] Institute of Clinical Research, University of Southern Denmark, 5000 Odense C, Denmark
*   Correspondence: ascholze@health.sdu.dk

Abstract: The nuclear factor erythroid 2-related factor 2 (Nrf2) protects the cell against oxidative damage. The Nrf2 system comprises a complex network that functions to ensure adequate responses to redox perturbations, but also metabolic demands and cellular stresses. It must be kept within a physiologic activity range. Oxidative stress and alterations in Nrf2-system activity are central for chronic-kidney-disease (CKD) progression and CKD-related morbidity. Activation of the Nrf2 system in CKD is in multiple ways related to inflammation, kidney fibrosis, and mitochondrial and metabolic effects. In human CKD, both endogenous Nrf2 activation and repression exist. The state of the Nrf2 system varies with the cause of kidney disease, comorbidities, stage of CKD, and severity of uremic toxin accumulation and inflammation. An earlier CKD stage, rapid progression of kidney disease, and inflammatory processes are associated with more robust Nrf2-system activation. Advanced CKD is associated with stronger Nrf2-system repression. Nrf2 activation is related to oxidative stress and moderate uremic toxin and nuclear factor kappa B (NF-κB) elevations. Nrf2 repression relates to high uremic toxin and NF-κB concentrations, and may be related to Kelch-like ECH-associated protein 1 (Keap1)-independent Nrf2 degradation. Furthermore, we review the effects of pharmacological Nrf2 activation by bardoxolone methyl, curcumin, and resveratrol in human CKD and outline strategies for how to adapt future Nrf2-targeted therapies to the requirements of patients with CKD.

Keywords: Nrf2; oxidative stress; CKD; bardoxolone methyl; fibrosis; inflammation; NQO1; kidney function; hemodialysis; curcumin; redox signaling

1. Introduction to Chronic Kidney Disease

Chronic kidney disease (CKD) comprises a heterogeneous group of kidney disorders and is defined by alterations in kidney function or structure for more than three months. CKD is classified and staged based on the underlying pathology, albuminuria category, and glomerular filtration rate (GFR) [1]. It represents a global public-health problem with a major effect on global morbidity and mortality. Better strategies for early detection and prevention of CKD as well as new effective therapies are needed. [2]. Factors that are associated with CKD progression include the cause of CKD, category of GFR and albuminuria, age, elevation of blood pressure, and history of cardiovascular disease (CVD) [1]. Inflammatory processes and oxidative damage are important pathomechanisms for CKD progression and CKD-attributable morbidity, such as CKD-associated early vascular aging [3,4], impaired immune function [5,6] or anemia [7,8]. An overview of all abbreviations used in the article is provided as Supplementary Table S1 online.

2. Introduction to the Nrf2 Pathway

Oxidative stress is one of the principal contributors to CKD development. CKD presents upregulation of NADPH oxidases and mitochondria dysfunction, favoring reactive-

Therapeutic Effect of Curcumin on 5/6Nx Hypertriglyceridemia: Association with the Improvement of Renal Mitochondrial β-Oxidation and Lipid Metabolism in Kidney and Liver

Zeltzin Alejandra Ceja-Galicia [1,2], Fernando Enrique García-Arroyo [1], Omar Emiliano Aparicio-Trejo [1], Mohammed El-Hafidi [3], Guillermo Gonzaga-Sánchez [1], Juan Carlos León-Contreras [4], Rogelio Hernández-Pando [4], Martha Guevara-Cruz [5], Armando R. Tovar [5], Pedro Rojas-Morales [1,2], Ana Karina Aranda-Rivera [2], Laura Gabriela Sánchez-Lozada [1], Edilia Tapia [1] and José Pedraza-Chaverri [2,*]

1. Department of Cardio-Renal Physiology, National Institute of Cardiology "Ignacio Chávez", Mexico City 14080, Mexico
2. Department of Biology, Faculty of Chemistry, National Autonomous University of Mexico, Mexico City 04510, Mexico
3. Department of Cardiovascular Biomedicine, National Institute of Cardiology "Ignacio Chávez", Mexico City 14080, Mexico
4. Department of Experimental Pathology, National Institute of Medical Science and Nutrition "Salvador Zubirán", Mexico City 14080, Mexico
5. Department of Nutrition Biology, National Institute of Medical Science and Nutrition "Salvador Zubirán", Mexico City 14080, Mexico
* Correspondence: pedraza@unam.mx

Abstract: Chronic kidney disease (CKD) prevalence is constantly increasing, and dyslipidemia in this disease is characteristic, favoring cardiovascular events. However, the mechanisms of CKD dyslipidemia are not fully understood. The use of curcumin (CUR) in CKD models such as 5/6 nephrectomy (5/6Nx) has shown multiple beneficial effects, so it has been proposed to correct dyslipidemia without side effects. This work aimed to characterize CUR's potential therapeutic effect on dyslipidemia and alterations in lipid metabolism and mitochondrial ß-oxidation in the liver and kidney in 5/6Nx. Male Wistar rats were subjected to 5/6Nx and progressed by 4 weeks; meanwhile, CUR (120 mg/kg) was administered for weeks 5 to 8. Our results showed that CUR reversed the increase in liver and kidney damage and hypertriglyceridemia induced by 5/6Nx. CUR also reversed mitochondrial membrane depolarization and β-oxidation disorders in the kidney and the increased lipid uptake and the high levels of proteins involved in fatty acid synthesis in the liver and kidney. CUR also decreased lipogenesis and increased mitochondrial biogenesis markers in the liver. Therefore, we concluded that the therapeutic effect of curcumin on 5/6Nx hypertriglyceridemia is associated with the restoration of renal mitochondrial ß-oxidation and the reduction in lipid synthesis and uptake in the kidneys and liver.

Keywords: curcumin; chronic kidney disease (CKD); lipid metabolism; dyslipidemia; mitochondrial dysfunction; liver alteration in CKD; hypertriglyceridemia; fatty acids ß-oxidation; antioxidant; triglycerides

1. Introduction

Chronic kidney disease (CKD) has an incidence of over 11% worldwide [1], making it one of the most important diseases on the earth. CKD is characterized by different symptoms such as a decrease in the glomerular filtration rate to less than 60 mL/min per 1.73 m^2 for 3 months or more, an increase in plasma nitrogenous compounds (creatinine and urea), hypertension, and dyslipidemia [2]. Dyslipidemia is characterized by high concentrations of plasma lipids, mainly triglycerides (TG) and cholesterol (CH), which are related to their

RONS and Oxidative Stress: An Overview of Basic Concepts

Ana Karina Aranda-Rivera [1,2,†] , **Alfredo Cruz-Gregorio** [1,†] , **Yalith Lyzet Arancibia-Hernández** [1] ,
Estefani Yaquelin Hernández-Cruz [1,2] and **José Pedraza-Chaverri** [1,*]

1   Laboratory F-315, Department of Biology, Faculty of Chemistry, National Autonomous University of Mexico, Mexico City 04510, Mexico
2   Postgraduate in Biological Sciences, National Autonomous University of Mexico, Mexico City 04510, Mexico
*   Correspondence: pedraza@unam.mx
†   These authors contributed equally to this work.

Abstract: Oxidative stress (OS) has greatly interested the research community in understanding damaging processes occurring in cells. OS is triggered by an imbalance between reactive oxygen species (ROS) production and their elimination by the antioxidant system; however, ROS function as second messengers under physiological conditions. ROS are produced from endogenous and exogenous sources. Endogenous sources involve mitochondria, nicotinamide adenine dinucleotide phosphate hydrogen (NADPH), oxidases (NOXs), endoplasmic reticulum (ER), xanthine oxidases (XO), endothelial nitric oxide synthase (eNOs), and others. In contrast, exogenous ROS might be generated through ultraviolet (UV) light, ionizing radiation (IR), contaminants, and heavy metals, among others. It can damage DNA, lipids, and proteins if OS is not controlled. To avoid oxidative damage, antioxidant systems are activated. In the present review, we focus on the basic concepts of OS, highlighting the production of reactive oxygen and nitrogen species (RONS) derived from internal and external sources and the last elimination. Moreover, we include the cellular antioxidant system regulation and their ability to decrease OS. External antioxidants are also proposed as alternatives to ameliorate OS. Finally, we review diseases involving OS and their mechanisms.

Keywords: oxidative stress; reactive oxygen species; antioxidants; redox signaling; ROS sources; antioxidant systems; cancer; kidney diseases

1. Introduction: Reactive Oxygen Species (ROS) and Reactive Nitrogen Species (RNS)

Reactive oxygen species (ROS) and reactive nitrogen species (RNS) are defined as unstable species containing oxygen (O_2) and nitrogen that react quickly with other molecules in the cells [1]. This review considers ROS and RNS as reactive oxygen and nitrogen species (RONS) for practical purposes. The RONS containing one or more unpaired electrons are known as free radicals, while RONS without unpaired electrons are called non-free radicals. Free radical species include superoxide anion radical ($O_2^{\bullet-}$), hydroxyl radical ($^{\bullet}OH$), alkoxyl ($^{\bullet}OR$), nitric oxide ($NO^{\bullet}$), and peroxyl radicals ($^{\bullet}OOR$); non-free radicals comprise hydrogen peroxide (H_2O_2), nitrogen dioxide (NO_2), and peroxynitrite ($ONOO^-$), among others [2]. $O_2^{\bullet-}$ is the principal precursor of RONS produced by the cells, and an increase in this radical is related to oxidative stress and cellular damage [3,4]. Thus, antioxidants are a powerful tool to control the overproduction of ROS and avoid oxidative damage.

While there are excellent reviews of redox state and oxidative stress [2,5,6], we wanted to review the basic concepts of oxidative stress, antioxidants, redox signaling, and RONS sources, having academic readers or those just starting out in this area of study in mind.

2. Signaling and Physiological Functions of RONS

RONS are products of aerobic metabolism that regulate cellular processes such as survival, growth, proliferation, apoptosis, and others. Although RONS can cause damage

Pathological Similarities in the Development of Papillomavirus-Associated Cancer in Humans, Dogs, and Cats

Alfredo Cruz-Gregorio ⬥, Ana Karina Aranda-Rivera ⬥ and José Pedraza-Chaverri *⬥

Laboratory F-315, Department of Biology, Faculty of Chemistry, National Autonomous University of Mexico, Mexico City 04510, Mexico
* Correspondence: pedraza@unam.mx

Simple Summary: Papillomavirus (PV) infection affects many species, including humans and domestic animals, such as dogs and cats. Some of these infections involve the development of cancer due to the presence of PV. There are similarities in the pathology of these three PV-associated cancers, which may provide crucial insights into cancer development in these species, extrapolating both markers and possible treatment in the three species. For example, the oncoproteins E5, E6, and E7 are the main causes of the development of cancer associated with PV, and the possible therapies associated with the blockage or reduction of these oncoproteins can be of great benefit for the reduction and/or elimination of cancer associated with PV. Thus, our review focuses on the similarities in the context of pathology and biomarkers in canine, feline, and human cancers associated with PV. We review the main biomarkers, E5, E6, and E7 oncoproteins, and their overexpression in *Canis familiaris*, *Felis catus*, and human papillomavirus and their association with the development of cancer. Furthermore, we also discuss that a potential treatment for PV-related cancer is the reduction or blocking of these oncoproteins.

Abstract: *Canis familiaris*, *Felis catus*, and human papillomavirus are nonenveloped viruses that share similarities in the initiation and development of cancer. For instance, the three species overexpress the oncoproteins E6 and E7, and *Canis familiaris* and human papillomavirus overexpress the E5 oncoprotein. These similarities in the pathophysiology of cancer among the three species are beneficial for treating cancer in dogs, cats, and humans. To our knowledge, this topic has not been reviewed so far. This review focuses on the information on cancer research in cats and dogs comparable to that being conducted in humans in the context of comparative pathology and biomarkers in canine, feline, and human cancer. We also focus on the possible benefit of treatment associated with the E5, E6, and E7 oncoproteins for cancer in dogs, cats, and humans.

Keywords: squamous cell carcinoma; *Canis familiaris* papillomavirus; *Felis catus* papillomavirus; human papillomavirus; pathological similarities in cancer; E5, E6, and E7 oncoproteins

1. Introduction

Canis familiaris (Cf), *Felis catus* (Fc), and human (H) papillomavirus (PV) are nonenveloped viruses with a capsid that envelops the genome of a single double-stranded deoxyribonucleic acid (dsDNA) molecule [1]. Both CfPV and HPV genomes are organized in three regions: (1) the long control region (LCR) that modulates viral replication and viral transcription, (2) the early region composed of six open reading frames (ORFs): E1, E2, E4, E5, E6, and E7, and (3) the late region formed by the ORFs of L1 and L2 that code for the proteins E1, E2, E4–E7, L1, and L2, respectively [2]. Unlike CfPV and HPV, the FcPC genome does not express the E4 and E5 proteins [3]. The E1 protein is a helicase implicated in viral replication, which needs E2 binding to increase E1 specificity to its DNA sequence target [2]. Importantly, the E2 protein also downregulates the viral transcription of E6 and E7 oncoproteins [4]. The release of virions by disrupting the

113

Article

Expression Profiles of Kidney Mitochondrial Proteome during the Progression of the Unilateral Ureteral Obstruction: Focus on Energy Metabolism Adaptions

Ariadna Jazmín Ortega-Lozano [1,†], Alexis Paulina Jiménez-Uribe [1,†], Ana Karina Aranda-Rivera [1], Leopoldo Gómez-Caudillo [1], Emmanuel Ríos-Castro [2], Edilia Tapia [3], Belen Bellido [1], Omar Emiliano Aparicio-Trejo [3], Laura Gabriela Sánchez-Lozada [3] and José Pedraza-Chaverri [1,*]

[1] Department of Biology, Faculty of Chemistry, National Autonomous University of Mexico (UNAM), Mexico City 04510, Mexico

[2] Genomic, Proteomic, and Metabolomic Unit (UGPM), LaNSE, Cinvestav-IPN, Mexico City 07360, Mexico

[3] Department of Cardio-Renal Physiopathology, National Institute of Cardiology "Ignacio Chávez", Mexico City 14080, Mexico

[*] Correspondence: pedraza@unam.mx; Tel./Fax: +52-55-5622-3878

[†] These authors contributed equally to this work.

Abstract: Kidney diseases encompass many pathologies, including obstructive nephropathy (ON), a common clinical condition caused by different etiologies such as urolithiasis, prostatic hyperplasia in males, tumors, congenital stenosis, and others. Unilateral ureteral obstruction (UUO) in rodents is an experimental model widely used to explore the pathophysiology of ON, replicating vascular alterations, tubular atrophy, inflammation, and fibrosis development. In addition, due to the kidney's high energetic demand, mitochondrial function has gained great attention, as morphological and functional alterations have been demonstrated in kidney diseases. Here we explore the kidney mitochondrial proteome differences during a time course of 7, 14, and 21 days after the UUO in rats, revealing changes in proteins involved in three main metabolic pathways, oxidative phosphorylation (OXPHOS), the tricarboxylic acid cycle (TCA), and the fatty acid (FA) metabolism, all of them related to bioenergetics. Our results provide new insight into the mechanisms involved in metabolic adaptations triggered by the alterations in kidney mitochondrial proteome during the ON.

Keywords: unilateral ureteral obstruction (UUO); kidney fibrosis; mitochondria proteome; energy metabolism

1. Introduction

Obstructive uropathy is a pathology characterized by the disruption of the normal urine flow caused by a great diversity of etiologies, such as urolithiasis, prostatic hyperplasia in males, tumors, congenital stenosis, and others. If the obstruction causes irreversible damage to the kidney, it is referred as obstructive nephropathy (ON). Some of the most noticeable events during the ON pathophysiology include increased intratubular pressure, an acute increase of renal blood flow (RBF) followed by its decrease, and the consequent reduction of glomerular filtration rate (GFR). As the obstruction persists, tubular acidification, apoptosis of epithelial cells, tubular atrophy, inflammation, fibrosis, and finally, renal failure occurs [1–4].

Unilateral ureteral obstruction (UUO) in rodents is an experimental model extensively used to explore the mechanisms and pathways involved in ON development. It replicates alterations in RBF and GFR, interstitial inflammation, tubular dilation, tubular atrophy, and the progressive development of fibrosis observed in clinics [5–8]. Moreover,
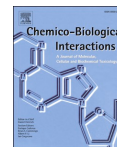
Review Article

Renal damage induced by cadmium and its possible therapy by mitochondrial transplantation

Estefani Yaquelin Hernández-Cruz [a,b], Isabel Amador-Martínez [a,b], Ana Karina Aranda-Rivera [a,b], Alfredo Cruz-Gregorio [a], José Pedraza Chaverri [a,*]

[a] *Laboratorio F-315, Departamento de Biología, Facultad de Química, Universidad Nacional Autónoma de México, 04510, Ciudad de México, Mexico*
[b] *Posgrado en Ciencias Biológicas, Universidad Nacional Autónoma de México, Ciudad Universitaria, Ciudad de México, 04510, Mexico*

A B S T R A C T

Cadmium (Cd) is one of the most toxic metals without biological function, and its accumulation in living organisms has been reported. The kidney is a target organ in Cd toxicity; it has been observed that Cd causes kidney damage even at low concentrations, and Cd damage can quickly progress to chronic kidney disease. The mitochondria play a fundamental role in the nephrotoxicity of Cd; Cd enters the mitochondria and affects the electron transport system (ETS), increases the production of reactive oxygen species (ROS), decreases the mitochondrial membrane potential (Δψm), alters mitochondrial dynamics, induces mutations in mitochondrial deoxyribonucleic acid (mtDNA) and decreased biogenesis leading to increased mitophagy, autophagy, and inevitably apoptosis. Existing therapies to treat Cd nephrotoxicity are currently based on antioxidant and chelating compounds, but despite their promising effects, they have some limitations; therefore, Cd nephrotoxicity continues to represent a global health problem. Mitochondrial transplantation is a new experimental approach with positive results by reversing mitochondrial alterations in cardiac and kidney dysfunction mainly caused by oxidative stress. Hence, the current review discusses the role of mitochondria in Cd-induced toxicity in the kidney and proposes mitochondrial transference as a novel therapy based on transplanting healthy mitochondria to cells with Cd-compromised mitochondria. This review is the first to propose mitochondrial transplantation as a treatment for heavy metal-induced kidney damage.

1. Introduction

Most living organisms reside in areas where environmental pollution exceeds the healthy limits [1,2]. Much of this pollution is due to the accumulation of heavy metals, widespread in various parts of the world, especially near industrial and urban areas [3]. Among the metals that have attracted attention for being one of the most toxic globally and representing a significant public health problem is cadmium (Cd) [4]. Chronic occupational or environmental exposure to Cd causes obstructive airway diseases, emphysema, end-stage renal failure, diabetic and renal complications, dysregulated blood pressure, bone disorders, and immunosuppression, as well as an increased risk cancer of lung, endometrial, bladder, prostate, nasopharynx, and breast [5–8]. In fact, human and animal studies have given sufficient evidence to classify Cd as a group 1 human carcinogen by the International Agency for Research on Cancer [9].

Cd can enter the body through the air, water, soil, and food. It has a long half-life (10–30 years) and mainly accumulates in the liver, bones, and other organs, causing irreversible damage. The kidneys are among the most affected by Cd toxicity [10,11], and it has been reported that about half of the total body load of Cd accumulates in the epithelial cells of the proximal tubule, causing proteinuria and disorders in the reabsorption process [12,13]. Prolonged exposure to Cd also increases calcium excretion and the risk of kidney stones [14]. Several studies report acute and chronic kidney disease induced by Cd, even at low levels of exposure. It has been reported that women, children, and people with health problems, such as diabetes, may be especially susceptible [15–21]. The main molecular mechanisms of Cd toxicity are oxidative stress and mitochondrial dysfunction [11,22,23]. Cd favors oxidative stress by increasing the formation of reactive oxygen species (ROS) and the alteration of the antioxidant system; it also causes damage to mitochondrial deoxyribonucleic acid (mtDNA), alters mitochondrial dynamics, and leads to cell death mainly by apoptosis [11,23]. It should be noted that the proximal tubule cells are the segment of the nephron

GK-1 Induces Oxidative Stress, Mitochondrial Dysfunction, Decreased Membrane Potential, and Impaired Autophagy Flux in a Mouse Model of Breast Cancer

Alfredo Cruz-Gregorio [1] , Ana Karina Aranda-Rivera [1] , Omar Emiliano Aparicio-Trejo [2],
Omar Noel Medina-Campos [1], Edda Sciutto [3] , Gladis Fragoso [3],* and José Pedraza-Chaverri [1],*

[1] Laboratorio F-315, Departamento de Biología, Facultad de Química, Universidad Nacional Autónoma de México (UNAM), Mexico City 04510, Mexico
[2] Departamento de Fisiopatología Cardio-Renal, Instituto Nacional de Cardiología "Ignacio Chávez", Mexico City 14080, Mexico
[3] Departamento de Inmunología, Instituto de Investigaciones Biomédicas, Universidad Nacional Autónoma de México (UNAM), Mexico City 04510, Mexico
* Correspondence: gladis@unam.mx (G.F.); pedraza@unam.mx (J.P.-C.)

Abstract: Breast cancer (BC) is the second most common cancer worldwide in women. During the last decades, the mortality due to breast cancer has progressively decreased due to early diagnosis and the emergence of more effective new treatments. However, human epidermal growth factor receptor 2 (HER2) and triple-negative breast cancer (TNBC) remain with poor prognoses. In our research group, we are proposing the GK-1 immunomodulatory peptide as a new alternative for immunotherapy of these aggressive tumors. GK-1 reduced the growth rate of established tumors and effectively reduced lung metastasis in the 4T1 experimental murine model of breast cancer. Herein, the effect of GK-1 on the redox state, mitochondrial metabolism, and autophagy of triple-negative tumors that can be linked to cancer evolution was studied. GK-1 decreased catalase activity, reduced glutathione (GSH) content and GSH/oxidized glutathione (GSSG) ratio while increased hydrogen peroxide (H_2O_2) production, GSSG, and protein carbonyl content, inducing oxidative stress (OS) in tumoral tissues. This imbalance between reactive oxygen species (ROS) and antioxidants was related to mitochondrial dysfunction and uncoupling, characterized by reduced mitochondrial respiratory parameters and dissipation of mitochondrial membrane potential ($\Delta\Psi$m), respectively. Furthermore, GK-1 likely affected autophagy flux, confirmed by elevated levels of p62, a marker of autophagy flux. Overall, the induction of OS, dysfunction, and uncoupling of the mitochondria and the reduction of autophagy could be molecular mechanisms that underlie the reduction of the 4T1 breast cancer induced by GK-1.

Keywords: GK-1; oxidative stress; VDAC; ATP synthase; mitochondrial dysfunction; autophagy flux

1. Introduction

Breast cancer (BC) is the most common cancer worldwide in women [1]. BC is highly heterogeneous, with different molecular alterations and clinical behavior differences [2]. This heterogeneity is associated with the expression of different immunohistochemical markers and categorized into four main molecular subtypes of BC tumors: luminal A, luminal B, human epidermal growth factor receptor 2 (HER2)-enriched, and basal-like also known as triple-negative (TNBC). For instance, luminal A and B tumors express the immunochemical markers estrogen receptor (ER) and progesterone receptor (PR) but do not express HER2. These tumors are low-grade, grow slowly, and have the best prognosis. HER2-enriched tumors express HER2 receptors but do not express ER and PR receptors. Regarding TNBC tumors, they do not express ER, PR, and HER2 receptors and are the most lethal and aggressive among BC. Because these tumors do not benefit from hormone

RESEARCH ARTICLE

WILEY

α-Mangostin induces oxidative damage, mitochondrial dysfunction, and apoptosis in a triple-negative breast cancer model

Alfredo Cruz-Gregorio [1,2] | Ana Karina Aranda-Rivera [2] |
Omar Emiliano Aparicio-Trejo [3] | Omar Noel Medina-Campos [2] |
Edda Sciutto [4] | Gladis Fragoso [4] | José Pedraza-Chaverri [2]

[1]Departamento de Biomedicina Cardiovascular, Instituto Nacional de Cardiología "Ignacio Chávez", CDMX, Mexico

[2]Laboratorio F-315, Departamento de Biología, Facultad de Química, Universidad Nacional Autónoma de México, CDMX, Mexico

[3]Departamento de Fisiopatología Cardio-Renal, Instituto Nacional de Cardiología "Ignacio Chávez", CDMX, Mexico

[4]Departamento de Inmunología, Instituto de Investigaciones Biomédicas, Universidad Nacional Autónoma de México, CDMX, Mexico

Correspondence
Alfredo Cruz-Gregorio, Departamento de Biomedicina Cardiovascular, Instituto Nacional de Cardiología "Ignacion Chávez", Juan Badiano 1, Belisario Domínguez Secc 16, Tlalpan, CDMX, 14080, Mexico.
Email: alfredo.cruz@cardiologia.org.mx

José Pedraza-Chaverri, Laboratorio F-315, Departamento de Biología, Facultad de Química, Universidad Nacional Autónoma de México, CDMX, 04510, Mexico.
Email: pedraza@unam.mx

Abstract

Triple-negative breast cancer (TNBC) does not express estrogen receptor, progesterone receptor, and human epidermal growth factor receptor; therefore, TNBC lacks targeted therapy, and chemotherapy is the only available treatment for this illness but causes side effects. A putative strategy for the treatment of TNBC could be the use of the polyphenols such as α-Mangostin (α-M), which has shown anticancerogenic effects in different cancer models and can modulate the inflammatory and prooxidant state in several pathological models. The redox state, oxidative stress (OS), and oxidative damage are highly related to cancer development and its treatment. Thus, this study aimed to evaluate the effects of α-M on redox state, mitochondrial metabolism, and apoptosis in 4T1 mammary carcinoma cells. We found that α-M decreases both protein levels and enzymatic activity of catalase, and increases reactive oxygen species, oxidized proteins and glutathione disulfide, which demonstrates that α-M induces oxidative damage. We also found that α-M promotes mitochondrial dysfunction by abating basal respiration, the respiration ligated to oxidative phosphorylation (OXPHOS), and the rate control of whole 4T1 cells. Additionally, α-M also decreases the levels of OXPHOS subunits of mitochondrial complexes I, II, III, and adenosine triphosphate synthase, the activity of mitochondrial complex I as well as the levels of peroxisome proliferator-activated receptor-gamma co-activator 1α, showing a mitochondrial mass reduction. Then, oxidative damage and mitochondrial dysfunction induced by α-M induce apoptosis of 4T1 cells, which is evidenced by B cell lymphoma 2 decrease and caspase 3 cleavage. Taken together, our results suggest that α-M induces OS and mitochondrial dysfunction, resulting in 4T1 cell death through apoptotic mechanisms.

KEYWORDS
4T1 cells, mitochondrial dysfunction, oxidative stress, triple-negative breast cancer (TNBC), α-Mangostin (α-M)

Alfredo Cruz-Gregorio and Ana Karina Aranda-Rivera contributed equally.

Review

The Development of Dyslipidemia in Chronic Kidney Disease and Associated Cardiovascular Damage, and the Protective Effects of Curcuminoids

Zeltzin Alejandra Ceja-Galicia [1,2], Ana Karina Aranda-Rivera [2], Isabel Amador-Martínez [1,2], Omar Emiliano Aparicio-Trejo [1], Edilia Tapia [1], Joyce Trujillo [3], Victoria Ramírez [4] and José Pedraza-Chaverri [2,*]

[1] Department of Cardio-Renal Physiopathology, National Institute of Cardiology Ignacio Chávez, Mexico City 14080, Mexico

[2] Department of Biology, Faculty of Chemistry, National Autonomous University of Mexico, Mexico City 04510, Mexico

[3] National Council on Science and Technology (CONACyT)-Instituto Potosino de Investigación Científica y Tecnológica-División de Materiales Avanzados (CONACyT-IPICYT-DMA), San Luis Potosí 78216, Mexico

[4] Department of Experimental Surgery, National Institute of Medical Science and Nutrition Salvador Zubirán (INCMNSZ), Mexico City 14080, Mexico

* Correspondence: pedraza@unam.mx

Abstract: Chronic kidney disease (CKD) is a health problem that is constantly growing. This disease presents a diverse symptomatology that implies complex therapeutic management. One of its characteristic symptoms is dyslipidemia, which becomes a risk factor for developing cardiovascular diseases and increases the mortality of CKD patients. Various drugs, particularly those used for dyslipidemia, consumed in the course of CKD lead to side effects that delay the patient's recovery. Therefore, it is necessary to implement new therapies with natural compounds, such as curcuminoids (derived from the *Curcuma longa* plant), which can cushion the damage caused by the excessive use of medications. This manuscript aims to review the current evidence on the use of curcuminoids on dyslipidemia in CKD and CKD-induced cardiovascular disease (CVD). We first described oxidative stress, inflammation, fibrosis, and metabolic reprogramming as factors that induce dyslipidemia in CKD and their association with CVD development. We proposed the potential use of curcuminoids in CKD and their utilization in clinics to treat CKD-dyslipidemia.

Keywords: curcumin; curcuminoids; chronic renal disease; cardiovascular disease (CVD); dyslipidemia; CKD

1. Introduction

Chronic kidney disease (CKD) is a global public health problem, with an incidence of >11.1% [1], corresponding to 843.6 million cases worldwide [2]. CKD significantly increases cardiovascular morbidity and mortality rates since CKD increases cardiovascular events by more than 50% [3–6]. Several risk factors are shared between CKD and cardiovascular disease (CVD), including diabetes, hypertension, lipid abnormalities, obesity, and smoking. CKD-induced dyslipidemia has been highlighted as a critical factor in CVD development [7,8]. CKD patient management involves using different drugs to reduce cardiovascular risk and prevent renal venous hypertension and congestion. These drugs include antihyperlipidemic combinations, renin-angiotensin-aldosterone system (RAAS) inhibitors, angiotensin receptor blockers, diuretics, vasodilators, inotropes, and β-blockers [8–10]. However, it has been reported that these drugs might cause side effects, doing more challenging to treat CKD patients [8]. Therefore, new treatment strategies are required to avoid or reduce dyslipidemia in CKD and the associated CVD without these side effects.

Targeting Mitochondrial Therapy in the Regulation of HPV Infection and HPV-Related Cancers

Alfredo Cruz-Gregorio [1,2] [iD], **Ana Karina Aranda-Rivera** [2] [iD], **Giovanni N. Roviello** [3,*] [iD] **and José Pedraza-Chaverri** [2,*] [iD]

1   Department of Cardiovascular Biomedicine, Ignacio Chávez National Institute of Cardiology, Juan Badiano No. 1, Colonia Section XVI, Tlalpan, Mexico City 14080, Mexico

2   Laboratory F-315, Department of Biology, Faculty of Chemistry, National Autonomous University of Mexico, Mexico City 04510, Mexico

3   Institute of Biostructures and Bioimaging, Italian National Council for Research (IBB-CNR), Area di Ricerca site and Headquarters, Via Pietro Castellino 111, 80131 Naples, Italy

*   Correspondence: giroviel@unina.it (G.N.R.); pedraza@unam.mx (J.P.-C.)

Abstract: It has been previously proposed that some types of cancer cells reprogram their metabolic pathways, favoring the metabolism of glucose by aerobic glycolysis (Warburg effect) instead of oxidative phosphorylation, mainly because the mitochondria of these cells are damaged, thus displaying mitochondrial dysfunction. However, in several cancers, the mitochondria do not exhibit any dysfunction and are also necessary for the tumor's growth and maintenance. Remarkably, if the mitochondria are dysfunctional, specific processes associated with the release of cytochrome c (cyt c), such as apoptosis, are significantly impaired. In these cases, cellular biotherapies such as mitochondrial transplantation could restore the intrinsic apoptotic processes necessary for the elimination of cancers. On the other hand, if the mitochondria are in good shape, drugs that target the mitochondria are a valid option for treating the related cancers. Famously, the mitochondria are targeted by the human papillomavirus (HPV), and HPV-related cancers depend on the host's mitochondria for their development and progression. On the other hand, the mitochondria are also important during treatment, such as chemotherapy, since they are key organelles for the increase in reactive oxygen species (ROS), which significantly increases cell death due to the presence of oxidative stress (OS). In this way, the mitochondria in HPV infection and in the development of HPV-related cancer could be targeted to reduce or eliminate HPV infections or HPV-related cancers. To our knowledge, there was no previous review specifically focusing on this topic, so this work aimed to summarize for the first time the potential use of mitochondria-targeting drugs, providing molecular insights on the main therapeutics developed so far in HPV infection and HPV-related cancer. Thus, we reviewed the mechanisms associated with HPV-related cancers, with their early proteins and mitochondrial apoptosis specifically induced by different compounds or drugs, in which these molecules induce the production of ROS, the activation of proapoptotic proteins, the deactivation of antiapoptotic proteins, the loss of mitochondrial membrane potential ($\Delta\psi m$), cyt c release, and the activation of caspases, which are all events which lead to the activation of mitochondrial apoptosis pathways. This makes these compounds and drugs potential anticancer therapeutics that target the mitochondria and could be exploited in future biomedical strategies.

Keywords: HPV infection; HPV-related cancer; mitochondria; oxidative stress; mitochondria therapy; compounds that target mitochondria

1. Introduction

According to the World Health Organization (WHO), cervical cancer is the fourth leading cause of cancer death in women worldwide [1]. It has been established that persistent infection with high-risk human papillomavirus (HR-HPV) constitutes a key risk factor for the development of cervical cancer [2]. HR-HPV is also related to the induction of

Review

Quercetin and Ferroptosis

Alfredo Cruz-Gregorio [1],* and Ana Karina Aranda-Rivera [2]

1 Departamento de Biomedicina Cardiovascular, Instituto Nacional de Cardiología Ignacio Chávez, Mexico City 14080, Mexico
2 Laboratorio F-315, Departamento de Biología, Facultad de Química, Universidad Nacional Autónoma de México, Mexico City 04510, Mexico; anitaaranda023@comunidad.unam.mx
* Correspondence: alfredo.cruzg@cardiologia.org.mx

Abstract: Quercetin is a flavonoid present in apples, onions, tea, red wines, and berries, and it has shown different beneficial effects, such as providing cardiovascular protection, possessing anti-inflammatory properties, and demonstrating anticancer activity, among others. These diseases are related to oxidizing molecules such as ROS because these species react and induce the oxidation of cellular biomolecules, such as proteins, lipids, DNA, or carbohydrates, which alters cellular homeostasis. Regarding lipids, the oxidation of these molecules induces lipid hydroperoxides which, if not decreased, particularly by GPX4, produce highly reactive aldehydes such as 4HNE and MDA. These oxidative conditions induce ferroptosis, a type of cell death associated with oxidation that differs from other types of cell death, such as apoptosis, necrosis, or autophagy. The induction of ferroptosis is desired in some diseases, such as cancer, but in others, such as cardiovascular diseases, this type of cell death is not wanted. The possible effects of quercetin associated with reducing or inducing ferroptosis have not been reviewed. Thus, this review focuses on the ability of quercetin to produce ferroptosis in diseases such as cancer as a treatment option and, conversely, on its role in deactivating ferroptosis to alleviate diseases such as cardiovascular diseases.

Keywords: quercetin; ferroptosis; cancer; renal injury; liver injury; inflammation

1. Introduction

Plants synthesize and accumulate a plethora of natural products such as alkaloids, flavonoids, and terpenoids. These compounds serve as messengers in different cell signaling pathways, e.g., as signals for nitrogen-fixing bacteria; they are also protective agents since they act as shields against ultraviolet light, attractants for pollination and oviposition, and even antimicrobial/antiviral agents [1]. Flavonoids are polyphenolic compounds found in fruits, vegetables, and cereals that have numerous actions, such as antioxidant activities, inducing phase II metabolizing enzymes via the activation of Nrf2, controlling cellular growth, and antiviral and antibacterial actions. Interestingly, these molecules are more effective antioxidants in vitro than vitamins E and C and have lower levels of toxicity [2]. Quercetin is a flavonoid characterized by its flavone nucleus, which is composed of two benzene rings linked with a heterocyclic pyrone ring. It is found in apples, onions, tea, red wines, and berries. Quercetin has different beneficial effects, such as providing cardiovascular protection, possessing anti-inflammatory properties, anticancer activity, and antiulcer effects, and demonstrating antiallergic and antiviral actions [3]. The diseases represented by the latter effects are related to oxidant molecules such as reactive oxygen species (ROS) because these species react and induce the oxidation of cell biomolecules, such as proteins, lipids, DNA, or carbohydrates, which impair cell homeostasis [4]. Regarding lipids, the oxidation of these molecules induces lipid hydroperoxides, which glutathione peroxidase 4 (GPX4) degrades; however, if GPX4 reduces its expression or activity, highly reactive aldehydes such as 4-Hydroxynonenal (4HNE) and malondialdehyde (MDA) are produced. These oxidative conditions induce a type of cell death associated with oxidation, ferroptosis,

Review article

Mitochondrial transplantation strategies in multifaceted induction of cancer cell death

Alfredo Cruz-Gregorio [a,*], Ana Karina Aranda-Rivera [b], Isabel Amador-Martinez [b], Paola Maycotte [c]

[a] *Departamento de Fisiología, Instituto Nacional de Cardiología Ignacio Chávez, 14080 Mexico City, Mexico*
[b] *Laboratorio F-315, Departamento de Biología, Facultad de Química, Universidad Nacional Autónoma de México, 04510 Mexico City, Mexico*
[c] *Centro de Investigación Biomédica de Oriente, Instituto Mexicano del Seguro Social, 74360 Puebla, Mexico*

A B S T R A C T

Otto Warburg hypothesized that some cancer cells reprogram their metabolism, favoring glucose metabolism by anaerobic glycolysis (Warburg effect) instead of oxidative phosphorylation, mainly because the mitochondria of these cells were damaged or dysfunctional. It should be noted that mitochondrial apoptosis is decreased because of the dysfunctional mitochondria. Strategies like mitochondrial transplantation therapy, where functional mitochondria are transplanted to cancer cells, could increase cell death, such as apoptosis, because the intrinsic apoptosis mechanisms would be reactivated. In addition, mitochondrial transplantation is associated with the redox state, which could promote synergy with common anticancer treatments such as ionizing radiation, chemotherapy, or radiotherapy, increasing cell death due to the presence or decrease of oxidative stress. On the other hand, mitochondrial transfer, a natural process for sharing mitochondrial between cells, induces an increase in chemoresistance and invasiveness in cancer cells that receive mitochondria from cells of the tumor microenvironment (TME), which indicates an antitumor therapeutic target. This review focuses on understanding mitochondrial transplantation as a therapeutic outcome induced by a procedure in aspects including oxidative stress, metabolism shifting, mitochondrial function, auto-/mitophagy, invasiveness, and chemoresistance. It also explores how these mechanisms, such as apoptosis, necroptosis, and parthanatos, impact cell death pathways. Finally, it discusses the chemoresistance and invasiveness in cancer cells associated with mitochondria transfer, indicating an antitumor therapeutic target.

1. Introduction

Mitochondria are responsible for a plethora of functions in cells [1,2]. These functions include metabolism, cell growth, cell survival, and apoptosis, essential in developing and maintaining cancer cells. For instance, in the mitochondria of eukaryotic cells, bioenergetic processes such as the tricarboxylic acid cycle (TCA), electron transport system (ETS), fatty acid oxidation (FAO), and oxidative phosphorylation (OXPHOS) are coordinated to obtain energy in the form of ATP. Biosynthetic processes such as amino acid (aa), lipid, and nucleotide synthesis are also enhanced to meet the needs of highly proliferating cancer cells [3]. Although OXPHOS yields 34 ATP molecules compared to glycolysis, which produces only 2 ATP molecules, their production is slow compared with glycolysis. This is because glycolysis can produce ATP with fast flux, more than 100-fold faster than OXPHOS, an effect needed in the rapid fluctuations of cancer cells. Thus, an increased glycolytic flux represents a metabolic strategy that allows cancer cells to meet their energetic demands [4]. Therefore, glycolysis is preferred in tumors because glycolytic ATP is obtained faster than mitochondrial ATP production from OXPHOS, allowing the high energy conditions demanded by tumor cells to be achieved and the production of metabolic intermediates for biosynthesis [5,6].

Moreover, increased lactate production due to an enhanced glycolytic flux decreases extracellular pH, which induces acidosis in the tumor microenvironment, contributing to immune escape, cancer invasion, metastasis, and even radiation and drug resistance [7]. Otto Warburg observed that cancer cells could reprogram their glucose metabolism, favoring glycolysis over OXPHOS, even in the presence of oxygen, a state

Review

Mitochondrial Impairment: A Link for Inflammatory Responses Activation in the Cardiorenal Syndrome Type 4

Isabel Amador-Martínez [1,2], Omar Emiliano Aparicio-Trejo [2], Bismarck Bernabe-Yepes [3], Ana Karina Aranda-Rivera [1,4], Alfredo Cruz-Gregorio [5], Laura Gabriela Sánchez-Lozada [2], José Pedraza-Chaverri [4] and Edilia Tapia [2,*]

1. Posgrado en Ciencias Biológicas, Universidad Nacional Autónoma de México, Ciudad Universitaria, Mexico City 04510, Mexico; amador_i@ciencias.unam.mx (I.A.-M.); anitaaranda023@comunidad.unam.mx (A.K.A.-R.)
2. Departamento de Fisiopatología Cardio-Renal, Instituto Nacional de Cardiología Ignacio Chávez, Mexico City 14080, Mexico; omar.aparicio@cardiologia.org.mx (O.E.A.-T.); laura.sanchez@cardiologia.org.mx (L.G.S.-L.)
3. Departamento de Biomedicina Cardiovascular, Instituto Nacional de Cardiología Ignacio Chávez, Mexico City 14080, Mexico; bis_by@comunidad.unam.mx
4. Laboratorio F-315, Departamento de Biología, Facultad de Química, Universidad Nacional Autónoma de México, Mexico City 04510, Mexico; pedraza@unam.mx
5. Departamento de Fisiología, Instituto Nacional de Cardiología Ignacio Chávez, Mexico City 14080, Mexico; alfredo.cruz@cardiologia.org.mx
*   Correspondence: edilia.tapia@cardiologia.org.mx

Abstract: Cardiorenal syndrome type 4 (CRS type 4) occurs when chronic kidney disease (CKD) leads to cardiovascular damage, resulting in high morbidity and mortality rates. Mitochondria, vital organelles responsible for essential cellular functions, can become dysfunctional in CKD. This dysfunction can trigger inflammatory responses in distant organs by releasing Damage-associated molecular patterns (DAMPs). These DAMPs are recognized by immune receptors within cells, including Toll-like receptors (TLR) like TLR2, TLR4, and TLR9, the nucleotide-binding domain, leucine-rich-containing family pyrin domain-containing-3 (NLRP3) inflammasome, and the cyclic guanosine monophosphate (cGMP)–adenosine monophosphate (AMP) synthase (cGAS)–stimulator of interferon genes (cGAS-STING) pathway. Activation of these immune receptors leads to the increased expression of cytokines and chemokines. Excessive chemokine stimulation results in the recruitment of inflammatory cells into tissues, causing chronic damage. Experimental studies have demonstrated that chemokines are upregulated in the heart during CKD, contributing to CRS type 4. Conversely, chemokine inhibitors have been shown to reduce chronic inflammation and prevent cardiorenal impairment. However, the molecular connection between mitochondrial DAMPs and inflammatory pathways responsible for chemokine overactivation in CRS type 4 has not been explored. In this review, we delve into mechanistic insights and discuss how various mitochondrial DAMPs released by the kidney during CKD can activate TLRs, NLRP3, and cGAS-STING immune pathways in the heart. This activation leads to the upregulation of chemokines, ultimately culminating in the establishment of CRS type 4. Furthermore, we propose using chemokine inhibitors as potential strategies for preventing CRS type 4.

Keywords: chronic kidney disease; cardiorenal syndrome type 4; mitochondria; innate immune response; chemokines; inflammation

1. Cardiorenal Syndrome Overview

The intrinsic association between cardiovascular disease (CVD) and kidney disease was first described by Robert Bright over a century ago [1]. This maladaptive link is termed cardiorenal syndrome (CRS) [2]. CRS comprises five distinct subtypes classified based on